Adaptive and maladaptive myocardial remodelling due to pressure overload do not evolve from a common hypertrophy precursor stage

Buermans, H.P.J.

2007

document version
Publisher's PDF, also known as Version of record

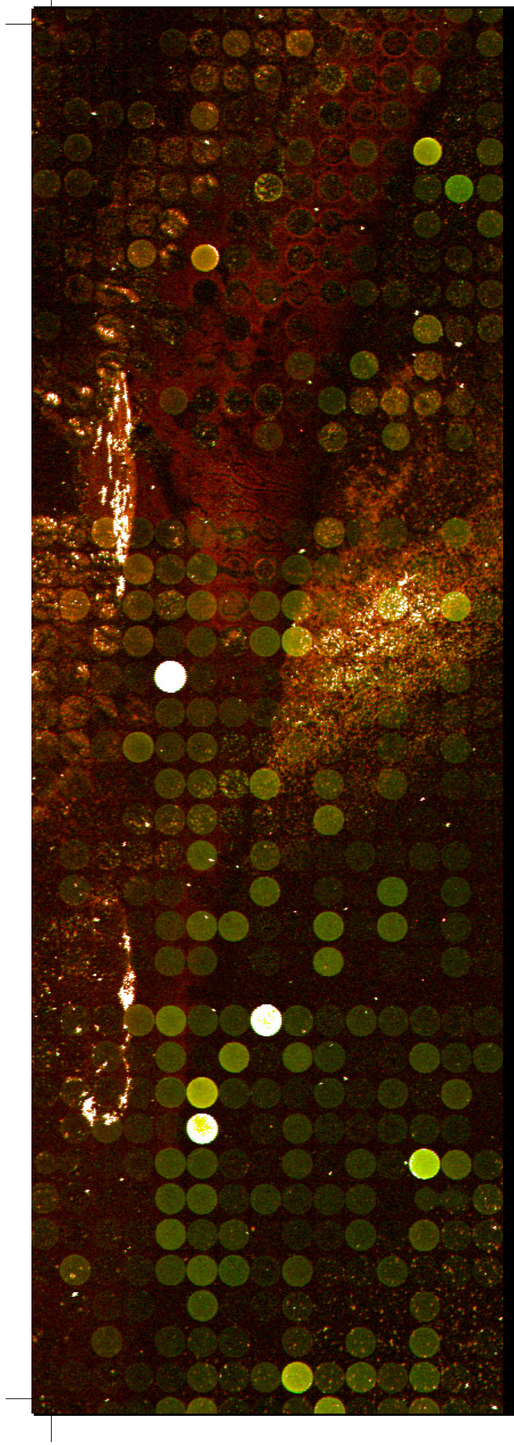

Adaptive and maladaptive myocardial remodelling due to pressure overload do not evolve from a common hypertrophy precursor stage

Henk P.J. Buermans

Adaptive and maladaptive myocardial remodelling due to pressure overload do not evolve from a common hypertrophy precursor stage

Characterization of ventricular
proteome and transcriptome profiles

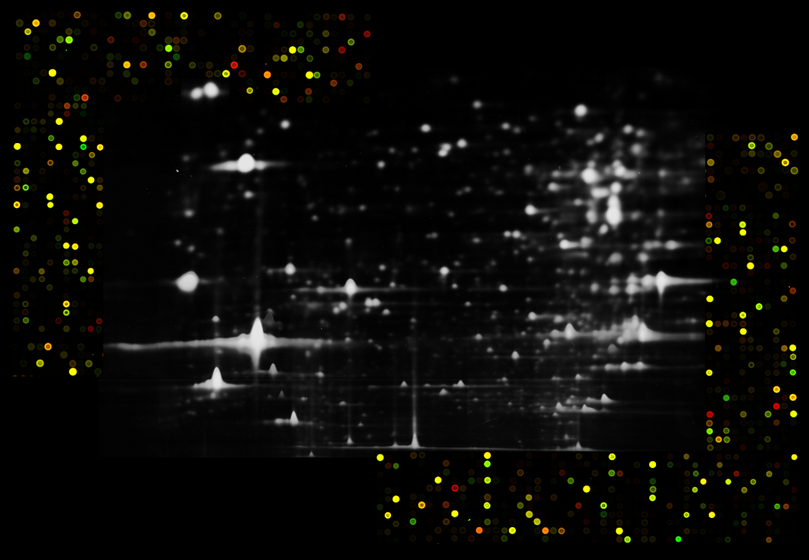

Henk P.J. Buermans

Uitnodiging

Voor het bijwonen van de
openbare verdediging
van het proefschrift van

Henk P.J. Buermans

Op dinsdag
13 februari 2006
om 15.45 uur

Aula Hoofdgebouw
Vrije Universiteit
De Boelelaan 1105
Amsterdam

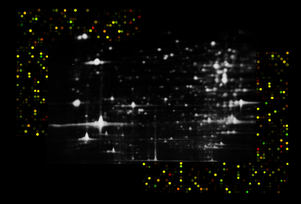

De paranimfen

Pierre Buermans
06-11406719
p.buermans@home.nl

Philip Hendriks
pe-hendriks@home.nl

Adaptive and maladaptive myocardial remodelling due to pressure overload do not evolve from a common hypertrophy precursor stage

Characterization of ventricular proteome and transcriptome profiles

Henk P.J. Buermans

The studies presented in this thesis were performed at the Laboratory for Physiology of the VU University Medical Center, van der Boechorststraat 7, 1081 BT Amsterdam, The Netherlands. Printing of this thesis was financially supported by:

Harlan Nederland
J.E. Jurriaanse Stichting
Netherlands Heart Foundation

Adaptive and maladaptive myocardial remodelling due to pressure overload do not evolve from a common hypertrophy precursor stage. Henk PJ. Buermans
ISBN: 90-9021041-5

This thesis was printed by GILDEPRINT BV, Enschede, The Netherlands

VRIJE UNIVERSITEIT

Adaptive and maladaptive myocardial remodelling due to pressure overload do not evolve from a common hypertrophy precursor stage

Characterization of ventricular proteome and transcriptome profiles

ACADEMISCH PROEFSCHRIFT

ter verkrijging van de graad Doctor aan
de Vrije Universiteit Amsterdam,
op gezag van de rector magnificus
prof.dr. L.M. Bouter,
in het openbaar te verdedigen
ten overstaan van de promotiecommissie
van de faculteit der Geneeskunde
op dinsdag 13 februari 2007 om 15.45 uur
in de aula van de universiteit,
De Boelelaan 1105

door

Hendrikus Petrus Josephus Buermans

geboren te Roosendaal

promotoren: prof.dr. F.C. Visser
prof.dr. W.J. Paulus

copromotor: dr. W.S. Simonides

Voor linnnn...

Table of contents

Chapter 1

General Introduction

Table of contents

1: Normal Heart Function

The Cardiac Cycle

The heart is a muscular pump, providing blood flow through the cardiovascular system, needed for normal body function. The cardiovascular system can be divided into a cardiac and a circulatory component. The cardiac component itself can be subdivided into the right heart side, supplying blood flow for the low pressure pulmonary circulation, and the left side, which provides blood flow for the high pressure coronary and systemic circulation (Figure 1). During a relaxation phase, i.e., diastole, the lumen of the ventricle is filled with blood. During systole, the ventricle wall contracts, reducing its lumen volume, and ejects the blood from the lumen into the arteries.

With each contraction, 55-75% of the blood in the ventricular cavity is ejected into the arteries under normal workload conditions, with mean arterial pressures of 15 mmHg and 90 mmHg developed by the right and left ventricle, respectively. This is sufficient to provide every organ with adequate blood flow.

Excitation – Contraction Coupling

The heart consists of several cell types, e.g., endothelial cells, smooth muscle cells, fibroblasts, pacemaker cells and cardiac myocytes. Cardiac myocytes are rod shaped cells with a diameter of 10-25 µm and a length of 100-200 µm. They are arranged in series, connected by intercalated discs forming myofibers. The outer or sarcolemmal membrane of a myocyte has deep invaginations called T-tubules, bordering the sarcomeres of the myofilaments. The sarcomeres are the

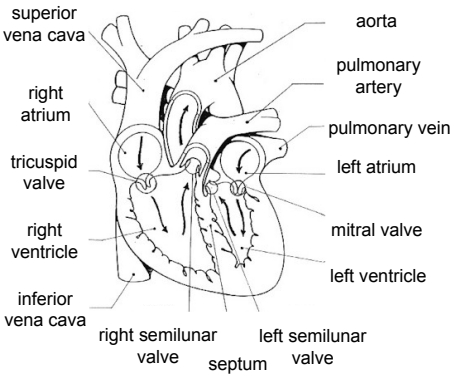

▲Figure 1 - Heart and circulation. Within each heart cycle, blood is collected in the right atrium (RA) from both the superior and inferior vena cava. The right ventricle (RV) is subsequently filled with blood from the RA during RV diastole and during RV systole, blood is ejected from the RV, passing the right semilunar valves, into the pulmonary arteries. In the lungs, carbon dioxide (CO_2) is released from the blood and oxygen (O_2) is bound to the hemoglobin of red blood cells. Parallel to the entry into the right side of the heart, blood is collected from the pulmonary veins in the left atrium (LA) and released into the left ventricle (LV) after which the blood is pumped during LV systole, passing the left semilunar valves, into the aorta. The heart itself is the first organ to be perfused by oxygenated blood via the coronary circulation. Each heart cycle is synchronized in a way that first both atria contract simultaneously, releasing blood into the ventricles. After a small pause, both ventricles will subsequently contract.

smallest functional units of the myofibers, consisting of myosin, forming the thick filaments and actin, tropomyosin and troponins in the thin filaments. The cardiac myocytes comprise approximately 75% of the total heart volume and convert the chemical energy stored in adenosine triphosphate (ATP) into mechanical energy, i.e., contraction, in a process called excitation contraction coupling (ECC). Central in the mechanism of ECC are fluctuations in intracellular calcium concentration ($[Ca^{2+}]_i$)[1]. Calcium is the second messenger that relays the signal of the action potential from the T-tubule of the sarcolemma to the contractile elements, initiating cross-bridge cycling of the actin and myosin filaments. The action potential triggers a rise in $[Ca^{2+}]_i$ through a calcium - induced - calcium – release (CICR) from the sarcoplasmatic reticulum (SR), which in turn initiates actin-myosin cross-bridge cycling and shortens the sarcomeres during systole (Figure 2). At end systole, $[Ca^{2+}]_i$ is reduced to baseline levels, allowing for the diastolic phase.

Calcium Handling

There are several transporter systems present in cardiac myocytes that mediate the decrease in $[Ca^{2+}]_i$ to baseline levels and thus terminate the ECC cycle. These systems balance the influx of calcium from beat to beat, maintaining a constant total calcium content of the myocyte. First, L-type channels (LTCC) are closed by a negative feedback loop responding to the increasing $[Ca^{2+}]_i$ itself, preventing more calcium from entering the cells. Reduction of $[Ca^{2+}]_i$ is driven by three routes, each with different contributions and transporting calcium from the cytosolic compartment to different locations[2]. A marginal percentage is handled by the sarcolemmal Ca^{2+}-ATPase and the mitochondrial Ca^{2+} uniporter, i.e., the slow systems, and these do not significantly contribute to the $[Ca^{2+}]_i$ fluxes. The sodium-calcium exchanger (NCX) which is located in the sarcolemma, transports calcium to the outside of the cellular compartment. The main contribution to the reduction of $[Ca^{2+}]_i$, however, is by the sarcoplasmic-endoplasmic reticulum Ca^{2+}-ATPase (SERCA2a), pumping calcium back into the SR (Figure 2, step 5). SERCA2a pump activity is increased when its inhibitory regulator protein phospholamban is phosphorylated by Ca-calmodulin-dependent protein kinase (CaMK) II and protein kinase A (PKA) at high $[Ca^{2+}]_i$ levels[1].

There are differences in the contribution of extracellular and SR calcium and hence the contribution of the different transport systems between species. Ferret, dog, cat, guinea-pig, rabbit and human myocytes show a similar distribution (70% SERCA2a vs. 28% NCX vs. 2% slow systems) in contrast to rat and mouse which are much more dependent on SERCA2a expression levels (92% SERCA2a vs. 7% NCX vs. 1% slow systems)[1].

Beta-Adrenergic Receptor Signalling

Cardiac output and contraction frequency can be varied by alterations in noradrenalin (NA) and adrenaline levels via modulation of beta-adrenergic receptor (βAR) signalling, allowing for acute responses to increased cardiac output demand. Of the subtypes of βAR expressed on cardiac myocytes, the β1 and β2 types have been shown to mediate positive inotropic effects in contrast to negative inotropic effects via β3 type signalling[3, 4]. Signalling through the βAR types 1 and 2 involves the stimulatory G protein ($G\alpha_s$) cascade, resulting in increased production of cAMP via adenylyl cyclase activation. Subsequently activated PKA modulates myocyte contraction via phosphorylation of many intracellular protein targets, resulting in

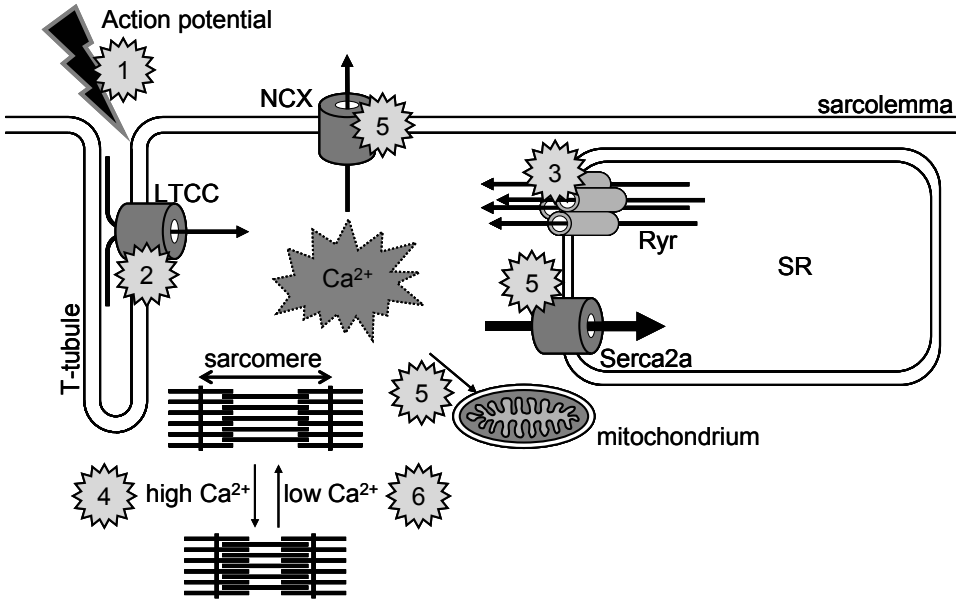

▲Figure 2 - Calcium Handling. When the sarcolemma is depolarized (step 1), a small amount of calcium enters the cell through opening of the L-type calcium channels (LTCC) (step 2). Within milliseconds, this small increase in $[Ca^{2+}]_i$ from the LTCC triggers a calcium - induced - calcium - release from the sarcoplasmatic reticulum (SR) through the ryanodine receptor complexes located in the SR membrane (step 3). This results in an approximately 100 fold increase in total free $[Ca^{2+}]_i$. Calcium binding to troponin C (TnC) induces a conformational change in troponin I (TnI), allowing actin-myosin cross-bridge cycling. When TnI inhibition is relieved, the myosin head reaches forward and binds to actin. Chemical energy from ATP hydrolysis is converted into mechanical energy when the myosin head bends through a 45º angle, sliding the actin and myosin filaments past each other, shortening the sarcomere and thus muscle fibre length (step 4). The actin-myosin complex dissociates at the end of the cycle when new ATP is bound. Myosin returns to its resting conformation, cleaves the ATP and resets the system to starting conditions, ready to repeat the cycle. This will continue for as long as there is enough calcium present to keep TnI in the disinhibiting conformation[2], allowing for relaxation only if the $[Ca^{2+}]_i$ has reached baseline levels again (step 6).

increased Ca^{2+} influx via the LTCC, increased Ca^{2+} re-uptake in the SR via PLB / SERCA2a and myofilament Ca^{2+} sensitivity via TnI. However, the β2 receptors are also coupled to the inhibitory G proteins ($G\alpha_i$), and thus may also reduce cAMP levels through inhibition of adenylyl cyclase. Consequently, the β1 to β2 receptor ratio is an important parameter.

Myocardial Energy Metabolism

During normal cardiac function, over 95% of all cellular ATP is produced via oxidative phosphorylation in the mitochondria, with only a small contribution from the glycolysis pathway. Approximately 60-70% of the total ATP content is used for sarcomere shortening during systole while the remaining 30-40% drives ion channels, primarily SERCA2a for calcium re-uptake into the SR.

Under normal conditions, approximately 70% of ATP generation depends on oxidation of fatty acids (FA). These FA are processed in the mitochondrial matrix by the fatty acid beta-oxidation pathway to yield acetyl-CoA and the reduced flavin adenine dinucleotide (FADH2). The remaining 30% of ATP generation depends primarily on pyruvate derived from glucose and lactate. Acetyl-CoA is also produced from pyruvate by the pyruvate-dehydrogenase (PDH) complex in the inner mitochondrial membrane. The acetyl-CoA from both these pathways enters the tricarboxylic acid (TCA) cycle to generate reduced nicotinamide adenine dinucleotide (NADH). The NADH and FADH2 from these pathways are used in the electron transport chain to build an electrochemical proton-gradient across the inner mitochondrial membrane, which enables ATP synthesis during oxidative phosphorylation.

2: Cardiomyopathy

Cardiac Adaptation

Cardiac function may be compromised following an "index event" leading to pressure or volume overload. As a direct result, the ventricles will sense an increase in wall stress, triggering a compensatory response that is aimed at normalizing wall stress and maintaining adequate blood flow. A general mechanism of the heart to compensate for this increased workload is hypertrophic remodelling of the ventricular wall. In the setting of pressure overload, which may for instance develop during (pulmonary) hypertension or aortic valve stenosis, the thickness of the ventricular wall will increase[5] due to the addition of new sarcomeres in parallel to already existing sarcomeres at the individual myocyte level. This is termed concentric hypertrophy. Cardiac hypertrophy, by definition, is the result of an abnormal increase in myocyte dimensions and not an increase in the number of these cells[6]. The adapted ventricle is then more capable of generating forces and pressures to cope with the increased workload, while the increased wall diameter normalizes wall stress (Figure 3). Volume overload may occur due to heart block, regurgitant mitral or aortic valves, atrial or ventricular septal defects, or other congenital diseases. Here also, new sarcomeres are added to existing ones, but in series rather than in parallel[5]. This hypertrophic response is called eccentric hypertrophy. It leads to an increase in end-diastolic volume of the ventricle, showing greater than normal cavity dimension at end-diastole, and results in an increased end-diastolic volume of the ventricular lumen, and a resulting rise in stroke volume, which compensates for excess blood remaining in the LV (Figure 3).

Adaptive vs. Maladaptive Remodelling

Cardiac hypertrophy is generally thought to be a necessary, beneficial, compensatory reaction in response to increased workload[7]. This was already recognized during the 18th and 19th century by JB. Morgagni[8], FA. Aran[9] and R. Virchow[10]. Indeed, many patients remain free of clinical events for a long time after the index event has occurred. In contrast to this adaptive (physiological) response, cardiac hypertrophy may progress to heart failure when the overload is too high or is maintained for too

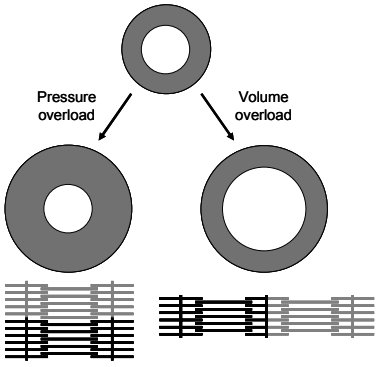

►**Figure 3 – Pressure and volume overload:** Schematic representation of sarcomere addition during pressure overload and volume overload (grey sarcomeres) to the pre-existing sarcomeres in the normal situation (black sarcomeres).

long a period of time (pathological hypertrophy).
A substantial amount of research over the last couple of decades has lead to important insights into processes that govern the development of ventricular hypertrophy and heart failure, e.g., alterations in signal transduction cascades, energy metabolism and calcium handling (for a detailed description of such processes, see section 3 and 4). However, it still remains an enigma which signalling pathway or combination of pathways is critical for the development of a pathological hypertrophic phenotype. Furthermore, it is unclear whether the alteration of these processes is predominantly qualitative or quantitative in nature.
Also, little information is available concerning the sequence in time at which these molecular alterations take place. For the majority of observed changes it is unknown whether these occur as a direct result of the pressure overload sensed by the myocardium, or, as a secondary response to preceding changes. Contemporary theory states that a compensated form of hypertrophy may either remain as a adaptive phenotype, or subsequently progress to a maladaptive phenotype. Progression to heart failure would be mediated by a deterioration of survival signalling, relative to the pro-hypertrophic stimuli. It remains to be seen whether a pathological phenotype is induced early during overload, as a function of the degree of mechanical overload, or, only as a secondary response when compensation is insufficient[11-13], i.e., end point trigger vs. early origin of differences between phenotypes.

Defining Heart Failure
Patients who have been diagnosed with heart failure, have hearts with depressed contractile capabilities, leading to decreased cardiac output. Heart failure contributed to approximately 287.200 deaths in the year 1999 in the United States and on average, 5 million cases of heart failure exist in the U.S alone. Two recent epidemiological studies[14, 15], based on two separate populations, indicated an overall higher incidence of heart failure in men, with no decreased incidence over time. For women however, one study showed decreased incidence[15] while the other indicated no change[14] during the last two decades. Both studies indicated an overall increase in the survival rate, in particular for men and young persons. However, this increase in survival rate was less prominent in women and the elderly. With an overall 5 year survival rate of 52% and an increasing elderly population, heart failure remains a major health problem. Similarly, an estimated 0.4 - 2% of the European population suffers from heart failure[16]. There is no single definition that fully describes heart failure in all its facets[17]. It is a clinical end-point of a syndrome characterized by a progressive loss of pump function, manifested by respiratory distress, pedal edema

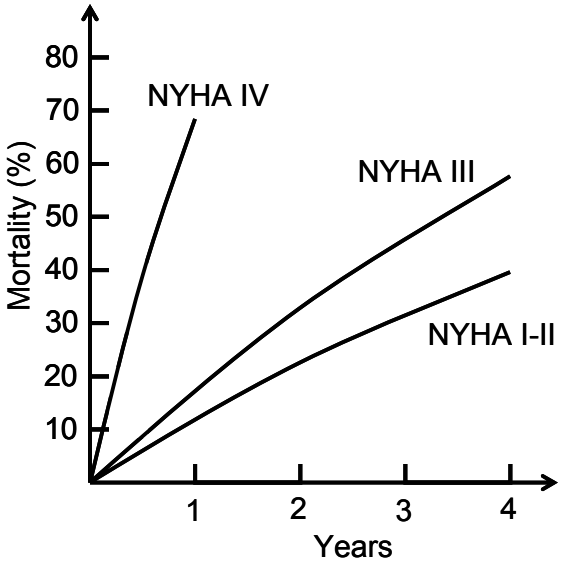

◄Figure 4: NYHA heart failure classification

Class I: patients with no limitation of activities; they suffer no symptoms from ordinary activities.

Class II: patients with slight, mild limitation of activity; they are comfortable with rest or with mild exertion.

Class III: patients with marked limitation of activity; they are comfortable only at rest.

Class IV: patients who should be at complete rest, confined to bed or chair; any physical activity brings on discomfort and symptoms occur at rest.

and ascites, and profound exercise intolerance. The New York Heart Association (NYHA) has provided a heart failure classifications framework (Figure 4), which classifies patients in four groups, according to the severity of the observed symptoms. However, heart failure may result from a wide variety of disorders, and, although the observed pathophysiological phenotype at end-point heart failure resulting from distinct etiologies may appear to be similar, the underlying changes at the molecular level can be profoundly different. Also, a single etiologic factor may result in a drastically different phenotype in individuals with a different genetic background. Furthermore, co-morbidities like viral infection, inflammation, hyperthyroidism and metabolic disease may significantly contribute to the progression to heart failure[18-20], indicating the importance of interactions between disease-related factors, the environment and genetic background. Recently, a new classification proposal was issued, which also classifies patients according to the specific etiology, in addition to the stage of development[20] potentially leading to a more specific and effective treatment of the patient.

3: Alterations During Ventricular Hypertrophy And Heart Failure

Characteristic features of hypertrophic remodelling at the cellular level, in addition to the aforementioned myofibrillar re-organization, are changes in calcium handling[21], evident from decreased peak systolic $[Ca^{2+}]_i$, increased diastolic $[Ca^{2+}]_i$ and prolonged diastolic $[Ca^{2+}]_i$ decay. Also, extracellular matrix composition[22, 23], cytoskeletal proteins[24], β-adrenergic receptor signalling[3, 4], mitochondrial energy metabolism[25], myocyte survival[26] and alterations in gene-expression patterns of both the messenger RNA (mRNA) and protein level can generally be observed. The main processes implicated in heart failure are briefly discussed in the following sections.

Fetal Gene Program

At the earliest stages of ventricular remodelling, a set of growth related genes is rapidly, yet transiently expressed in the myocardium. These are the first changes to be detected after the rise in pressure, and were subsequently called the "immediate early genes" (IEG). Typical members of this group of genes are members of the early growth response (Egr) family and the proto-onco genes c-fos and c-jun[27] in addition to GATA-4, Nkx-2.5/Csx, myocyte enhancing factor (MEF)-2 and the HAND family[28]. These genes encode transcription factors that can subsequently stimulate alterations in gene-expression patterns. These changes in gene-expression are indicative for the initiation of a hypertrophic or fetal gene program, in which the adult protein isoforms are replaced by their fetal counterparts. Typical changes are increases in skeletal a-actin with concomitant decreases in a-cardiac actin[29], and a switch in the myosin heavy chain (MHC) α to MHCβ expression ratio[30, 31]. Also depressed SERCA2a[23, 32] levels and increased natriuretic peptide type A and B (ANP and BNP) expression are observed[29].

Altered Beta-Adrenergic Receptor Signalling

Absolute cardiac βAR expression levels are at 50-70 fmol/mg membrane protein. In the normal heart, the β1 to β2 expression ratio is approximately 70:30, at which catecholamine stimulation would lead to an overall increase in cAMP production. During heart failure, although the β2 levels are unaffected, β1 expression levels are reduced to such an extent that the β1 to β2 ratio may reach 50:50. Relatively increased $G\alpha i$ contributions in this situation, results in a decreased generation of, and response to, cAMP upon catecholamine stimulation. In addition, hypertrophic remodelling has also been associated with an increased activity of G protein receptor kinases (GRKs), in particular the GRK2 (βARK1). These kinases trigger the internalization and degradation of βARs. Both the receptor degradation and the

reduction of cAMP effectively lead to a desensitization to catecholamine drive. This appears to be an adaptive response since sympathetic activation is inversely correlated with survival[33]. Although it is generally thought that β1 and β2-ARs mediate pro- and anti-apoptotic signalling respectively, the precise mediators for these effects remain to be identified.

Changes In Energy Metabolism

In general, during the earliest stages in the development of heart failure through pressure overload, energy substrate distribution is relatively normal. However, in the advanced stages, a severe downregulation in fatty acid oxidation is observed, accompanied by increased glycolysis and glucose oxidation, reduced respiratory chain activity and impaired reserve for mitochondrial oxidative flux and reduced myocardial ATP content[34]. However, despite the strong association between the substrate switch and the development of heart failure, there is evidence that supports a beneficial role of this change[35, 36]. In addition, theoretically, glucose and lactate yield approximately 11% more ATP per oxygen used than fatty acids do[37]. However, ATP yield will be decreased for both glucose / lactate and fatty acid oxidation (FAO) if the inner mitochondrial membrane is uncoupled, and thus is unable to take full advantage of the proton-gradient. This is particularly important since FA have been shown to be able to uncouple oxidative phosphorylation.

The basis for this switch away from FAO can be found at both the transcription and protein activity level of peroxisome proliferator activated receptor-α (PPARα) and the transcription factor PPARα coactivator-1a (PGC-1a). In the normal postnatal heart a complex of PPARα, retinoid x receptor-α (RXRα) and PGC-1a, bound to a PPAR responsive element (PPRE) in the promotor region of a FAO related gene, functions as a lipid sensor switch. Upon fatty acid binding, the complex is activated and gene transcription can commence, in principle allowing for the simultaneous regulation of many related genes with PPRE motifs[38].

A decrease in both PPARα[39] and PGC-1a[40] has been demonstrated in the pressure-overloaded heart and several signalling cascades have been shown to mediate these changes. Cardiac specific over expression of a constitutively active form of protein kinase B (PKB / Akt), lead to the decreased expression of both PPARα and PGC-1a[41]. In addition, PGC-1a has been shown to be inhibited via ERK1/2 signalling, while it is stimulated by calcineurin A, CaMK, nitric oxide / cGMP, β-adrenergic / cAMP signalling and p38 MAPK[25].

Mitochondrial Structure And Biogenesis

Mitochondria are small subcellular organelles 1-4 μm in length which comprise 30-50% of the total cardiac myocyte volume. Their best known function is the generation of high energy ATP from adenosine diphosphate (ADP) through oxidative phosphorylation. In addition, mitochondria are involved in processes like apoptosis, regulation of the cellular redox state, heme synthesis, steroid synthesis and heat production. They consist of a highly folded inner membrane, forming cristae, surrounding the matrix compartment. This inner membrane contains, in addition to a number of highly selective transporter complexes, a crucial series of proteins needed for respiratory chain function, i.e., NADH dehydrogenase (Complex I), succinate dehydrogenase (Complex II), cytochrome-C reductase (Complex III; also known as the cytochrome B-C1 complex), cytochrome C oxidase (Complex IV) and ATP synthase (Complex V). Surrounding the mitochondrion is the outer membrane, containing a large number of pore-forming complexes that control transport in and out of the intermembrane space, however, molecules smaller than 15kD are able to diffuse freely in and out of the intermembrane space. The integrity of these two membranes is imperative for proper mitochondrial function.

Mitochondria contain 5-10 copies of double stranded, circular mitochondrial DNA (mtDNA), each approximately 16.5 kb long, coding for 22 tRNAs, two rRNA and 13 protein subunits for complexes I, III and IV of the respiratory chain. These genes have no introns, and the two non-coding regions contain the two promotor regions for transcription initiation and the origin of replication. After both strands are completely transcribed, strands for mRNA, rRNA and tRNA are excised and non-coding RNA is degraded. The majority of the estimated 1000 proteins comprising mature mitochondria are so called nuclear-encoded mitochondrial (NEM) genes, i.e., respiratory chain complex subunits, membrane carriers, matrix enzymes and transcription-translation related proteins. Fully functioning protein complexes are formed with their mtDNA-encoded counterparts, after these proteins have been imported into mitochondria via translocator complexes of the outer and inner membranes, TOM and TIM, respectively, which are structured at contact sites (CS) which fuse the inner and outer membranes.

PGC-1a is not only involved in transcriptional gene-expression regulation of FAO-related proteins, it is also directly involved in mitochondrial biogenesis through regulation of increased nuclear respiratory factor (NRF) 1 and NRF-2 expression, which in turn are almost exclusively involved in the regulation of NEM genes. Of these genes, it is the mitochondrial transcription factor A (TFAM), which is crucial for the replication, maintenance, and transcription of the mitochondrial genome. Genetically modified mice with a cardiac-specific deletion of the TFAM gene, showed

severe respiratory chain deficiency in addition to characteristic gene-expression alterations for heart failure[42, 43] and apoptosis[42]. Also, profound alterations in calcium-handling genes were observed, e.g., decreased expression of Ryr, calsequestrin 2, LTCC, NCX and SERCA2a[44]. Interestingly, TFAM has been shown to be downregulated in a model for pressure overload at end-point heart failure, accompanied by reduced expression levels of nuclear and mitochondrial subunits for complex IV of the respiratory chain[40]. Furthermore, mice over-expressing human TFAM showed reduced LV remodelling and mortality after myocardial infarction[45].

Mitochondrial Dysfunction

Altered structure, function and number of mitochondria in the cell may indicate mitochondrial dysfunction, which leads to impaired energy production, loss of contractility and cell death[46]. The development of heart failure may involve an abnormally high frequency of myocyte apoptosis that can persist for a prolonged period of time[47, 48]. Apoptosis can be triggered via various stimuli, including ischemia-reperfusion, β1-adrenergic stimulation, stretch, angiotension II, tumor necrosis factor–α and oxidative stress[49]. One inherent by-product of normal cellular activity is the production of a small amount of reactive oxygen species (ROS) from 1-5% of the oxygen that is consumed during cellular respiration in the mitochondrial respiratory chain[50], meaning that conditions that demand higher levels of oxygen consumption consequently result in higher levels of cellular ROS. Of the many possible sources of ROS, mitochondria, xanthine oxidase and the non-phagocytic NADPH oxidases (Noxs), are the predominant sources of ROS in heart failure. Under normal conditions, the ROS species are effectively scavenged by antioxidant systems, including the mitochondrial superoxide dismutase 2. Evidence exists that excess ROS production causes myocyte dysfunction and apoptosis[51, 52]. Increased mitochondrial ROS production may severely impair cellular and mitochondrial function, by damaging proteins, lipids and mtDNA, which in turn may lead to increased generation of ROS. In contrast to genomic DNA, mtDNA is relatively unprotected and resides in close proximity to the inner mitochondrial membrane where ROS is generated. It is therefore much more susceptible to ROS damage than the nuclear genome. Mutations in the mtDNA may lead to non-functional respiratory-chain proteins and impaired mitochondrial replication.

Increased cellular ROS, but also long chain fatty acids and calcium, may lead to the opening of the mitochondrial permeability transition pore (mtPTP), which is a channel, with the adenine nucleotide translocase 1 (ANT1) and the voltage dependent anion channel 1 (VDAC1) located on the inner and outer membranes, respectively, as part of the membrane contact sites. mtPTP opening leads to the loss

of the membrane potential ($\Delta\psi$) and cytochrome-C release from the intermembrane space into the cytosol, activation of caspase3 and subsequently to apoptosis.

Extracellular Matrix Composition

The extracellular matrix (ECM) is crucial for maintaining the integrity and normal geometry of the heart. It does not merely provide a supportive scaffold by surrounding and interconnecting the cardiac myocytes, aligning them in muscle fibers, but the matrix also plays a complex and divergent role in influencing cell behaviour, e.g., cell migration, proliferation, adhesion, and cell-to-cell signalling[53]. The primary constituents are elastin and collagen fibers, of which five forms are expressed in the heart, i.e., collagens I, III, IV, V and VI. Collagen type I, comprising approximately 85% of the total collagen content, has a tensile strength close to iron, enabling the heart to resist deformation, while collagen type III (11% of the total content) displays more flexible properties. Collagen types IV and VI are involved in cellular adhesion via integrins as components of the basal lamina. Other constituents of the ECM are adhesive proteins (fibronectin and laminin), anti-adhesive proteins (tenascin, thrombospondin and osteopontin) as well as proteoglycans, integrins and metalloproteinases[54, 55].

There is a balance between ECM degradation and formation. Matrix metalloproteinases (MMP) are endopeptidases, predominantly produced by fibroblasts[56] and mast cells[57], that degrade elements of the ECM. Four groups of MMPs can be discerned, based on their primary specificity for matrix components, i.e., collagenases (MMP-1 and MMP-13), gelatinases (MMP-2 and MMP-9), stromelysins (MMP-3), and membrane-type MMPs (MT1-MMP)[58]. They are secreted into the ECM in an inactive state zymogen, and are activated by cleavage by serine proteases like cathepsin G, trypsin and plasmin. MMPs induce collagen degradation by cleavage of these proteins at a site near the C-terminal domain. The remaining fragments are unstable and are denatured, leaving them susceptible to degradation by non-specific proteases. A family of four endogenous proteins called the tissue inhibitors of metalloproteinases (TIMP1 to TIMP4) inhibit MMP activity by binding MMPs in a 1:1 ratio, completely abolishing their activity to degrade their substrates.

Examinations of failing hearts, provided evidence of abnormal ECM turnover, e.g., alterations in the amount, type, stability, and organization of fibrillar collagen. More specifically, MMP dysregulation appears to be associated with heart-failure development[56, 58-60]. Also, MMPs produced by mast cells have been implicated in the development of heart failure[61]. Moreover, the use of an MMP inhibitor was able to significantly reduce LV dilatation and preserve systolic function in a study using SHHF rats[62].

4: Signal Transduction Cascades Involved In Myocardial Hypertrophy

Hormones from autocrine/paracrine or neuroendocrine origin and different forms of stress, e.g., altered hemodynamic loading, toxic insults and infections, initiate and activate signal transduction cascades that can lead either to acute responses, or on the longer term, to alterations in gene-transcription activity. Multiple signal transduction cascades, with considerable cross-talk, have been shown to be involved in hypertrophic remodelling and heart failure[12, 63-65].

Mitogen-Activated Protein Kinase Cascades

The mitogen-activated protein kinase (MAPK) pathways represent three parallel branches of successive, serine threonine kinases named after their terminal effector kinases, i.e., the extracellular signal-regulated protein kinases (ERK), c-Jun NH2-terminal kinases (JNK) and p38, which are activated by dual phosphorylation on a threonine and a tyrosine residue lying within a T–X–Y motif. Unambiguous roles for each of these three signalling branches have yet to be defined, however, reports indicate both pro and anti-apoptotic effects for JNK and p38 while ERK appears to be predominantly involved in survival signalling[65, 66].

Calcineurin/NFAT Signalling

Calcineurin (Cn), a serine threonine protein phosphatase, is activated during sustained elevations in $[Ca^{2+}]_i$, essentially linking impaired calcium handling to alterations in gene-expression. Activated Cn dephosphorylates a family of transcription factors called the nuclear factors of activated T-cells (NFAT), which subsequently translocate to the nucleus and, in cooperation with other active transcription factors, are involved in the regulation of transcription initiation of various genes. Activation of the Cn/NFAT pathway manifests itself as a "two-edged sword". While a transient activation antagonizes myocyte apoptosis, prolonged activation induced myocyte hypertrophy with deleterious effects ultimately leading the heart failure[65, 67, 68].

PI3K / Akt / Gsk3β Cascades

The phosphatidylinositol 3-kinase / protein kinase B (PI3K/Akt) signalling cascade is implicated in adaptive cardiac hypertrophy. Overexpression of either constitutively active PI3K or Akt leads to concentric hypertrophy with preserved function and without signs of fibrosis[69-71]. Glycogen synthase kinase 3β (Gsk3β), an ubiquitously expressed and constitutively active serine/threonine kinase, is involved in processes like development, cytoskeletal turnover, apoptosis, cell cycle, metabolism and gene-

expression. Under normal, un-stimulated conditions, it is active and serves as a negative regulator of cardiac hypertrophy by actively inhibiting downstream signalling cascades[72-75]. Gsk3β is able to interfere with the activity of specific transcription factors through the triggering of a nuclear exit signal, e.g., GATA4, NFAT and STAT, or, by attenuation of DNA binding, e.g., CREB, c-Jun, junD and HSF-1[72]. Phosphorylation at the Ser9 residue, which may occur due to multiple upstream kinases, including Akt, disinhibits its negative regulatory actions, allowing for hypertrophic signals to continue uninterrupted.

GATA4 Transcription Factor

GATA4 is one of the earliest transcription factors expressed in developing cardiac myocytes[76]. Both the ERK and p38 MAPK cascades regulate the activity of the GATA4 transcription factor, by phosphorylation of Ser105[77, 78] and mediates gene-expression alterations during cardiac hypertrophy through interaction with several other transcription factors and/or nuclear co-factors, e.g., p300, serum response factor (SRF), Nkx2.5, MEF2 and NFAT[79]. Moreover, GATA4 appears to mediate anti-apoptotic effects, making it a myocyte survival factor[80, 81].

5: Controlled Induction Of Adaptive Or Maladaptive Hypertrophy

Many animal models are available of human myocardial hypertrophic responses due to pressure overload. Although interspecies differences are known to exist, e.g., calcium handling, action potential, heart rate and MHC α to β ratio, animal studies are necessary to define the essential mechanisms underlying myocardial disease states[82].

One frequently used animal model to study the processes associated with myocardial dysfunction is the monocrotaline (MCT) model for pulmonary hypertension and subsequent RV hypertrophy due to pressure overload[83-86]. MCT is a pyrrolizidine alkaloid derived from *Crotolaria spectabilis* and after a single subcutaneous injection, the MCT is biotransformed in the liver to its active metabolite monocrotaline-pyrrole (MCTP) by the cytochrome P-450 3a system[87, 88]. The MCTP has a very short half-life in aqueous solutions and only through stabilisation and transportation via red blood cells is the MCTP able to reach the pulmonary vascular endothelium[89]. In the lungs, the MCTP injures the vascular endothelium and induces pulmonary vasculitis with a subsequent increase in vascular resistance and pulmonary arterial pressure, resulting in RV hypertrophic remodelling. Alterations characteristic of hypertrophic remodelling were shown at the gene-expression level, e.g., a progressive down-regulation of SERCA2a[83, 84], an increase in MHC β to α[84] expression ratio[83] and increased ANP expression levels[90]. Also a decrease in noradrenalin transporter density as well as activity and a reduction in βAR receptor density was reported[91-93].

With the MCT doses generally used in rats (40-60 mg/kg body weight) the developed hypertrophy progressed to heart failure and death at around day 25-28 after injections, with typically a 1.6 and 2 fold increase in lung and RV weight, respectively. However, in up to 50% of the animals, the hypertrophic response resulted in a compensated phenotype with no signs of heart failure[21, 83, 84, 91, 93-97]. Although compensated or decompensated hypertrophic phenotypes do emerge, they cannot reliably be discerned until around day 25-28. Hence, early events occurring during the development of either phenotype cannot be studied. A recently introduced modification to the standard MCT model does allow for the controlled induction of a compensated or decompensated hypertrophic phenotype by using a dose of either 30 or 80 mg/kg bw, respectively. Both doses lead to an initial phase of compensated RV hypertrophy (day 14-19). From day 19 on, the low dose continues to remain compensated. However, the high dose progresses towards decompensated phenotype and premature death around days 25-28[98]. This model provides the unique opportunity to study, and define, critical factors for the development of either phenotype.

6: Rationale For Genomics Research

One should realize that during the development of stable ventricular hypertrophy or heart failure, the activation of the aforementioned signal transduction routes and subsequent changes in structure and function of the myocardium may occur simultaneously. Moreover, even if the contribution of each of these alterations to the overall phenotype is relatively small, the sum of all known and unknown factors involved will amount to a very complex system indeed. Also, it is a false assumption that a pathological phenotype consists solely of detrimental processes, as is the assumption that a non-pathological phenotype will be driven only by beneficial events. Rather, in both these conditions, adaptive and maladaptive processes will manifest, and, depending on the prevalence of either, the compensated or decompensated phenotype will eventually "prevail". Furthermore, it is unknown whether the drive of detrimental signals initiates the development of a pathological phenotype early during myocardial remodelling or at a late event during hypertrophic remodelling.

The ability to dissect specific molecular and cellular events that distinguish between putative hypertrophic events and events that underlie the development of either maladaptive or adaptive myocardial hypertrophy, will be crucial for our understanding of key signalling cascades involved in processes leading to either of these phenotypes. A reductionsts approach of one, or a few, genes at a time is not sufficient for the analysis of the complex parallel cellular events that characterize the hypertrophic response. Consequently, to achieve these goals there is a pressing need for novel techniques that are capable of accurately assessing a significant portion of cellular events, occurring either at the transcriptome, proteome or metabolome level, in combination with the analysis of patho-physiological parameters.

7: Large Scale Screening Methods

The large scale analysis of the genome and transcriptome of a given tissue in combination with functional data constitutes the field of functional genomics. The DNA in the nucleus of each cell contains a full set of information for the estimated 32.000 - 38000 genes of a typical mammalian genome. However, only a subset of these genes is expressed in each cell under a given condition at a certain time, which determines the unique properties of each cell type. The transcriptome is the full collection of activated genes, mRNAs and transcripts present in a cell. It is thought that the cardio-vascular system expresses approximately 70% of the total number of genes[99].

Gene Expression Alterations

A series of interdependent events regulate the processes that are needed from the initial signal to change gene-expression, commence protein synthesis and the emergence of a fully functional protein[100]. Transcription regulation of protein-coding genes depends on a complex interplay between gene-specific regulators, signal-transduction pathways, general transcription factors, RNA polymerase II (RNAPII) and co-regulatory protein complexes as well as chromatin modification[101, 102]. This regulation of chromatin structure has serious implications in gene-expression modulation, i.e., a gene and its regulatory elements may no longer be regarded as a stand alone unit. Rather, it may be viewed as part of a larger context, in which neighbouring genes influence each others expression[103]. This complex control of gene-expression regulation allows for dynamic cellular responses to changes in

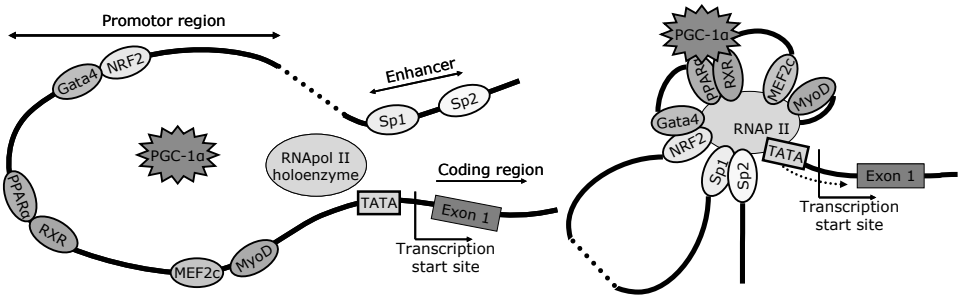

▲**Figure 5: Transcription-initiation complex.** Schematic representation of the formation and activation of the transcription-initiation complex of a gene. Left: The DNA-binding domains of activated transcription factors associate with their corresponding short specific DNA motifs within the promotor sequence. Co-activators, e.g., PGC1a, may mediate and enhance the activity of the transcription factors via protein-protein interactions. Right: Binding of the activation domains of the transcriptions factors with the RNApolII complex stabilizes the initiation complex and facilitates its positioning on the TATA box.

environmental conditions and/or developmental alterations, not only by acting as an on/off switch, but also by enabling increases and decreases in gene-expression to occur.
Gene-expression alterations can often be considered a *primum mobile*, i.e., both the origin and the effector of a response, in which the information stored in the genome is interpreted and employed to provide the means required for an appropriate response. Monitoring gene-expression alterations may thus provide insights into cellular responses to specific patho-physiological stimuli.

Formation And Activation Of The Transcription Initiation Complex
The whole process of transcription can be divided into three steps, i.e., initiation, elongation and termination, with transcription initiation by the activation of the RNAPII holoenzyme complex being the most important control point in gene-expression. This 2MDa holoenzyme is a complex consisting of at least 50 proteins and is thought to exist in a preassembled state in the nuclear compartment. Central to the function of this complex are the TATA-binding protein (TBP), several general transcription factors (TF) and the RNAPII with its C-terminal domain (CTD).
Transcription initiation of a gene will only commence when a specific set of signals reach, and activate, the appropriate set of transcription factors that are needed. The DNA binding domain of these transcriptions factors will then associate with short specific DNA motifs in the gene's enhancer and promotor regions. In general, such regulatory regions contain binding motifs for several TF, allowing multiple signal transduction cascades to activate one single gene. Interaction of the TF's activation domains with the holoenzyme complex in concert with alterations in the DNA condensation status, and looping of the DNA strands, facilitates the positioning of the RNAPII complex on the transcription start site (Figure 5). The RNAPII reads the DNA sequence when moving along the DNA sense strand from the 3'-end to the 5'-end, and builds the mRNA strand according to normal Watson-Crick base-pairing principles, with the exception that the thymidine base is substituted by uracil in the mRNA strand. The finished mRNA strand is bound by specific proteins that facilitate its translocation from the nuclear compartment to the cytosol, where it is translated and further processed to yield a fully functioning protein.

Micro-Array Methodology
Methods to determine gene-expression have been available for over two decades, e.g., polymerase chain reaction introduced by Kary Mullis in 1985[104] and northern blotting by E.M. Southern in the 1970s. Although many assays may be run in parallel, these techniques basically process one gene at a time. It was in 1995 that a

large scale gene-expression method was described by Velculescu *et al*. termed Serial analysis of gene-expression (SAGE)[105], that allowed the quantitative and simultaneous analysis of a large number of transcripts.

Micro-arrays also have the potential to simultaneously perform transcription analysis on thousands of genes. A micro-array essentially consists of a glass slide, which acts as a solid support surface material, upon which gene-specific DNA sequence strands, either DNA, cDNA, or oligonucleotides, have been accurately deposited as distinct spots in a well defined grid, using high speed robotics. Three types of arrays can be discerned, i.e., those used in comparative genome hybridization (CGH) to assay genomic gains and losses[106], SNP-chips that are able to detect single nucleotide polymorphisms[107] and expression arrays that can be used to assess global transcriptome profiles. The latter are used to compare expression-profiles between phenotypes resulting from different experimental conditions[108].

The first micro-array experiments were performed by Schena *et al*. at Stanford University in 1995[108], using arrays representing 45 Arabidopsis genes. From then on, the micro-array technology has undergone rapid development, leading to the contemporary arrays, with the potential to perform genome-wide transcription analyses, in a wide variety of biological samples. Arrays are available for several species, including *Arabidopsis thaliana*[109], *Saccharomyces cerevisiae*[110], *Mus Musculus*[111], *Rattus Norvegicus*[112] and *Homo Sapiens*[113].

Simple Steps To Perform A Micro-Array Experiment

In the Nature Genetics supplement issue of 1999, a standard nomenclature system was introduced referring to the hybridization pairs which interact during hybridization[114]. The definitions are based upon the principle that a micro-array is a reversed dot-blot, in which the probe, with a known sequence, is essentially used to identify and quantify the target. Conversely, in a standard micro-array setup, the probe is the gene-specific DNA sequence which is immobilized on the micro-array surface and the target is the labelled cDNA strand in the hybridization mixture. Micro-arrays intrinsically exploit the ability of the probe and target strands to form a sequence specific DNA-DNA hybrid complex by standard Watson-Crick base pairing.

The laboratory aspects of performing micro-array experiments consists of a set of relatively simple and straightforward steps (Figure 6). First, experimental conditions of interest need to be defined, appropriate samples collected and handled to allow the extraction of high quality total RNA or mRNA. Per array, the expression levels of each gene can be compared for two experimental conditions. For each experimental condition the mRNA pool needs to be reverse transcribed into complementary DNA (cDNA) strands, with incorporation of the standard dATP, dCTP, dGTP and dTTP

nucleotides as well as an aminoallyl-modified dUTP nucleotide (aa-dUTP). To allow the expression levels of each gene per sample to be differentiated within each array in subsequent steps, each of the two conditions is labelled with a different fluorescent tag at the aa-dUTP, e.g., Fluorolink Cy3 or Cy5 mono-functional dyes. The two samples can than be mixed and applied onto the micro-array for hybridization, without loss of information concerning the expression levels of the genes in the separate conditions. The labelled cDNA stands, e.g., the targets, bind to the gene-specific, immobilized, probe strands on the array surface. After a series of washing steps to remove all non-specific binding from the arrays, the total amount of

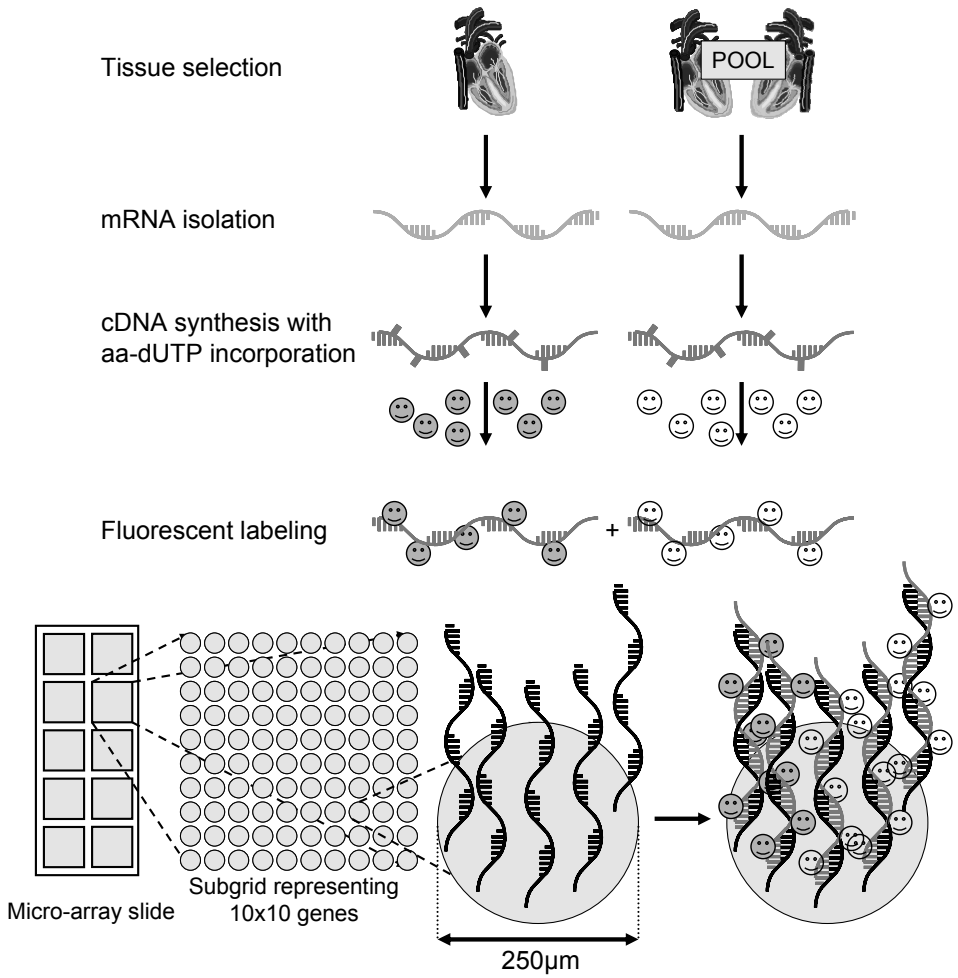

▲Figure 6: Micro-array labeling and hybridization. See accompanying text in section *Simple Steps To Perform A Micro-Array Experiment.*

specifically bound cDNA at each spot can be measured by confocal laser scanning microscopy for both fluorescent tags. A micro-array experiments thus yields two individual images representing the spot abundance intensities for each fluorescent tag used. Specialized image analysis software is able to determine and extract the total fluorescent signal intensity per spot. A fundamental assumption is that the measured signal intensity is proportional to the original mRNA abundance in the biological sample, which allows the comparison of gene-expression levels between different biological samples by comparing the level of fluorescent intensities per gene per array.

Figure 7A illustrates a typical example of the two separate channel images in addition to the combined overlay image resulting from a single array experiment where the control and treatment group were labelled with Cy5 and Cy3, respectively. These images show circular spots with homogenous intensity and low background signals. The colours in the Cy5-Cy3-overlay image can be easily interpreted. A highly expressed gene results in a spots with high colour intensity, and conversely, low expression genes result in low intensity spots, while genes that are not expressed at all, yield black spots. Green spots are indicative for genes that have increased expression levels in the treatment sample relative to the control situation, i.e., Cy3 > Cy5, while the red spots, represent genes with lower expression levels in the treatment sample, i.e., Cy3 < Cy5. Yellow spots represent genes with similar expression levels in both samples, i.e., the Cy3 and Cy5 spot intensities are equal.

A scatter plot is a simple way to visualize the gene-expression differences between the two biological samples used in each array experiment. It is compiled by plotting the expression ratio for each individual spot against a measure for the total spot intensity, e.g., $\log_2(Cy3/Cy5)$ vs. $\log_{10}(Cy3*Cy5)$ or $\log_2(Cy3+Cy5 / 2)$. A whole spectrum of ratios can be appreciated from figure 7B, most of which can be found between the +1 and -1 ratio boundaries. The lower intensities display a higher variation in ratios due to detection limitations for the lower gene-expression levels, while at the high intensity levels variation is relatively small. This means that one cannot simply apply a standard ratio cut-off to determine differential expression, which may prove to be biased at low and too conservative at high expression levels. Scatter plots are also generally used to examine the arrays for potential artefacts, such as systemic intensity-dependent effects, which are characterized by a structural deviation from the Y=0 axis of the spots in the plot at the lower intensity range. When such artefacts are observed, specific within-array transformation algorithms are available to correct for these artefacts in order to avoid biased results in the subsequent analysis steps, which are generally called within-array transformations. Between-array transformations, standardization and normalization steps are

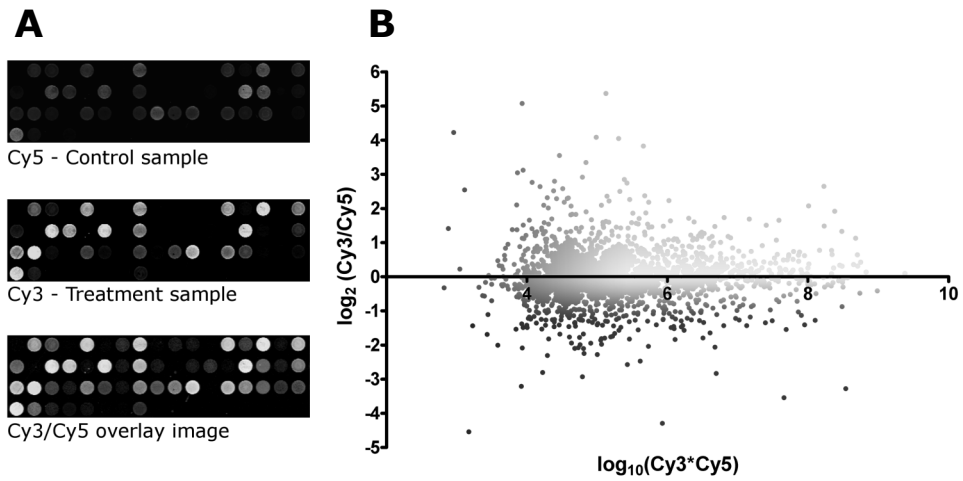

▲Figure 7: Array channel images and scatter plot. See accompanying text in section *Simple Steps To Perform A Micro-Array Experiment.*

subsequently needed to allow all separate arrays to be incorporated into a single dataset and to be reliably analysed [115-121].

Experiment Design

In the simple experimental setup described in the previous paragraph of a direct comparison on one slide of a control sample vs. a treatment sample, a systemic error may be introduced due to the different excitation-emission properties of the Cy3 and Cy5 fluorescent dyes. These errors appear as systemic differences in the Cy3 and Cy5 signal intensities, leading to biased results, even when the two different channels originated from an identical source sample, i.e., a self vs. self experiment. These biases may be corrected for by imposing specific transformation and/or normalization procedures, though whether these manipulation are able to completely correct for these dye-biases remains questionable. This dye-bias may also be compensated for by performing dye-swap experiments, in which the control and treatment samples on the first array are labelled using the Cy5 and Cy3 dyes, respectively, while on the second array, the labels are switched.

The experiment described in the previous section of a direct comparison between samples, lacks the ability to efficiently compare gene-expression between samples representing more than two biological phenotypes. To handle the comparison for multiple biological samples two alternative approaches are available, i.e., experimental designs that employ a common reference or those that use a loop design, both of which have advantages as well as disadvantages. Figure 8 displays

characteristics for both the loop and reference designs. At a first glance, if enough sample material is available, the loop design appears to be the best choice. However, when more than three samples are to be compared, the loop designs may become very complex, making deconvolution of the data structure into comprehensible results complicated. Also, if one of the arrays in the loop is of dubious quality, it may seriously affect the accuracy of the whole experiment.

For experimental designs that employ a common reference, high quality RNA of standardized composition may be obtained commercially, though it is costly. This is an RNA pool that represents all of the target organisms' genes, yielding a signal in almost all of the spots on the array. Conversely, one can prepare a custom pool of RNA from various tissue sources, both physiological and pathological in origin, preferably related to the samples of interest. This approach ensures that at least all targets of potential biological interest are present in the reference sample. In this experimental setup, all subsequent samples are hybridized against an aliquot of the reference sample. A disadvantage of the reference design is that one needs a large pool of high-quality RNA to ensure all samples of interest can be included in the experiment. Dye-swaps may be incorporated to reduce the average variance in half, though total cost of the experiments will then at least double. Also, half of all resources are allocated to this reference, thus accounting for half of all expenses. However, samples can easily be replaced or added without problems, making it a very flexible setup to use.

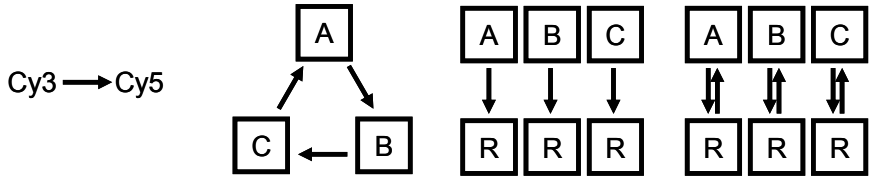

	Loop	Reference	Reference + dye swap
Average variance	0.67	2	1
Slides	3	3	6
Aliquots per sample [A=B=C]	2	1 + 3x REF	2 + 6x REF
Distance between samples in arrays	1	2	2

▲Figure 8: Experiment design. See accompanying text in section *Experiment Design*. Adapted from[121].

Considerations On Data Mining

During the last five years, the procedures to analyse gene-expression data derived from micro-array studies have evolved profoundly. The relative ease and large scale of data generation calls for standardized methods that guide unbiased data mining and interpretation. However, the collective contribution from many research fields, e.g., biology, statistics, bioinformatics and software engineering, have yet to result in a "one size fits all" consensus to handle and interpret genome-wide expression data. Nevertheless, some concepts appear to have emerged.

Comparing Two Conditions

Several approaches are available when comparing two conditions. Initially, studies used an arbitrary fold-change cut-off value between group averages as a criterion for differential expression. This, however, cannot be considered a statistical test, i.e., it does not take into account the gene-specific variances within or between groups. T-tests do estimate group variances, but due to the low number of replicates that are usually available in expression array studies, the t-test may have low power. Also, this low number of samples may lead to small variance estimates by chance alone, which could lead to high t-statistic values, even when the fold change between the groups is small. Estimating the error variance by pooling variances from across all genes that were analysed is possible, however under the assumption that the individual gene variances are homogenous among the genes. The resulting statistic is essentially reduced to a fold-change test that does not estimate the individual gene variances. Other approaches using modifications to the normal t-test remove some of the problems of the original t-test and are therefore more reliable, e.g., significance analysis of microarrays (SAM) by adding a small constant to the denominator[122] and the regularized t-test by combining a weighted average of the gene-specific and global average variance estimates[123].

Comparing More Than Two Conditions

When comparing more than two groups, the F-tests contained within the analysis of variance (Anova) statistical framework may provide the necessary method[124-126], in which the spot intensities are used instead of calculated ratios between the channels of the arrays. Of note is that the Anova tests can also be applied when comparing two groups. These F-tests are generalizations of the t-test that determine any pattern of differential expression between more than two groups by comparing the within- and between-group variance estimates. In parallel to the different variations in t-tests, several F-test are available to choose from[124, 126]. The classic F-test, i.e., generalization of the t-test, operates on a gene-by-gene basis for variance estimates

and is likely to result in low statistical power. F-tests that assume a common error variance across genes and use a pooled error variance (F3), or that are analogue to the regularized t-test (F2), are able to incorporate information from across genes to estimate the error variance. However, taking the simple average of variance estimates may lead to biased results and is hard to justify. The Fs test compiles estimators of variance depending on the variability of the individual gene variances, without making any prior assumptions about their distribution. If a homogenous distribution is present, i.e., individual variance estimates are similar, a pooled estimate is used. However, when the individual variances are dissimilar, indicating heterogeneity, more weight is attributed to the gene-specific variances.

It is important to keep in mind that in principle micro-array data do not follow the standard Gaussian null-distribution and that non-parametric approaches have preference. Permutation analysis allows for empirical estimation of the null distribution of the data-set. It is widely applicable due to its flexibility, but a large number of permutations needs to be performed for reliable results.

Gene-Ontology Analyses

A typical micro-array experiment series may result in the identification of a few to several hundreds of differentially expressed genes. Although many tools are available to assist the researcher[127-131], interpreting the biological significance of these findings remains the most challenging aspect of a micro-array experiment. In general, these tools assess whether predefined classes of genes are more present or enriched in the list of significantly regulated genes than is to be expected on the basis of chance alone. The gene-ontology project (www.geneontology.org) provides a classification for gene products into three categories, i.e., molecular function, cellular component and biological function. Other widely used classifications are the KEGG[132] and GenMapp[133] pathways.

The power of these tools lies in the unbiased analysis of any large number of significantly regulated genes for common features, e.g., muscle development, MAPK signalling, cell-cycle activity. Also, compared to manual Pubmed literature searches, these automated tools may drastically cut down the total time needed for the interpretation of a large sets of data. The return output lists a series of categories with associated genes and p-values for over-representation. Several statistical methods are used to calculate the p-values, e.g., Fisher exact test[134-137] and χ^2 test[138, 139].

Proteomics

In parallel to the transcriptome, the proteome represents the total protein complement of a cell at a given time and condition. As a direct result of patho-

physiological changes, the proteome may be subject to post-transcriptional modifications (PTM), e.g., conformation changes, proteolytic cleavage, acetylation, phoshorylation, oxidation, nitrosylation and glycosylation, which may affect both the intrinsic iso-electric point (pI) and mass (Mr) of a protein.

The application of two dimensional gel electrophoresis (2DGE) in mammals was pioneered by J. Klose *et al*.[140, 141]. Although protein micro-arrays are available[142, 143], 2DGE remains the most used method for the separation of complex protein mixtures containing a large number of polypeptides in a single experiment. An advantage of the 2DGE approach is the ability to detect PTM alterations on both the pI and/or Mr levels. Proteins are separated in the first dimension on the basis of their pI in an isoelectric focussing (IEF) step and in the second dimension on the basis of their Mr in a SDS-PAGE step. Increased resolution in the first dimension can be gained by using several more focussed pH ranges in parallel IEF sessions of the same sample of interest, while the mass separation can be modulated by different gradations in acrylamide/duracryl composition of the SDS-PAGE gel. Further augmentation of the specificity of 2DGE may be achieved by using specific subcellular fractions, e.g, mitochondria, SR, nuclear envelope, myofilaments or the cytoplasm, though only the soluble fractions of these compartments can be separated using the 2DGE technique.

After visualization by silver, coomassie or sypro ruby staining, individual PTM of proteins will appear as separate spots on the SDS-PAGE gel. Computer assisted matching of corresponding protein spots between individual gels is generally performed with specific software, e.g., PDQuest®, which can also determine the spot intensities for each spot on each SDS-PAGE gel and subsequently use these intensities to test for significant differences in protein-expression levels between groups. The identity of significantly regulated proteins needs to be determined with matrix-assisted laser desorption/ionization time-of-flight (MALDI-TOF) mass spectrometry[144]. To do this, the spot is physically excised from the SDS-PAGE gel and subjected to trypsin digestion to yield polypeptide fragments from the native protein. After purification of these fragments they are embedded into a crystaline layer of MALDI-matrix on a solid support surface, i.e. the MALDI-chip. Documentation and data-base searches, cross-referencing the fragment-ion-mass fingerprints of the specific individual peptides fragments may lead to the identification of the protein in question.

Aim And Outline Of This Thesis

The general aim of this thesis was to explore alterations on either the transcriptome or proteome level during RV remodelling due to pressure overload for events that are associated with the development of either an adaptive or maladaptive hypertrophic phenotype. Knowledge of the composition and timing of these critical events may lead to a more thorough understanding of the pathophysiological processes involved in the development of either hypertrophic phenotype. In addition, assessment of gene-expression that specifically correlate with either adaptive or maladaptive remodelling could potentially lead to bio-marker discovery and to improved diagnosis of the pathological phenotype in patients.
The large-scale, high-throughput analyses techniques used to measure alterations on either the transcriptome or proteome level were expression micro-arrays and 2DGE, respectively. Both of these methods allow for the analysis of thousands of mRNA transcripts or proteins simultaneous.

To achieve the goals described above, an animal model was needed that allows for the controlled induction of either the adaptive or maladaptive phenotype well before phenotypical differences become apparent. This model is introduced in **Chapter 2**. Gene-expression profiles from right-ventricular tissue were compared between animals developing adaptive or maladaptive hypertrophy and control animals at 14 days after the imposition of pressure overload.
In **Chapter 3** a time-course experiment is presented describing gene-expression alterations during adaptive and maladaptive ventricular remodelling at 10, 19 and 25 days after the imposition of pressure overload.
In parallel to the gene-expression analyses, RV myocardial protein-expression profiles obtained from animals at 10 days after MCT injections were compared using 2-dimensional gel-electrophoresis in **Chapter 4**.
In **Chapter 5** the experimental data presented in this thesis are placed in a broader perspective and discussed in relation to recent publications concerning adaptive and maladaptive hypertrophy.

As in the case of left ventricular (LV) hypertrophy, the concept of compensated or adaptive hypertrophy in aortic stenosis (AS) has been questioned. Kupari *et al*. (Eur Heart J. 2005 Sep;26(17):1790-6), stated that: ”LV hypertrophy may be maladaptive rather than beneficial in AS in man”. The evidence provided by Kupari *et al*. are discussed in **Chapter 6**.

Reference List

(1) Bers DM. Cardiac excitation-contraction coupling. *Nature* 2002 January 10;415(6868):198-205.

(2) Bassani JW, Bassani RA, Bers DM. Relaxation in rabbit and rat cardiac cells: species-dependent differences in cellular mechanisms. *J Physiol* 1994 April 15;476(2):279-93.

(3) Dorn GW, II, Molkentin JD. Manipulating Cardiac Contractility in Heart Failure: Data From Mice and Men. *Circulation* 2004 January 20;109(2):150-8.

(4) Lohse MJ, Engelhardt S, Eschenhagen T. What Is the Role of {beta}-Adrenergic Signaling in Heart Failure? *Circ Res* 2003 November 14;93(10):896-906.

(5) Carabello BA. Concentric versus eccentric remodeling. *Journal of Cardiac Failure* 2002 December;8(6, Part 2):S258-S263.

(6) Dorn GW, II, Robbins J, Sugden PH. Phenotyping Hypertrophy: Eschew Obfuscation. *Circ Res* 2003 June 13;92(11):1171-5.

(7) Grossman W, Jones D, McLaurin LP. Wall stress and patterns of hypertrophy in the human left ventricle. *J Clin Invest* 1975 July;56(1):56-64.

(8) Morgagni JB. The seats and causes of diseases investigated by anatomy (translated by B. Alexander). 1769. London, UK.

(9) Aran FA. Practical manual of the diseases of the heart and great vessels (translated by W. A. Harris). 1843. Philadelphia, PA, Barrington and Haswell.

(10) Virchow R. Cellular pathology (translated by F. Chance). 1860. London, UK.

(11) Morisco C, Sadoshima J, Trimarco B, Arora R, Vatner DE, Vatner SF. Is treating cardiac hypertrophy salutary or detrimental: the two faces of Janus. *Am J Physiol Heart Circ Physiol* 2003 April 1;284(4): H1043.

(12) Frey N, Olson EN. Cardiac Hypertrophy: The Good, the Bad, and the Ugly. *Annu Rev Physiol* 2003 January 1;65(1):45.

(13) van Empel VPM, De Windt LJ. Myocyte hypertrophy and apoptosis: a balancing act. *Cardiovascular Research* 2004 August 15;63(3):487-99.

(14) Roger VL, Weston SA, Redfield MM, Hellermann-Homan JP, Killian J, Yawn BP, Jacobsen SJ. Trends in Heart Failure Incidence and Survival in a Community-Based Population. *JAMA* 2004 July 21;292(3):344-50.

(15) Levy D, Kenchaiah S, Larson MG, Benjamin EJ, Kupka MJ, Ho KKL, Murabito JM, Vasan RS. Long-Term Trends in the Incidence of and Survival with Heart Failure. *N Engl J Med* 2002 October 31;347 (18):1397-402.

(16) Mosterd A, Hoes AW, de Bruyne MC, Deckers JW, Linker DT, Hofman A, Grobbee DE. Prevalence of heart failure and left ventricular dysfunction in the general population; The Rotterdam Study. *Eur Heart J* 1999 March 2;20(6):447-55.

(17) Coronel R, de Groot JR, van Lieshout JJ. Defining heart failure. *Cardiovascular Research* 2001 June;50(3):419-22.

(18) Follath F. Nonischemic heart failure: epidemiology, pathophysiology, and progression of disease. *J Cardiovasc Pharmacol* 1999 June;33 Suppl 3:S31-S35.

(19) Franz WM, Muller OJ, Katus HA. Cardiomyopathies: from genetics to the prospect of treatment. *The Lancet* 2001 November 10;358(9293):1627-37.

(20) Giles TD, Chatterjee K, Cohn JN, Colucci WS, Feldman AM, Ferrans VJ, Roberts R. Definition, classification, and staging of the adult cardiomyopathies: A proposal for revision. *Journal of Cardiac Failure* 2004 February;10(1):6-8.

(21) Brunner F, Wolkart G, Haleen S. Defective Intracellular Calcium Handling in Monocrotaline-Induced Right Ventricular Hypertrophy: Protective Effect of Long-Term Endothelin-A Receptor Blockade with 2-Benzo[1,3]dioxol-5-yl-3-benzyl-4-(4-methoxy-phenyl-)- 4-oxobut-2-enoate-sodium (PD 155080). *J Pharmacol Exp Ther* 2002 February 1;300(2):442-9.

(22) Wang D, Oparil S, Feng JA, Li P, Perry G, Chen LB, Dai M, John SWM, Chen YF. Effects of Pressure Overload on Extracellular Matrix Expression in the Heart of the Atrial Natriuretic Peptide-Null Mouse. *Hypertension* 2003 May 19;01.

(23) Wong K, Boheler KR, Petrou M, Yacoub MH . Pharmacological Modulation of Pressure-Overload Cardiac Hypertrophy : Changes in Ventricular Function, Extracellular Matrix, and Gene Expression. *Circulation* 1997 October 7;96(7):2239-46.

(24) Casademont J, Miro O. Electron transport chain defects in heart failure. *Heart Fail Rev* 2002 April;7(2):131-9.

(25) Huss JM, Kelly DP. Mitochondrial energy metabolism in heart failure: a question of balance. *J Clin Invest* 2005 March 1;115(3):547-55.

(26) Weiss JN, Korge P, Honda HM, Ping P. Role of the Mitochondrial Permeability Transition in Myocardial Disease. *Circ Res* 2003 August 22;93(4):292-301.

(27) Chien KR, Knowlton KU, Zhu H, Chien S. Regulation of cardiac gene expression during myocardial growth and hypertrophy: molecular studies of an adaptive physiologic response. *FASEB J* 1991 December 1;5(15):3037-46.

(28) Bar MH, Kreuzer J, Cojoc A, Jahn L. Upregulation of embryonic transcription factors in right ventricular hypertrophy. *Basic Res Cardiol* 2003 September;98(5):285-94.

(29) Adachi S, Ito H, Ohta Y, Tanaka M, Ishiyama S, Nagata M, Toyozaki T, Hirata Y, Marumo F, Hiroe M. Distribution of mRNAs for natriuretic peptides in RV hypertrophy after pulmonary arterial banding. *Am J Physiol Heart Circ Physiol* 1995 January 1;268(1):H162-H169.

(30) Izumo S, Lompre AM, Matsuoka R, Koren G , Schwartz K, Nadal-Ginard B, Mahdavi V. Myosin heavy chain messenger RNA and protein isoform transitions during cardiac hypertrophy. Interaction between hemodynamic and thyroid hormone-induced signals. *J Clin Invest* 1987 March;79(3):970-7.

(31) Lompre AM, Schwartz K, d'Albis A, Lacombe G, Van Thiem N, Swynghedauw B. Myosin isoenzyme redistribution in chronic heart overload. *Nature* 1979 November 1;282(5734):105-7.

(32) Nagai R, Zarain-Herzberg A, Brandl CJ, Fujii J, Tada M, MacLennan DH, Alpert NR, Periasamy M. Regulation of Myocardial Ca2+-ATPase and Phospholamban mRNA Expression in Response to Pressure Overload and Thyroid Hormone. *PNAS* 1989 April 15;86(8):2966-70.

(33) Packer M. Neurohormonal interactions and adaptations in congestive heart failure. *Circulation* 1988 April;77(4):721-30.

(34) Stanley WC, Recchia FA, Lopaschuk GD. Myocardial Substrate Metabolism in the Normal and Failing Heart. *Physiol Rev* 2005 July 1;85(3):1093-129.

(35) Bersin RM, Wolfe C, Kwasman M, Lau D, Klinski C, Tanaka K, Khorrami P, Henderson GN, de Marco T, Chatterjee K. Improved hemodynamic function and mechanical efficiency in congestive heart failure with sodium dichloroacetate. *Journal of the American College of Cardiology* 1994 June 1;23(7):1617-24.

(36) Chandler MP, Stanley WC, Morita H, Suzuki G, Roth BA, Blackburn B, Wolff A, Sabbah HN. Short-Term Treatment With Ranolazine Improves Mechanical Efficiency in Dogs With Chronic Heart Failure. *Circ Res* 2002 August 23;91(4):278-80.

(37) Stanley WC, Chandler MP. Energy Metabolism in the Normal and Failing Heart: Potential for Therapeutic Interventions. *Heart Failure Reviews* 2002 April;7(2):115-30.

(38) Lehman JJ, Kelly DP. Gene regulatory mechanisms governing energy metabolism during cardiac hypertrophic growth. *Heart Fail Rev* 2002 April;7(2):175-85.

(39) Sack MN, Disch DL, Rockman HA, Kelly DP . A role for Sp and nuclear receptor transcription factors in a cardiac hypertrophic growtháprogram. *PNAS* 1997 June 10;94(12):6438-43.

(40) Garnier A, Fortin D, Delomenie C, Momken I, Veksler V, Ventura-Clapier R. Depressed mitochondrial transcription factors and oxidative capacity in rat failing cardiac and skeletal muscles. *J Physiol (Lond)* 2003 September 1;551(2):491-501.

(41) Cook SA, Matsui T, Li L, Rosenzweig A. Transcriptional Effects of Chronic Akt Activation in the Heart. *J Biol Chem* 2002 June 14;277(25):22528.

(42) Wang J, Silva JP, Gustafsson CM, Rustin P, Larsson NG. Increased in vivo apoptosis in cells lacking mitochondrial DNA gene expression. *PNAS* 2001 March 27;98(7):4038-43.

(43) Hansson A, Hance N, Dufour E, Rantanen A, Hultenby K, Clayton DA, Wibom R, Larsson NG. A switch in metabolism precedes increased mitochondrial biogenesis in respiratory chain-deficient mouse hearts. *PNAS* 2004 March 2;101(9):3136-41.

(44) Tavi P, Hansson A, Zhang SJ, Larsson NG , Westerblad H. Abnormal Ca2+ release and catecholamine-induced arrhythmias in mitochondrial cardiomyopathy. *Hum Mol Genet* 2005 April 15;14(8):1069-76.

(45) Ikeuchi M, Matsusaka H, Kang D, Matsushima S, Ide T, Kubota T, Fujiwara T, Hamasaki N, Takeshita A, Sunagawa K, Tsutsui H. Overexpression of Mitochondrial Transcription Factor A Ameliorates Mitochondrial Deficiencies and Cardiac Failure After Myocardial Infarction. *Circulation* 2005 August 2;112(5):683-90.

(46) Capetanaki Y. Desmin Cytoskeleton: A Potential Regulator of Muscle Mitochondrial Behavior and Function. *Trends in Cardiovascular Medicine* 2002 November;12(8):339-48.

(47) Condorelli G, Morisco C, Stassi G, Notte A, Farina F, Sgaramella G, de Rienzo A, Roncarati R, Trimarco B, Lembo G. Increased Cardiomyocyte Apoptosis and Changes in Proapoptotic and Antiapoptotic Genes bax and bcl-2 During Left Ventricular Adaptations to Chronic Pressure Overload in the Rat. *Circulation* 1999 June 15;99(23):3071-8.

(48) Galiuto L, Lotrionte M, Crea F, Anselmi A, Biondi-Zoccai GGL, De Giorgio F, Baldi A, Baldi F, Possati G, Gaudino M, Vetrovec GW, Abbate A. Impaired coronary and myocardial flow in severe aortic stenosis is associated with invreased apoptosis: a transthoracic Doppler and myocardial contrast echocardiography study. *Heart* 2005 May 20;hrt.

(49) Crow MT, Mani K, Nam YJ, Kitsis RN. The Mitochondrial Death Pathway and Cardiac Myocyte Apoptosis. *Circ Res* 2004 November 12;95(10):957-70.

(50) Papa S. Mitochondrial oxidative phosphorylation changes in the life span. Molecular aspects and physiopathological implications. *Biochim Biophys Acta* 1996 September 12;1276(2):87-105.

(51) Siwik DA, Tzortzis JD, Pimental DR, Chang DLF, Pagano PJ, Singh K, Sawyer DB, Colucci WS. Inhibition of Copper-Zinc Superoxide Dismutase Induces Cell Growth, Hypertrophic Phenotype, and Apoptosis in Neonatal Rat Cardiac Myocytes In Vitro. *Circ Res* 1999 July 23;85(2):147-53.

(52) Rosenberg P. Mitochondrial dysfunction and heart disease. *Mitochondrion* 2004 September;4(5-6):621-8.

(53) Deschamps AM, Spinale FG. Disruptions and detours in the myocardial matrix highway and heart failure. *Curr Heart Fail Rep* 2005 March;2(1):10-7.

(54) D'Armiento J. Matrix Metalloproteinase Disruption of the Extracellular Matrix and Cardiac Dysfunction. *Trends in Cardiovascular Medicine* 2002 April;12(3):97-101.

(55) Jane-Lise S, Corda S, Chassagne C, Rappaport L. The Extracellular Matrix and the Cytoskeleton in Heart Hypertrophy and Failure. *Heart Failure Reviews* 2000 October;5(3):239-50.

(56) Polyakova V, Hein S, Kostin S, Ziegelhoeffer T, Schaper J. Matrix metalloproteinases and their tissue inhibitors in pressure-overloaded human myocardium during heart failure progression. *Journal of the American College of Cardiology* 2004 October 19;44(8):1609-18.

(57) Brower GL, Chancey AL, Thanigaraj S, Matsubara BB, Janicki JS. Cause and effect relationship between myocardial mast cell number and matrix metalloproteinase activity. *Am J Physiol Heart Circ Physiol* 2002 August 1;283(2):H518-H525.

(58) Fedak PWM, Verma S, Weisel RD, Li RK. Cardiac remodeling and failure: From molecules to man (Part II). *Cardiovascular Pathology* 2005;14(2):49-60.

(59) Ju H, Dixon IM. Extracellular matrix and cardiovascular diseases. *Can J Cardiol* 1996 December;12(12):1259-67.

(60) Nagatomo Y, Carabello BA, Coker ML, McDermott PJ, Nemoto S, Hamawaki M, Spinale FG. Differential effects of pressure or volume overload on myocardial MMP levels and inhibitory control . *American Journal of Physiology - Heart and Circulatory Physiology* 2000;278(1 47-1):H151-H161.

(61) Hara M, Ono K, Hwang MW, Iwasaki A, Okada M, Nakatani K, Sasayama S, Matsumori A. Evidence for a Role of Mast Cells in the Evolution to Congestive Heart Failure. *J Exp Med* 2002 February 4;195(3):375-81.

(62) Peterson JT, Hallak H, Johnson L, Li H, O'Brien PM, Sliskovic DR, Bocan TMA, Coker ML, Etoh T, Spinale FG. Matrix Metalloproteinase Inhibition Attenuates Left Ventricular Remodeling and Dysfunction in a Rat Model of Progressive Heart Failure. *Circulation* 2001 May 8;103(18):2303-9.

(63) Hwang JJ, Dzau VJ, Liew CC. Genomics and the pathophysiology of heart failure. *Curr Cardiol Rep* 2001 May;3(3):198-207.

(64) Dorn GW, II, Force T. Protein kinase cascades in the regulation of cardiac hypertrophy. *J Clin Invest* 2005 March 1;115(3):527-37.

(65) Baines CP, Molkentin JD. STRESS signaling pathways that modulate cardiac myocyte apoptosis. *Journal of Molecular and Cellular Cardiology* 2005 January;38(1):47-62.

(66) Ravingerova T, Barancik M, Strniskova M. Mitogen-activated protein kinases: a new therapeutic target in cardiac pathology. *Mol Cell Biochem* 2003 May;247(1-2):127-38.

(67) Molkentin JD. Calcineurin and beyond: cardiac hypertrophic signaling. *Circ Res* 2000 October 27;87(9):731-8.

(68) Wilkins BJ, Molkentin JD. Calcium-calcineurin signaling in the regulation of cardiac hypertrophy. *Biochemical and Biophysical Research Communications* 2004 October 1;322(4):1178-91.

(69) Condorelli G, Drusco A, Stassi G, Bellacosa A, Roncarati R, Iaccarino G, Russo MA, Gu Y, Dalton N, Chung C, Latronico MVG, Napoli C, Sadoshima J, Croce CM, Ross J, Jr. Akt induces enhanced myocardial contractility and cell size in vivo in transgenic mice. *PNAS* 2002 September 17;99(19):12333-8.

(70) Shioi T, Kang PM, Douglas PS, Hampe J, Yballe CM, Lawitts J, Cantley LC, Izumo S. The conserved phosphoinositide 3-kinase pathway determines heart size in mice. *EMBO J* 2000 June 1;19(11):2537-48.

(71) Matsui T, Li L, Wu JC, Cook SA, Nagoshi T, Picard MH, Liao R, Rosenzweig A. Phenotypic Spectrum Caused by Transgenic Overexpression of Activated Akt in the Heart. *J Biol Chem* 2002 June 14;277(25):22896-901.

(72) Hardt SE, Sadoshima J. Glycogen Synthase Kinase-3{beta}: A Novel Regulator of Cardiac Hypertrophy and Development. *Circ Res* 2002 May 31;90(10):1055-63.

(73) Badorff C, Ruetten H, Mueller S, Stahmer M, Gehring D, Jung F, Ihling C, Zeiher AM, Dimmeler S. Fas receptor signaling inhibits glycogen synthase kinase 3{beta} and induces cardiac hypertrophy following pressure overload. *J Clin Invest* 2002 February 1;109(3):373-81.

(74) Antos CL, McKinsey TA, Frey N, Kutschke W, McAnally J, Shelton JM, Richardson JA, Hill JA, Olson EN. Activated glycogen synthase-3beta suppresses cardiac hypertrophy in vivo. *PNAS* 2002 January 22;99(2):907-12.

(75) Haq S, Choukroun G, Kang ZB, Ranu H, Matsui T, Rosenzweig A, Molkentin JD, Alessandrini A, Woodgett J, Hajjar R, Michael A, Force T. Glycogen Synthase Kinase-3{beta} Is a Negative Regulator of Cardiomyocyte Hypertrophy. *J Cell Biol* 2000 October 3;151(1):117-30.

(76) Heikinheimo M, Scandrett JM, Wilson DB. Localization of Transcription Factor GATA-4 to Regions of the Mouse Embryo Involved in Cardiac Development. *Developmental Biology* 1994 August;164(2):361-73.

(77) Liang Q, Wiese RJ, Bueno OF, Dai YS, Markham BE, Molkentin JD. The Transcription Factor GATA4 Is Activated by Extracellular Signal-Regulated Kinase 1- and 2-Mediated Phosphorylation of Serine 105 in Cardiomyocytes. *Mol Cell Biol* 2001 November 1;21(21):7460-9.

(78) Charron F, Tsimiklis G, Arcand M, Robitaille L, Liang Q, Molkentin JD , Meloche S, Nemer M. Tissue-specific GATA factors are transcriptional effectors of the small GTPase RhoA. *Genes Dev* 2001 October 15;15(20):2702-19.

(79) Liang Q, Molkentin JD. Divergent Signaling Pathways Converge on GATA4 to Regulate Cardiac Hypertrophic Gene Expression. *Journal of Molecular and Cellular Cardiology* 2002 June;34(6):611-6.

(80) Aries A, Paradis P, Lefebvre C, Schwartz RJ, Nemer M. Essential role of GATA-4 in cell survival and drug-induced cardiotoxicity. *PNAS* 2004 May 4;101(18):6975-80.

(81) Suzuki YJ, Evans T. Regulation of cardiac myocyte apoptosis by the GATA-4 transcription factor. *Life Sciences* 2004 February 27;74(15):1829-38.

(82) Hasenfuss G. Animal models of human cardiovascular disease, heart failure and hypertrophy. *Cardiovascular Research* 1998 July 1;39(1):60-76.

(83) Wassen FW, Schiel AE, Kuiper GG, Kaptein E, Bakker O, Visser TJ, Simonides WS. Induction of thyroid hormone-degrading deiodinase in cardiac hypertrophy and failure. *Endocrinology* 2002 July;143(7):2812-5.

(84) Kogler H, Hartmann O, Leineweber K, van Nguyen P, Schott P, Brodde OE, Hasenfuss G. Mechanical Load-Dependent Regulation of Gene Expression in Monocrotaline-Induced Right Ventricular Hypertrophy in the Rat. *Circ Res* 2003 July 3;01.

(85) Ecarnot-Laubriet A, Assem M, Poirson-Bichat F, Moisant M, Bernard C, Lecour S, Solary E, Rochette L , Teyssier J-R. Stage-dependent activation of cell cycle and apoptosis mechanisms in the right ventricle by pressure overload. *Biochimica et Biophysica Acta (BBA) - Molecular Basis of Disease* 2002 April 24;1586(3):233-42.

(86) Jones JE, Mendes L, Rudd MA, Russo G, Loscalzo J, Zhang YY. Serial noninvasive assessment of progressive pulmonary hypertension in a rat model. *Am J Physiol Heart Circ Physiol* 2002 July 1;283(1):H364-H371.

(87) Wilson DW, Segall HJ, Pan LC, Lame MW, Estep JE, Morin D. Mechanisms and pathology of monocrotaline pulmonary toxicity. *Crit Rev Toxicol* 1992;22(5-6):307-25.

(88) Kasahara Y, Kiyatake K, Tatsumi K, Sugito K, Kakusaka I, Yamagata S, Ohmori S, Kitada M, Kuriyama T. Bioactivation of monocrotaline by P-450 3A in rat liver. *J Cardiovasc Pharmacol* 1997 July;30(1):124-9.

(89) Estep JE, Lame MW, Morin D, Jones AD, Wilson DW, Segall HJ. [14C]monocrotaline kinetics and metabolism in the rat. *Drug Metab Dispos* 1991 January 1;19(1):135-9.

(90) Comini L, Agnoletti G, Panzali A, Mantero G, Pasini E, Gaia G, Albertini A, Ferrari R. Activation of ANP synthesis during congestive heart failure in rats treated with monocrotaline. *Am J Physiol* 1995 January;268(1 Pt 2):H391-H398.

(91) Leineweber K, Brandt K, Wludyka B, Beilfuss A, Ponicke K, Heinroth-Hoffmann I, Brodde OE. Ventricular Hypertrophy Plus Neurohumoral Activation Is Necessary to Alter the Cardiac {beta}-Adrenoceptor System in Experimental Heart Failure. *Circ Res* 2002 November 29;91(11):1056-62.

(92) Leineweber K, Seyfarth T, Brodde OE. Chamber-specific alterations of noradrenaline uptake (uptake1) in right ventricles of monocrotaline-treated rats. 2000 December;131(7):1438-44.

(93) Seyfarth T, Gerbershagen HP, Giessler C, Leineweber K, Heinroth-Hoffmann I, Ponicke K, Brodde OE. The Cardiac [beta] -Adrenoceptor-G-protein(s)-adenylyl Cyclase System in Monocrotaline-treated Rats. *Journal of Molecular and Cellular Cardiology* 2000 December;32(12):2315-26.

(94) Ceconi C, Condorelli E, Quinzanini M, Rodella A, Ferrari R, Harris P. Noradrenaline, atrial natriuretic peptide, bombesin and neurotensin in myocardium and blood of rats in congestive cardiac failure. *Cardiovasc Res* 1989 August;23(8):674-82.

(95) Bernocchi P, Ceconi C, Pedersini P, Pasini E, Curello S, Ferrari R. Skeletal muscle metabolism in experimental heart failure. *J Mol Cell Cardiol* 1996 November;28(11):2263-73.

(96) Wolkart G, Stromer H, Brunner F. Calcium Handling and Role of Endothelin-1 in Monocrotaline Right Ventricular Hypertrophy of the Rat. *Journal of Molecular and Cellular Cardiology* 2000 November;32(11):1995-2005.

(97) Schott P, Singer SS, Kogler H, Neddermeier D, Leineweber K, Brodde OE, Regitz-Zagrosek V, Schmidt B, Dihazi H, Hasenfuss G. Pressure overload and neurohumoral activation differentially affect the myocardial proteome. *Proteomics* 2005 April;5(5):1372-81.

(98) Buermans HPJ, Redout EM, Schiel AE, Musters RJP, Zuidwijk M, Eijk PP, van Hardeveld C, Kasanmoentalib S, Visser FC, Ylstra B, Simonides WS. Microarray analysis reveals pivotal divergent mRNA expression profiles early in the development of either compensated ventricular hypertrophy or heart failure. *Physiol Genomics* 2005 May 11;21(3):314-23.

(99) Dempsey AA, Dzau VJ, Liew CC. Cardiovascular genomics: estimating the total number of genes expressed in the human cardiovascular system. *J Mol Cell Cardiol* 2001 October;33(10):1879-86.

(100) Orphanides G, Reinberg D. A unified theory of gene expression. *Cell* 2002 February 22;108(4):439-51.

(101) Hochheimer A, Tjian R. Diversified transcription initiation complexes expand promoter selectivity and tissue-specific gene expression. *Genes Dev* 2003 June 1;17(11):1309-20.

(102) Lee TI, Young RA. Transcription Of Eukaryotic Protein-Coding Genes. *Annual Review of Genetics* 2000;34(1):77-137.

(103) Sproul D, Gilbert N, Bickmore WA. The Role Of Chromatin Structure In Regulating The Expression Of Clustered Genes. *Nat Rev Genet* 2005 October;6(10):775-81.

(104) Mullis KB. Target amplification for DNA analysis by the polymerase chain reaction. *Ann Biol Clin (Paris)* 1990;48(8):579-82.

(105) Velculescu VE, Zhang L, Vogelstein B, Kinzler KW. Serial analysis of gene expression. *Science* 1995 October 20;270(5235):484-7.

(106) Kallioniemi OP, Kallioniemi A, Sudar D, Rutovitz D, Gray JW, Waldman F , Pinkel D. Comparative genomic hybridization: a rapid new method for detecting and mapping DNA amplification in tumors. *Semin Cancer Biol* 1993 February;4(1):41-6.

(107) Gunderson KL, Steemers FJ, Lee G, Mendoza LG, Chee MS. A genome-wide scalable SNP genotyping assay using microarray technology. *Nat Genet* 2005 May;37(5):549-54.

(108) Schena M, Shalon D, Davis RW, Brown PO . Quantitative monitoring of gene expression patterns with a complementary DNA microarray. *Science* 1995 October 20;270(5235):467-70.

(109) Vandepoele K, Vlieghe K, Florquin K, Hennig L, Beemster GTS, Gruissem W, Van de Peer Y, Inze D, De Veylder L. Genome-Wide Identification of Potential Plant E2F Target Genes. *Plant Physiol* 2005 September 1;139(1):316-28.

(110) Arava Y, Wang Y, Storey JD, Liu CL, Brown PO, Herschlag D. Genome-wide analysis of mRNA translation profiles in Saccharomycescerevisiae. *PNAS* 2003 April 1;100(7):3889-94.

(111) Frey BJ, Mohammad N, Morris QD, Zhang W, Robinson MD, Mnaimneh S, Chang R, Pan Q, Sat E, Rossant J, Bruneau BG, Aubin JE, Blencowe BJ, Hughes TR. Genome-wide analysis of mouse transcripts using exon microarrays and factor graphs. *Nat Genet* 2005 September;37(9):991-6.

(112) Kawahara N, Wang Y, Mukasa A, Furuya K , Shimizu T, Hamakubo T, Aburatani H, Kodama T, Kirino T. Genome-wide Gene Expression Analysis for Induced Ischemic Tolerance and Delayed Neuronal Death Following Transient Global Ischemia in Rats. 2004 February;24(2):212-23.

(113) Togashi A, Katagiri T, Ashida S, Fujioka T, Maruyama O, Wakumoto Y, Sakamoto Y, Fujime M, Kawachi Y, Shuin T, Nakamura Y. Hypoxia-Inducible Protein 2 (HIG2), a Novel Diagnostic Marker for Renal Cell Carcinoma and Potential Target for Molecular Therapy. *Cancer Res* 2005 June 1;65(11):4817-26.

(114) Phimister B. Going global. *Nat Genet* 1999;21 Suppl(1).

(115) Schuchhardt J, Beule D, Malik A, Wolski E, Eickhoff H, Lehrach H, Herzel H. Normalization strategies for cDNA microarrays. *Nucleic Acids Res* 2000 May 15;28(10):E47.

(116) Quackenbush J. Microarray data normalization and transformation. *Nat Genet* 2002 December;32 Suppl:496-501.

(117) Huber W, Von Heydebreck A, Sultmann H, Poustka A, Vingron M. Variance stabilization applied to microarray data calibration and to the quantification of differential expression. *Bioinformatics* 2002 July;18 Suppl 1:S96-S104.

(118) Durbin BP, Hardin JS, Hawkins DM, Rocke DM. A variance-stabilizing transformation for gene-expression microarray data. *Bioinformatics* 2002 July 1;18(90001):105S-110.

(119) Kepler T, Crosby L, Morgan K. Normalization and analysis of DNA microarray data by self-consistency and local regression. *Genome Biology* 2002;3(7):research0037.

(120) Yang YH, Dudoit S, Luu P, Lin DM, Peng V, Ngai J, Speed TP. Normalization for cDNA microarray data: a robust composite method addressing single and multiple slide systematic variation. *Nucl Acids Res* 2002 February 15;30(4):e15.

(121) Tseng GC, Oh MK, Rohlin L, Liao JC, Wong WH. Issues in cDNA microarray analysis: quality filtering, channel normalization, models of variations and assessment of gene effects. *Nucl Acids Res* 2001 June 15;29(12):2549-57.

(122) Tusher VG, Tibshirani R, Chu G. Significance analysis of microarrays applied to the ionizing radiation response. *PNAS* 2001 April 24;98(9):5116-21.

(123) Baldi P, Long AD. A Bayesian framework for the analysis of microarray expression data: regularized t -test and statistical inferences of gene changes. *Bioinformatics* 2001 June 1;17(6):509-19.

(124) Cui X, Churchill G. Statistical tests for differential expression in cDNA microarray experiments. *Genome Biology* 2003;4(4):210.

(125) Kerr MK, Martin M, Churchill GA. Analysis of variance for gene expression microarray data. *J Comput Biol* 2000;7(6):819-37.

(126) Cui X, Hwang JTG, Qiu J, Blades NJ, Churchill GA. Improved statistical tests for differential gene expression by shrinking variance components estimates. *Biostat* 2005 January 1;6(1):59-75.

(127) Dennis G, Sherman B, Hosack D, Yang J, Gao W, Lane H, Lempicki R. DAVID: Database for Annotation, Visualization, and Integrated Discovery. *Genome Biology* 2003;4(9):R60.

(128) Hosack D, Dennis G, Sherman B, Lane H, Lempicki R. Identifying biological themes within lists of genes with EASE. *Genome Biology* 2003;4(10):R70.

(129) Bouton CMLS, Pevsner J. DRAGON View: information visualization for annotated microarray data. *Bioinformatics* 2002 February 1;18(2):323-4.

(130) Subramanian A, Tamayo P, Mootha VK, Mukherjee S, Ebert BL, Gillette MA , Paulovich A, Pomeroy SL, Golub TR, Lander ES, Mesirov JP. Gene set enrichment analysis: A knowledge-based approach for interpreting genome-wide expression profiles. *PNAS* 2005 September 30;0506580102.

(131) Curtis RK, Oresic M, Vidal-Puig A. Pathways to the analysis of microarray data. *Trends in Biotechnology* 2005 August;23(8):429-35.

(132) Kanehisa M, Goto S, Kawashima S, Okuno Y, Hattori M. The KEGG resource for deciphering the genome. *Nucleic Acids Res* 2004 January 1;32(1):D277-D280.

(133) Doniger S, Salomonis N, Dahlquist K, Vranizan K, Lawlor S, Conklin B. MAPPFinder: using Gene Ontology and GenMAPP to create a global gene-expression profile from microarray data. *Genome Biology* 2003;4(1):R7.

(134) Zeeberg BR, Feng W, Wang G, Wang MD, Fojo AT, Sunshine M, Narasimhan S, Kane DW, Reinhold WC, Lababidi et a. GoMiner: a resource for biological interpretation of genomic and proteomic data. *Genome Biology* 2003;4(4):R28.

(135) Beissbarth T, Speed TP. GOstat: find statistically overrepresented Gene Ontologies within a group of genes. *Bioinformatics (Oxford, England)* 2004 June 12;20(9):1464-5.

(136) Grosu P, Townsend JP, Hartl DL, Cavalieri D. Pathway Processor: a tool for integrating whole-genome expression results into metabolic networks. *Genome Res* 2002 July;12(7):1121-6.

(137) Pandey R, Guru RK, Mount DW. Pathway Miner: extracting gene association networks from molecular pathways for predicting the biological significance of gene expression microarray data. *Bioinformatics (Oxford, England)* 2004 September 1;20(13):2156-8.

(138) Cheng J, Sun S, Tracy A, Hubbell E, Morris J, Valmeekam V, Kimbrough A, Cline MS, Liu G, Shigeta et a. NetAffx Gene Ontology Mining Tool: a visual approach for microarray data analysis. *Bioinformatics (Oxford, England)* 2004 June 12;20(9):1462-3.

(139) Zhong S, Li C, Wong WH. ChipInfo: Software for extracting gene annotation and gene ontology information for microarray analysis. *Nucl Acids Res* 2003 July 1;31(13):3483-6.

(140) Klose J, Kobalz U. Two-dimensional electrophoresis of proteins: an updated protocol and implications for a functional analysis of the genome. *Electrophoresis* 1995 June;16(6):1034-59.

(141) Klose J. Protein mapping by combined isoelectric focusing and electrophoresis of mouse tissues. A novel approach to testing for induced point mutations in mammals. *Humangenetik* 1975;26(3):231-43.

(142) MacBeath G. Protein microarrays and proteomics. *Nat Genet* 2002 December;32 Suppl:526-32.

(143) Walter G, Bussow K, Lueking A, Glokler J. High-throughput protein arrays: prospects for molecular diagnostics. *Trends in Molecular Medicine* 2002 June 1;8(6):250-3.

(144) Nordhoff E, Egelhofer V, Giavalisco P, Eickhoff H, Horn M, Przewieslik T, Theiss D, Schneider U, Lehrach H, Gobom J. Large-gel two-dimensional electrophoresis-matrix assisted laser desorption/ionization-time of flight-mass spectrometry: an analytical challenge for studying complex protein mixtures. *Electrophoresis* 2001 August;22(14):2844-55.

Chapter 2

Micro-Array Analysis Reveals Pivotal Divergent mRNA Expression Profiles Early In The Development Of Either Compensated Ventricular Hypertrophy Or Heart Failure

Henk P.J. Buermans[1], Everaldo M. Redout[1], Anja E. Schiel[1]
René J.P. Musters[1], Marian Zuidwijk[1], Paul P. Eijk[3]
Cornelis van Hardeveld[1], Soemini Kasanmoentalib[3]
Frans C. Visser[2], Bauke Ylstra[3], Warner S. Simonides[1]

1. Laboratory for Physiology, Institute for Cardiovascular Research (ICaR-VU), VU University Medical Center, Van der Boechorststraat 7, 1081 BT Amsterdam, The Netherlands.

2. Department of Cardiology, Institute for Cardiovascular Research (ICaR-VU), VU University Medical Center, De Boelelaan 1117, 1081 HV Amsterdam, The Netherlands.

3. Micro-array core facility, VU University Medical Center, Van der Boechorststraat 7, 1081 BT Amsterdam, The Netherlands.

Published in:
Physiological Genomics, May 2005; 21: 314 - 323

Table of contents

Abstract

Myocardial right-ventricular (RV) hypertrophy due to pulmonary hypertension is aimed at normalizing ventricular wall stress. Depending on the degree of pressure overload, RV hypertrophy may progress to a state of impaired contractile function and heart failure, but this can not be discerned during the early stages of ventricular remodelling. We tested whether critical differences in gene-expression profiles exist between ventricles before the ultimate development of either a compensated or decompensated hypertrophic phenotype. Both phenotypes were selectively induced in Wistar rats by a single subcutaneous injection of either a low or a high dose of the pyrrolizidine alkaloid monocrotaline (MCT). Spotted oligonucleotide micro-arrays were used to investigate pressure-dependent cardiac gene-expression profiles at two weeks after the MCT injections, between control rats and rats that would ultimately develop either compensated or decompensated hypertrophy. Clustering of significantly regulated genes revealed specific expression profiles for each group, although the degree of hypertrophy was still similar in both. The ventricles destined to progress to failure showed activation of pro-apoptotic pathways, particularly related to mitochondria, while the group developing compensated hypertrophy showed blocked pro-death effector signalling via p38 MAPK, through upregulation of MKP1.

In summary, we show that already at an early time point, pivotal differences in gene expression exist between ventricles that will ultimately develop either a compensated or a decompensated phenotype, depending on the degree of pressure overload. These data reveal genes that may provide markers for the early prediction of clinical outcome as well as potential targets for early intervention.

Introduction

Myocardial ventricular hypertrophy is a major risk factor that is associated with a higher incidence of clinical events, morbidity and mortality from cardiovascular disease[1], generally leading to heart failure. Right-ventricular (RV) hypertrophy is a general adaptive mechanism of the heart to increased workload, resulting from, i.e., chronic pulmonary hypertension, valvular disease or left-ventricular (LV) dysfunction. RV hypertrophy is aimed at normalizing ventricular wall stress and, as in the case of LV overload, depending on the degree or duration of the pressure overload, RV-hypertrophy may progress from a compensated state into a pathological state with progressive myocyte apoptosis and compromised cardiac function, ultimately leading to congestive heart failure[2]. Multiple signal transduction pathways are known to be involved in the remodelling of the heart[3], and hypertrophy and failure are characterized to varying degrees by changes in extracellular matrix composition, energy metabolism, contraction, adrenergic signalling and calcium handling[4]. Which of these changes is critical in the ultimate transition to heart failure is a matter of debate. More importantly, it remains unclear which signalling pathway or combination of signalling pathways mediate the development of pathological hypertrophy and whether the pathological phenotype is induced early during overload as a function of the degree of mechanical overload, or only as a secondary response when compensation is insufficient[3, 5].

To address this question we used the established monocrotaline (MCT) model of chronic pulmonary hypertension and subsequent RV hypertrophy to determine gene transcription profiles early in the development of compensated and decompensated hypertrophy[6]. MCT is a pyrrolizidine alkaloid and its bioactive metabolite, which has a short half-life, selectively injures the vascular endothelium of the lung and induces pulmonary vasculitis and an increase in vascular resistance and pulmonary arterial pressure[7]. With the MCT doses typically used in rats, the RV hypertrophy progresses to failure and death around day 28 in most animals, but up to 50% of the animals may develop compensated RV hypertrophy with no signs of failure[8-13]. Detailed analyses of the development of heart failure in this model have shown that critical changes in contractile function and expression of proteins involved in beta-adrenergic signalling and calcium handling, do not become apparent until after three weeks[14, 15]. Furthermore, pressure-dependent activation of pro-apoptotic pathways in the hypertrophied RV are suggested to underlie the transition to failure around this time[16]. However, comparative analyses of the compensated and heart failure groups are few, and limited to late stages when the separate groups can be identified[8, 9, 11, 13]. Following earlier work in our laboratory[13, 17, 18] we now refined the MCT model to allow

the selective induction of either compensated or decompensated RV hypertrophy by using a low or a high dose of MCT, respectively. Animals developing the pathological, decompensated phenotype die of congestive heart failure (CHF) four weeks following MCT injection, while animals in the low-dose group developed a stable compensated hypertrophic phenotype (HYP) showing no signs of failure. Because the outcome of the hypertrophic process is known for both groups, early stages in the development of compensated and decompensated hypertrophy can be investigated with this model before phenotypical differences become apparent.

In the present study we used spotted oligonucleotide micro-arrays representing 4803 known genes to analyze ventricular gene expression of control, HYP and CHF animals early at the onset of myocardial ventricular hypertrophy, i.e., two weeks following MCT administration. Analysis of the expression profiles revealed quantitative but also qualitative differences in gene expression in the hypertrophying RV that may be crucial for the ultimate development of either the compensated or the decompensated state.

Methods

Animals

Animals were treated according to the national guidelines and with the permission of the Institutional Animal Care and Use Committee (IACUC) of the VU University Medical Center Amsterdam, the Netherlands. Male Wistar Rats, weighing 180-200 g (Harlan, Zeist, The Netherlands) were housed individually (250 cm^2/animal) and received food and water *ad libitum*.

A total of 58 animals were randomly assigned to three groups. All animals received a single subcutaneous injection with either saline (control group: CON, n=18), 30 mg MCT/kg body weight (hypertrophy group: HYP, n=20) or 80 mg MCT/kg body weight (congestive heart failure group: CHF, n=20). Two weeks after treatment 12 animals from each group were randomly picked and killed with a halothane overdose and heart and lungs were excised. A total of 2 mL of blood was taken and stored for subsequent measurement of plasma thyroid hormone level (T3) by specific RIA as previously described[19]. Hearts were rinsed by perfusion and the left and right ventricles and septum were separated. All tissues were weighed and snap frozen in liquid nitrogen and stored at –80 ºC. At four weeks after treatment the remaining animals were killed and blood samples, heart and lungs were collected.

Total RNA Isolation

Total RNA isolation from the left and right ventricles from each animal was performed using the TriZol (Invitrogen) method according to the manufacturer's protocol. Total RNA was quantified by A260 measurement and the A260/A280 ratio was used to check for possible contaminations. Sample integrity was also checked on a Agilent 2100 bioanalyzer. A common reference pool was constructed by pooling equal amounts of RNA from all samples used in the micro-array experiments. Samples were dissolved in 100% formamide and stored at –80 ºC prior to use. RNA from six RVs and two LVs per group were used in the micro-array hybridizations for myocardial gene expression profiling. The remaining RV samples were used for the real time PCR confirmation of the micro-array results.

Quantitative Real-Time PCR

Gene-specific primers (Invitrogen) were designed using Primer Express v2.0 to generate amplicons with a length of 75-125 bp spanning exon-exon junctions. Primer pairs were checked for a linear response over a large cDNA input range and for non-specific products with dissociation curves and 2% agarose gel electrophoresis.

Hypoxanthine-guanine phosporibosyltransferase (HPRT) was used as an internal control to normalize gene expression.
A total of 5 µg total RNA was used to generate cDNA strands in a 20 µL reaction volume using the Cloned AMV First Strand Synthesis Kit (Invitrogen). An equivalent of 25 ng total RNA was subsequently used in the amplification with 50 nmol/L gene-specific primers and 4 µL SYBR green master-mix (Applied Biosystems) in a total volume of 8 µL, using standard cycle parameters on an Applied Biosystems model 7700.

Western Blotting
Right and left ventricular tissue was homogenized in modified 1D-buffer (15% glycerol, 1% SDS, 0.0625 mol/L TrisCl pH6.8, 500 µg/mL DTT (MP Biochemicals, Inc.), 500 µg/mL Pefabloc SC (Roche) and 5 µL/mL Phosphatase inhibitor cocktail 1 (Sigma). Samples were then sonicated for 30 min, incubated at 80°C for 5 min and centrifuged for 20 min at 14.000 rpm. The protein samples were immunoblotted for phospho-p38 and MKP-1 (Santa Cruz).
Western-blotting reagents were purchased from Amersham International (Amersham, UK). Equal amounts of protein (50 µg; BCA assay) were separated by electrophoresis (10% SDS-PAGE) and transferred to nitrocellulose membranes. Protein transfer was confirmed by Ponceau staining of the blot. Membranes were blocked with 5% non-fat milk in TBS-T for 1 h at room temperature. Phospho-specific p38 and MKP-1 antibodies were separately incubated in TBS-T containing 5% nonfat milk (Biorad) overnight at 4°C. After membranes were washed with TBS-T, they were incubated with the appropriate secondary antibodies conjugated to horseradish peroxidase for 1 h at room temperature. Bands were visualized by enhanced chemiluminescence and quantified using a FujiFilm LAS 3000 laser densitometer.

Micro-Array Printing, Probe Generation, Hybridization And Washing
The Compugen Rat OligoLibrary™ was purchased from Sigma-Aldrich. Oligos were resuspended to a concentration of 20 µmol/L in a 150 mmol/L sodium phosphate buffer, pH8.5 and printed on Motorola CodeLink™ activated slides using an Amersham Pharmacia Biotech Spotter. Features were spotted as duplicates on the micro-array with pairs divided over two different regions.
cDNA probes were generated from 100 µg total RNA, with an oligo-dT [(dT)20-VN] primer (Invitrogen) and SuperScript™ II Reverse Transcriptase (Invitrogen), with incorporation of aminoallyl-dUTP. Probes were indirectly labelled with Fluorolink Cy3 (sample) or Cy5 (reference pool) mono-functional dyes.

Hybridization protocol was adapted from Snijders *et al.*[20] with minor modifications. In brief, Cy3 and Cy5 labelled probes were combined and the hybridization mixture was prepared containing a final concentration of 2 µg/µL yeast tRNA, 0.4 µg/µL polyA and 0.8 µg/µL human Cot-1 DNA in 91.2 µL H_2O, 7.6 µL 10 % SDS, 30.4 µL glycerol and 250.8 µL master mix (1 g dextran sulfate, 6 mL formamide, 1 mL, 20x SSC). Probe mix was denaturated at 70 ºC for 15 min and incubated at 30 ºC for 60 min Pre-hybridization mixture was identical to the probe-mix but probe was substituted with salmon sperm DNA to a final concentration of 1 µg/µL.
Several layers of rubber cement were applied closely around the array area to form a hydrophobic well to which the pre-hybridization mix was added. Pre-hybridization was maintained for 45 min at room temperature. Probe hybridization was initiated by gently removing as much of the pre-hybridization mix as possible without generating any dry areas on the array and applying the probe-hybridization mix. Hybridization was maintained for 16 h at 30 ºC on a rocking table (~1 rpm). To prevent liquid evaporation the arrays were kept at high humidity by placing them in separate containers situated in a larger, air tight, humid container.
After hybridization excess hybridization mixture was rinsed off with PI buffer (0.1 mol/L sodium phosphate, 0.1 % Igepal CA630, pH8), then washed once in 50% formamide, 2x SSC, pH7 at 35 ºC for 15 min followed by 15 min in PI buffer at RT. Excess salt was removed by subsequently rinsing in 0.2x SSC and 0.1x SSC for 1 min at RT. Slides were dried by centrifugation at 1000 rpm for 3 min For our most recent protocols see: http://www.vumc.nl/microarrays/onderzoek/protocols.html.

Data Acquisition And Analysis
Slides were scanned at a 10 µm resolution for Cy3 and Cy5 intensities using a Perkin-Elmer Multi Laser Micro-Array Scanner operated by the ScanArray Express v1.0 software. Array images were processed with Imagene v5.1. Flagged features were excluded from further analysis. Mean Cy3 and Cy5 intensities were background corrected. Because there was only a very small location effect, the duplicate signals for each gene were averaged. The mean Cy3 and Cy5 channel intensities were balanced, and the Cy3 to Cy5 log2-ratios were standardized to a Z-score with the fitted value as mean (µ) and the mean absolute distance as standard deviation (σ). Genes were considered to be suitable for further analysis if for all three RV groups, genes were present in at least three out of the six arrays per group. For the LV analysis, each gene had to be present in all six LV arrays to be accepted. These data have been deposited in the Gene Expression Omnibus[21] as series GSE1652.

Significance Analysis

Clustering of the significantly regulated genes was performed on the basis of their significant differences as determined in the three pair-wise comparisons. If there was a significant difference between the CON and HYP group, it was denoted with a "1", or, if there was no difference observed, a "0". This was also done for CON vs. CHF and HYP vs. CHF respectively. These "1" and "0" notations where then combined as x - x - x representing the CON vs. HYP, CON vs. CHF and HYP vs. CHF comparisons respectively. With three pair-wise comparisons, there are a total of seven combinations possible. A gene with no significant difference between CON vs. HYP [0], a significant difference between CON vs. CHF [1] as well as a difference between HYP vs. CHF [1], would then be assigned to cluster 0-1-1. In the remainder of this article, these clusters will be referred to as clusters I through VII (see Table 3 in the Results section).

Note that this is a method that clusters only on the basis of significant differences between groups. It does not take the direction of change into account, i.e., up and downregulated genes can be assigned to the same cluster.

Initially, differential expression between the CON, HYP and CHF groups was assessed with the significance analysis of microarrays program, SAM[22]. However, in contrast to 33 upregulated genes, only four were found that were downregulated (data not shown). This imbalance in direction of regulation lead to search for alternative analysis methods for our data-set.

According to the theorem of Stouffer-Hemelrijk[23] the sum of n standardized log ratios has a normal distribution with mean of zero and standard deviation of $\sqrt{n}$. So its quotient $Z = \sum z_i / \sqrt{n}$ has a standard normal distribution with a mean of zero and a standard deviation of 1.

If $z_i (z_1, z_2, ...z_n) \sim N(0,1)$

Then its sum

$\sum z_i = (z_1 + z_2 + ... + z_n) \sim N(0, \sqrt{n})$

and

$\text{mean-}Z_{(CON,HYP \text{ or } CHF)} = \sum z_i / \sqrt{n} \sim N(0,1)$

The difference between two pair-wise conditions was tested on significance by Zscore in the following way.

$$Z_{score} = (Z_2 - Z_1) / \sqrt{2} \qquad \sim \qquad N(0,1)$$

For each group the mean-Z was calculated. Gene expression was considered to be significantly different if the absolute Z score value was greater than 2, which corresponds with a p-value < 0.025.

Statistical Analysis For RT-PCR And Hypertrophic Parameters

Relevant parameters were evaluated for significant differences between groups with a one-way ANOVA using the SPSS v9.0 statistical package with the Bonferroni correction for multiple testing. Differences with a p value smaller than 0.05 were considered significant.

Results

Mct-Induced Development Of Compensated RV Hypertrophy Or Heart Failure

In previous studies the use of a single dose of MCT of 40-60 mg/kg typically resulted in a mixed population of animals, developing either compensated hypertrophy or progressing to heart failure[8-13]. We found that administration of a high dose of MCT (80 mg/kg) induced RV hypertrophy which in all cases progressed to congestive heart failure (CHF). In contrast, 30 mg MCT/kg induced exclusively compensated RV hypertrophy (HYP). Figure 1 shows average growth curves of animals in both groups over a period of four weeks. MCT administration resulted in a slight reduction of the rate of growth, but animals in the HYP group did not cease to grow, while the CHF group started loosing weight around day 20. Apart from the progressive weight loss, all animals in this group showed secondary signs of right-sided CHF, including pleural effusion and ascites at the time of sacrifice at four weeks. No such signs were present in any of the animals in the HYP group. In a parallel study four HYP animals were sacrificed at twelve weeks and non of these animals showed signs of heart failure (not shown).

Table 1 summarizes organ and body weights of animals sacrificed at four weeks or at two weeks. The latter group was used in the micro-array analysis described in the next section. The significantly greater increase in lung weight in the CHF versus the HYP group is indicative of the more extensive proliferative pulmonary vasculitis induced by the high dose of MCT[24]. The increase is not related to edema, since dry-to-wet weight ratios of lung tissue did not differ between the groups at any time (not shown). Both groups developed a significant degree of RV hypertrophy in response to the increased pulmonary resistance, as evidenced by a 20% increase in the RV/LV+S weight ratio already at two weeks. The degree of hypertrophy was significantly greater in the CHF group (135%), compared to the HYP group (95%) after four weeks. In line with the development of severe heart failure, plasma thyroid hormone

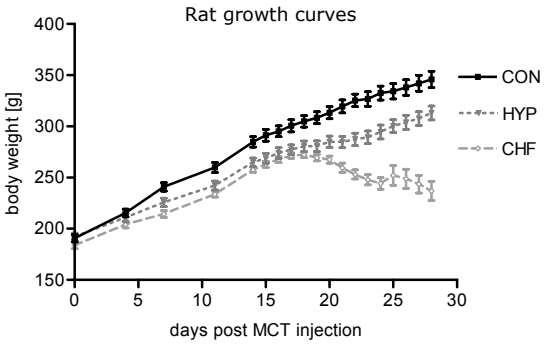

◄**Figure 1**: Body weight (g) was measured throughout the four week period after MCT treatment. Black, blue and red lines represent control, hypertrophic and heart failure rats respectively. Plotted is the mean body weight per group ± SEM confidence interval.

	2 weeks			4 weeks		
	CON	HYP	CHF	CON	HYP	CHF
BW (g)	284 ± 4	258 ± 5 *	244 ± 4 *	352 ± 14	332 ± 10	250 ± 6 *†
Heart (mg)	924 ± 28	835 ± 31	812 ± 28 *	980 ± 27	1090 ± 30	1007 ± 38
Heart/BW (mg/g)	3.25 ± 0.08	3.23 ± 0.08	3.32 ± 0.07	2.80 ± 0.09	3.29 ± 0.11 *	4.03 ± 0.09 *†
RV (mg)	162 ± 8	170 ± 9	167 ± 9	167 ± 11	304 ± 23 *	334 ± 11 *†
RV/BW (mg/g)	0.57 ± 0.02	0.65 ± 0.03 *	0.68 ± 0.03 *	0.47 ± 0.02	0.93 ± 0.09 *	1.33 ± 0.02 *†
RV / LV + S (mg/mg)	0.21 ± 0.01	0.25 ± 0.01 *	0.26 ± 0.01 *	0.20 ± 0.01	0.40 ± 0.04 *	0.50 ± 0.02 *
Lung(g)	1.48 ± 0.03	1.54 ± 0.03	1.75 ± 0.05 *†	1.33 ± 0.11	1.65 ±0.042 *	2.24 ± 0.09 *†
Lung/BW (mg/g)	5.12 ± 0.05	5.74 ± 0.08 *	6.99 ± 0.10 *†	3.72 ± 0.15	4.96 ± 0.19 *	9.00 ± 0.42 *†
Plasma T3 (nmol/L)	1.10 ± 0.05	1.20 ± 0.05	1.03 ± 0.05	0.98 ± 0.06	1.00 ± 0.05	0.33 ± 0.06 *†

▲**Table 1**: Animals were sacrificed two or four weeks after receiving either saline (CON), 30 mg MCT/kg (HYP) or 80 mg MCT/kg (CHF). Mean values ± SEM of body weight (BW), plasma T3 level, tissue wet weights of whole heart, right ventricle (RV) and lung are given, as well as tissue to body weigth ratios. RV/LV+S denotes the wet weight ratio of RV over the combined weight of left ventricle (LV) and septum (S). Data were analysed as described in the Materials and Methods section and * indicates $P<0.05$ relative to CON and † indicates $P<0.05$ relative to HYP, n=12 for all parameters at two weeks, except for lung weight (n=6); n=8 for all parameters at four weeks, except for the CON group (n=6).

levels (T3) were significantly reduced at four weeks in the CHF group only.

In an initial analysis of RV gene expression in this model we determined mRNA levels of sarcoplasmic-endoplasmic reticulum Ca^{2+}-ATPase (SERCA2a) and atrial natriuretic factor (ANF) as representative hallmark genes regulated in hypertrophy (Table 2). As expected, changes in the levels of SERCA2a and ANF message correlated with the severity of the hypertrophy. The data showed a progressive increase in ANF mRNA at two and four weeks, which reached significance only in the CHF group. The levels of SERCA2a mRNA were reduced at four weeks, and significantly more so in CHF compared to HYP animals. At two weeks, however, no change was detectable in either group relative to controls.

Taken together, these data indicate that the low and high dose of MCT induce different degrees of pulmonary hypertension and ensuing RV hypertrophy, which in the latter case progresses to failure. A large scale analysis of ventricular gene expression was next performed in the control, HYP and CHF groups at two weeks to assess early differences in gene expression.

	2 weeks			4 weeks		
	CON (6)	HYP (8)	CHF (8)	CON (6)	HYP (8)	CHF (8)
ANF mRNA (%)	100 ± 22	244 ± 33	317± 57 *	100 ± 33	450 ± 85	905 ± 145 *
SERCA2a mRNA (%)	100 ± 4	100 ± 6	93 ± 3	100 ± 11	64 ± 6 *	37 ± 3 * †

▲**Table 2**: Right ventricles and plasma of 6-8 animals sacrificed two or four weeks after receiving either saline (CON), 30 mg MCT/kg (HYP) or 80 mg MCT/kg (CHF), were analyzed for tissue mRNA levels using slot-blot hybridization, as previously described[13]. All RNA samples were analyzed on the same blot and normalized to the mRNA level of glyceraldehyde-3-phosphate dehydrogenase (GAPDH). Levels of ANF and SERCA2a mRNA are expressed relative to their average control level (100%). All data are the means ± SEM of (n) samples. Data were analyzed as described in the Materials and Methods section and * indicates $P<0.05$ relative to CON and † indicates $P<0.05$ relative to HYP.

Cluster	CON vs. HYP	CON vs. CHF	HYP vs. CHF	Genes	Up / Down
I [1-1-1]	1	1	1	6	6 / 0
II [0-1-0]	0	1	0	69	52 / 17
III [1-1-0]	1	1	0	22	17 / 5
IV [0-1-1]	0	1	1	31	25 / 6
V [1-0-1]	1	0	1	6	2 / 4
VI [0-0-1]	0	0	1	20	11 / 9
VII [1-0-0]	1	0	0	25	11 / 14
				Total 179	124 up, 55 down

◄**Table 3**: Classification of genes into 7 separate clusters based on the significant differences between the three RV groups for all significantly regulated genes. Cluster [1-0-1] indicates: a significant difference between CON vs. HYP [first digit], no significant difference between CON vs. CHF [second digit] and a difference between HYP vs. CHF [third digit]. In the last two columns, for each cluster the total number of genes and the number of up or downregulated are specified.

Micro-Array Analysis

For the RV micro-arrays, 3010 unique genes of the total 4803 (62%) passed the required criteria for further analysis. All three RV groups were pair-wise analyzed by a Z-test. All Z-test scores with an absolute value higher than 2 ($|Z\text{-score}| > 2.0$) were considered to be significant, which resulted in a total of 179 unique genes. Overall there were more genes upregulated than downregulated in the RV, as can be seen in Table 3.

An analysis of the left ventricular myocardium resulted in ten differentially expressed genes, four of which were also regulated in the RV, although with different expression profiles between the three groups. We considered these left ventricular changes of minor importance in our model.

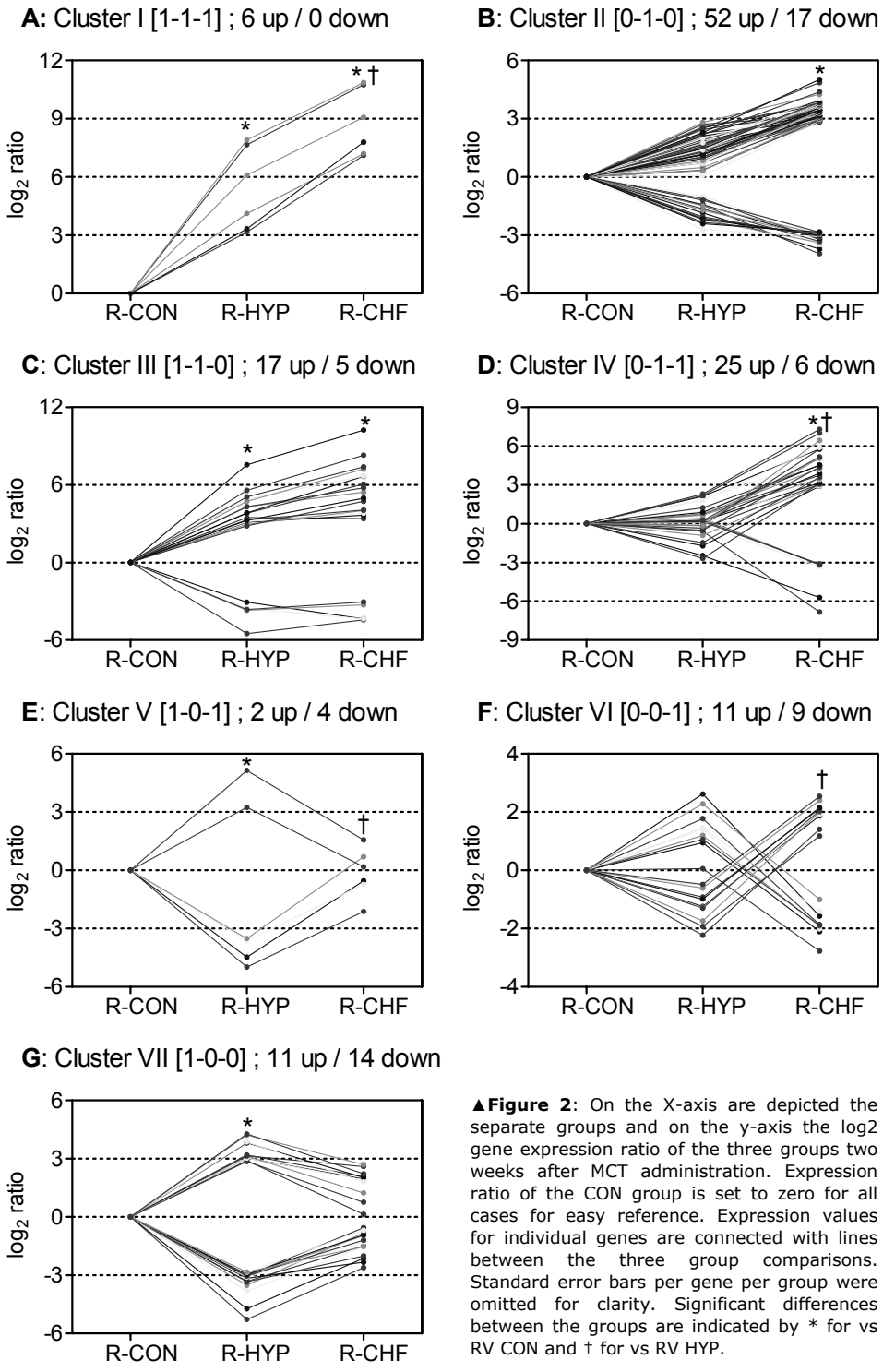

▲**Figure 2**: On the X-axis are depicted the separate groups and on the y-axis the log2 gene expression ratio of the three groups two weeks after MCT administration. Expression ratio of the CON group is set to zero for all cases for easy reference. Expression values for individual genes are connected with lines between the three group comparisons. Standard error bars per gene per group were omitted for clarity. Significant differences between the groups are indicated by * for vs RV CON and † for vs RV HYP.

All further analysis were performed on the 179 right ventricular genes only. A list of all differentially regulated left and right ventricular genes is available at http://physiolgenomics.physiology.org/cgi/content/full/00185.2004/DC1.

Gene Cluster Classification

To classify the identified genes, they were clustered on the basis of their significant differences in expression between the three RV groups. This lead to 7 clusters (Table 3), of which four contain genes with a significant difference in expression between the RV HYP and RV CHF groups, i.e., clusters I, IV, V and VI. Expression plots of all seven clusters are shown in Figure 2A through G. Genes in these separate clusters may be involved in hypertrophic processes that determine the specific development of the compensated and decompensated phenotypes.

Cluster I (Fig 2A) contains genes with an expression profile that correlates with the degree of pressure overload, i.e., there is a significantly higher expression in CHF than the HYP groups, both of which are also significantly different from CON levels. Genes like these are likely to be associated with general hypertrophic remodelling processes that appear to be load-dependent. Two of these genes, alpha-skeletal actin[25] and myosin binding protein C[26], have both been shown to be involved in myocardial hypertrophy. Genes in cluster II (Fig 2B) show an expression profile that is highly similar to cluster I, even though they only display significant differences in the CON vs. CHF comparisons. However these genes still appear to display a load-dependent gene expression profile. Some downregulated genes in this cluster are cytosolic phospholipase A2, Selenoprotein W and dihydropryridine-sensitive calcium channel alpha-1, while beta-catenin (Catnb), cyclin D1 and alpha tubulin were upregulated in CHF relative to CON. Similar to cluster I, cluster III (Fig 2C) is comprised of genes which appear to be associated with a general hypertrophy transcription program, however their expression level is not sensitive to the difference in load between the HYP and CHF groups. Carnitine palmitoyltransferase 1 beta (Cpt1b) was downregulated, while alpha-smooth muscle actin was upregulated in this cluster. Cluster IV (Fig 2D) contains genes that are regulated only in the CHF group. These genes may ultimately be associated with the development of a decompensated phenotype, since they are not differentially expressed in the HYP group at this point in time. In this cluster several mitochondria-related genes were significantly regulated, i.e., the mitochondrial transcription factor A (mtTFA) was downregulated in contrast to the upregulation of the mitochondrial voltage-dependent anion channel (VDAC1) and mitochondrial adenine nucleotide translocator (ANT1) genes.

In contrast to cluster IV, cluster V (Fig 2E) represents those genes which are either up or downregulated in the HYP group when compared to both the CON and CHF groups. These genes may ultimately be associated with the development of compensated hypertrophy since they are not differentially expressed in CHF. This cluster showed the upregulation of a protein tyrosine phosphatase (Genbank U02553). A locuslink query on this gene showed it encodes a dual specificity phosphatase known as mitogen-activated protein kinase (MAPK) phosphatase-1 (MKP-1). MKP-1 is a predominantly nuclear protein which recognizes and de-activates MAPKs, such as p38-MAPK, by dephosphorylating the threonine and tyrosine residues with the T-X-Y sequence. MAPK signalling and in particular the activation of p38-MAPK has been implicated in the development of decompensated hypertrophy and heart failure. Consequently, the upregulation of MKP-1 HYP could be critical in adaptive remodelling in the HYP group (see next section and Discussion).
Assigning a patho-physiological role to the last two clusters is more difficult. Cluster VI (Fig 2F) contains genes that are either up or downregulated in the CHF group relative to the HYP group only, with no significant differences relative to CON. Some of these genes show comparable expression profiles to cluster IV, while others show resemblance to genes in cluster V. However, since these genes do show a significant difference between the HYP and CHF group, they may still contribute to the distinct process leading to either compensated hypertrophy or heart failure.
A nuclear receptor co activator, transcriptional intermediary factor 2, was found to be significantly downregulated in CHF relative to HYP, while the endothelin receptor-B and the calcitonin receptor-like receptor were upregulated in the CHF group.
Finally, cluster VII (Fig 2G) contains genes that are only regulated in the HYP relative to the CON group, but not significantly different from CHF. This cluster showed a decrease in expression of gamma-butyrobetaine hydroxylase (BBH) and platelet-derived growth factor B chain precursor. Thrombospondin 4 and the plasma protein alpha1-fetoprotein were upregulated in this cluster.
These data indicate that early in the development of either compensated or decompensated right ventricular hypertrophy, qualitative differences in addition to quantitative differences in mRNA expression already exist between both hypertrophic phenotypes.

p38-MAPK Phosphorylation In HYP And CHF

As mentioned in the previous section, MKP-1 mediated deactivation of p38-MAPK might play a role in the differentiation between compensated and decompensated hypertrophy.

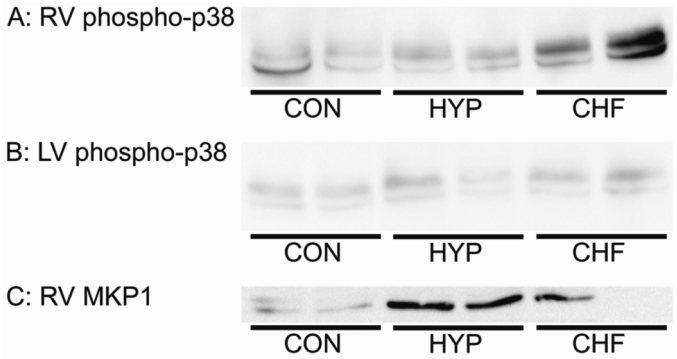

◄**Figure 3**: Western blot analysis of phospho-p38 MAPK levels and MKP1 in right and left ventricular samples. From top to bottom: A: RV phospho-p38, B: LV phospho-p38, C: RV MKP1.

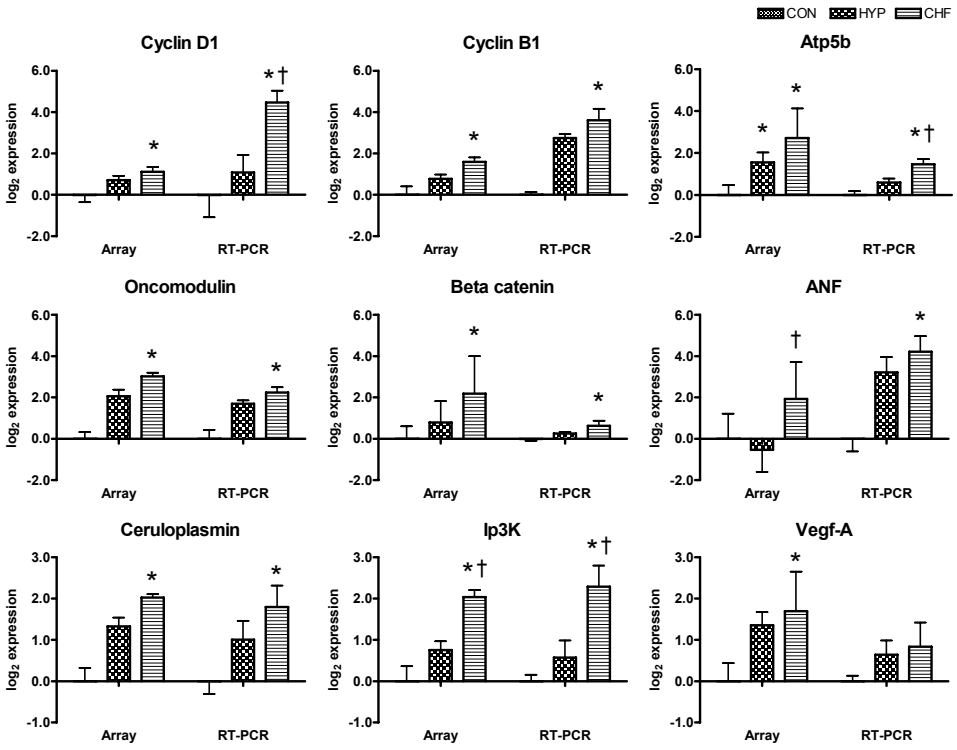

▲**Figure 4**: Real-time PCR confirmations for beta-catenin, mitochondrial ATP synthase beta subunit (ATP5b) atrial natriuretic factor (ANF), ceruloplasmin, cyclinD1, inositol 1,4,5-triphosphate 3-kinase (Ip3k), cyclinB1, oncomodulin and vascular endothelial growth factor A (vegfA). Control expression values for both the array and RT-PCR data have been set to 1. In each graph the expression levels are displayed for array-CON, HYP, CHF and PCR-CON, HYP, CHF from left to right respectively. Significant differences relative to the CON or HYP group are indicated by * or † respectively.

Therefore, we first assessed p38-MAPK activation in RV samples from CON, HYP and CHF animals. Western blot analysis of phospho p38-MAPK levels showed marked activation in the CHF group only (Fig 3a). This activation was restricted to the RV, since an analysis of the LV showed no difference in phospho p38-MAPK levels between the three groups (Fig 3b). Next, we examined whether the absence of p38-MAPK activation in the HYP group was associated with increased MKP-1 expression as suggested by the micro-array expression data. Indeed, MKP1 protein levels in the RV of the HYP group were clearly increased relative to control levels, with considerably less expression in the CHF group (Fig 3c).

Real-Time PCR Gene Confirmations

From the significantly regulated genes, twelve were selected to be confirmed by real-time PCR. Nine of these showed expression profiles in agreement with the micro-array data, although with occasional differences in the fold changes that were observed (Fig 4). Three of the twelve genes showed no change in expression (monoamine oxidase A and calpain 3), or a decrease in expression where an increase was expected (SUP) (data not shown).

Discussion

In this study, we used 65-mer spotted oligonucleotide micro-arrays representing 4803 known rat genes, to probe the ventricular myocardial transcriptome for differential expression of genes at an early stage of development of either compensated or decompensated RV hypertrophy. Although the degree of RV hypertrophy was similar in both MCT-treated groups two weeks following injections, their gene-expression profiles were strikingly different. Clustering revealed expression profiles that were uniquely associated with the development of either the compensated or decompensated hypertrophic phenotype. As we will discuss later, we found genes which were not previously associated with hypertrophy and heart failure, as well as genes which are well known to be involved. Some of these may prove to be pivotal in the ultimate development of either compensated hypertrophy or failure, such as the genes involved in MAPK signalling and apoptosis pathways.
These divergent transcription profiles, caused by different degrees of pressure overload, were generated by using a novel adaptation of the monocrotaline model for RV hypertrophy.

Model
The rat MCT model is widely used to study right-ventricular hypertrophy in response to a chronically elevated hemodynamic load, with most studies reporting progression of RV hypertrophy to failure and death in the majority of animals around day 28 following a single injection of 40-60 mg of MCT/kg. However, using these doses of MCT, up to 50% of the animals may develop stable compensated RV hypertrophy with no signs of failure[8-13]. The animals that do progress to failure show a significantly greater degree of RV hypertrophy and more pronounced changes in RV gene expression, reflecting the development of higher pulmonary arterial pressures[13,27,28]. A single dose of MCT may thus induce a graded response, which is most likely related to differences between individual animals in rate of MCT metabolism, or susceptibility to its bioactive metabolite. The MCT model could therefore provide a valuable tool to study the development of compensated hypertrophy or failure in response to pressure-overload, but a comparison of early stages has not been possible, because both groups cannot be reliably distinguished until after three weeks, when differences become apparent[14, 15].
In the present study we show that a dose of 80 mg MCT/kg consistently induced RV hypertrophy progressing to congestive heart failure (CHF), whereas 30 mg MCT/kg induced only compensated RV hypertrophy (HYP). The values for body weight, plasma T3 levels and index of RV hypertrophy, i.e., RV/LV+S weight, for the CHF

group at four weeks (Table 1), are identical to those reported earlier for the sub-group of animals that developed CHF following a dose of 40 mg MCT/kg[13]. Furthermore, the parameters of the animals that developed compensated hypertrophy in that study, are identical to those in the present HYP group (Table 1), with a significantly smaller degree of RV hypertrophy in the HYP relative to the CHF group[13]. The reduced levels of plasma T3 at four weeks in the CHF group only, may serve as an indicator of the severity of heart failure. In our earlier study we showed that the ultimate 60% drop in plasma T3 is characteristic of severe non-thyroidal illness and, although in part related to a diminished caloric intake, it is primarily the effect of the condition of heart failure[29]. The more pronounced reduction of RV mRNA levels of SERCA2a in CHF versus HYP at four weeks (Table 2), also confirms our earlier observation and those made by others[15]. At two weeks we already find significant RV hypertrophy, in line with previous findings[27], but the degree of hypertrophy is the same for both groups. Nevertheless, lung weight was already significantly more increased in the CHF compared to the HYP group (Table 1), indicating more extensive vascular injury and proliferative vasculitis in this group (the weight increase was not associated with edema)[27, 28]. A consequently higher hemodynamic load and RV wall stress in this group is indicated by the greater increase in ANF mRNA expression in RV from the CHF group (Table 2), which is in agreement with earlier studies[16, 30, 31]. Furthermore, the absence of an effect on SERCA2a expression in either group at two weeks supports the notion that essential changes in gene expression occur after this time[14, 15].

It cannot be ruled out that the dose of 80 mg/kg has additional effects compared to the low dose of MCT, that are not related to the degree of pulmonary vasculitis and subsequent RV hypertrophy. However, with respect to ventricular gene expression such additional systemic effects of MCT appear to be marginal, given that only ten LV genes were differentially regulated in the analysis of all groups. Taken together, the data indicate that our current MCT-protocol predictably induces different degrees of pulmonary hypertension, leading to either compensated or decompensated RV hypertrophy and failure.

Expression Profile Clusters

Clustering the regulated RV genes on the basis of their significant differences between the three groups classified them to the seven distinct groups of genes (Fig 2A - 2G). For the majority of the genes, when either up or downregulated in the HYP relative to the CON group, the expression in the CHF group showed a greater change in the same direction, i.e., clusters I, II and III. Genes in these clusters appear to be

load sensitive and are associated with general hypertrophic remodelling in both compensated and decompensated hypertrophy.
There were two clusters of genes that were uniquely associated with either the compensated hypertrophic phenotype (cluster V) or decompensated phenotype (cluster IV). This indicates that heart failure is not merely a result of quantitative gene expression differences, but that there is a certain group of genes whose expression is associated with the development of either maladaptive ventricular remodelling or adaptive hypertrophy (see discussion below). Our data indicate that, although the compensated and decompensated myocardium do have a lot of regulated genes in common, their expression profiles are in fact strikingly different.

Altered Gene Expression In HYP And CHF
In addition to several well known genes involved in hypertrophic remodelling, e.g., alpha-smooth muscle actin , alpha skeletal actin, and alpha-tubulin[4], several other genes emerged as well.
In pressure overload induced cardiac hypertrophy and heart failure, myocardial energy utilization is switched from fatty acids to glucose as a substrate. In line with this, Cpt1b and BBH were downregulated in clusters III and VII. Cpt1b is situated in the outer mitochondrial membrane, where it is involved in the transport of long-chain fatty acyl-CoAs from the cytoplasm into the mitochondria, thereby regulating mitochondrial beta-oxidation rates[32]. BBH catalyzes the formation of L-carnitine from gamma-butyrobetaine and is essential for the transport of activated fatty acids across the mitochondrial membrane[33].
Although HIF1 alpha was not significantly regulated in our analysis, a more hypoxia-responsive gene, hypoxia inducible factor 3 alpha (HIF3a)[34], was found to be upregulated in cluster III. This indicates some degree of cellular hypoxia in both HYP and CHF. We did not find a change in HIF3a gene expression in the left ventricular myocardium, thereby excluding systemic hypoxia as a cause for the expression of this gene in the RV.
In cluster IV we found the metabotropic glutamate receptor 1 (mGLUR1) to be specifically downregulated in the CHF group. mGLUR1 has been shown to be expressed in the central nervous system, where it is involved in preventing neuronal apoptosis via HOMER - PIKE-L complex interaction, leading to PI3K activation[35]. A patho-physiological role for mGLUR1 in the heart has not been described, although cardiac mGLUR1 expression has been reported[36]. Downregulation of this gene in the heart in CHF could impair anti-apoptotic effects, which might be crucial in the development of the decompensated phenotype. However, more research will be needed to confirm a role for mGLUR1 in heart failure.

Interestingly, the growth hormone (GH) receptor was upregulated in HYP (cluster VII). Although no other groups showed a significant difference in expression, the HYP vs. CHF comparison, with a |Z-score| of 1.95, was almost significantly different. The expression profile of this gene shows a striking similarity to cluster V, the HYP specific cluster. Recently, González-Juanatey *et al.* showed that GH attenuated apoptosis in cardiac myocytes via calcineurin signalling. In addition to this, they showed a decrease in p38-MAPK phosphorylation level after GH treatment[37]. As will be discussed in the next section, p38-MAPK signalling in relation to apoptosis may play a pivotal role in the development of the HYP and CHF phenotypes.

Putative Mediators In Compensated Hypertrophy Or Heart Failure

It is impossible within the limits of this paper to present a full description of the possible functional significance of regulated genes. However, we did find several genes that may play a crucial role in the development of either compensated or decompensated ventricular hypertrophy.

Our data show the HYP-specific upregulation of Mitogen-activated protein kinase (MAPK) phosphatase-1 (MKP-1), in cluster V. MKP-1 recognizes and de-activates MAPKs with higher preference for p38-MAPK and c-Jun N-terminal kinases (JNK1/2) than for extracellular signal-related kinases (ERK1/2). Evidence is accumulating that MKP-1 is involved in a negative feedback loop mechanism suppressing MAPK signalling activity. MAPK pathway activation ultimately leads to the phosphorylation and activation of one of three end effectors, i.e., p38-MAPK, JNK1/2 or ERK1/2, all of which can activate a wide array of transcription factors, thereby contributing to altered gene expression. MAPK signalling has repeatedly been shown to be of major importance in ventricular remodelling due to pressure overload[38]. Recently, it has been shown that p38-MAPK acts as a pro-death effector, and that attenuation of p38-MAPK phosphorylation was associated with the upregulation of anti-apoptotic bcl-2, both in vitro and in vivo[39]. In a study of MCT-induced RV hypertrophy, an increase in bcl-2 expression was observed in an early stage of hypertrophy, while it was markedly downregulated in the transition to heart failure, where it was associated with severe apoptosis[16]. Transient MKP-1 over-expression reduced myocardial hypertrophy associated gene expression as evidenced by attenuated ANF, beta-myosin heavy chain and alpha skeletal muscle actin promotor activity after phenyleprine (PE) stimulation of isolated rat neonatal ventricular cardiomyocytes[40]. MKP-1 transgenic mice also showed in addition to blocked activation of p38-MAPK, JNK1/2 and ERK1/2 following acute catecholamine stimulation, that expression of MKP-1 attenuated hypertrophy both in response to pressure-overload and prolonged isoproterenol infusion[41].

Our observation that MKP-1 is specifically upregulated in the HYP group suggests blocked pro-death signalling mediated via p38-MAPK de-phosphorylation which is not present in the CHF group. Western analysis indeed confirmed the upregulation of MKP-1 in the RVs of the HYP group which consequently showed no p38-MAPK activation, in contrast to the RVs of the CHF group.

Subsequent increases in bcl-2 levels in the HYP group will then exert their anti-apoptotic effects in the compensated hypertrophic myocardium only. High levels of bcl-2 were indeed found at an early stage of hypertrophy by Ecarnot *et al.*[16], while it was markedly downregulated in the subsequent transition to heart failure. This decrease in bcl-2 levels coincided with a stimulation of cyclin D1 expression, a pro-apoptotic mediator, leading to extensive myocardial apoptosis. Indeed, our array data show a significant increase in cyclin D1 expression in the CHF group relative to CON (cluster II), which was confirmed by realtime-PCR.

In addition to the above mentioned alterations in the expression of key pro-apoptotic and pro-survival signalling molecules, we found that the genes encoding the two major components of the mitochondrial permeability transition pore complex (PTPC), i.e., the mitochondrial adenine nucleotide translocator 1 (ANT1) and the mitochondrial voltage dependent anion channel 1 (VDAC1), were significantly overexpressed in CHF, but not in HYP. This is particularly relevant in light of the potential role of p38 and JNK in the mitochondrial death pathway[42, 43]. However, western blot analysis did not yet indicate altered expression of either VDAC1 or ANT1 at this point in ventricular remodelling (data not shown). This could be explained by a time lag between mRNA and actual protein expression, which is supported by the observation that apoptosis is not yet detected at day 14 in the MCT model[16].

Mitochondrial involvement was also suggested by the significantly reduced expression of the mitochondrial transcription factor A (mtTFA) in CHF, but not in HYP. mtTFA controls mitochondrial replication and transcription[44, 45]. Mitochondrial synthesis and function require an estimated 1000 polypeptides, 37 of which are encoded by mitochondrial (mt)DNA, the rest by nuclear (n)DNA[46]. This suggests that reduced mitochondrial biogenesis via mtTFA downregulation and associated mitochondrial dysfunction may play a role in development of pathological hypertrophy. Reduced mtTFA levels were also found at end point heart failure in a study of aortic stenosis-induced LV hypertrophy six months after surgery[47]. In fact, mitochondrial dysfunction enhances oxidative stress, which may directly trigger mitochondrial membrane permeabilization and subsequent apoptosis by opening of the PTPC[48, 49].

The changes described above, see also Figure 5 for a schematic summary, indicate that there is a fundamental shift in the balance of pro-apoptotic vs anti-apoptotic signalling in the two different hypertrophic phenotypes studied. Already early in

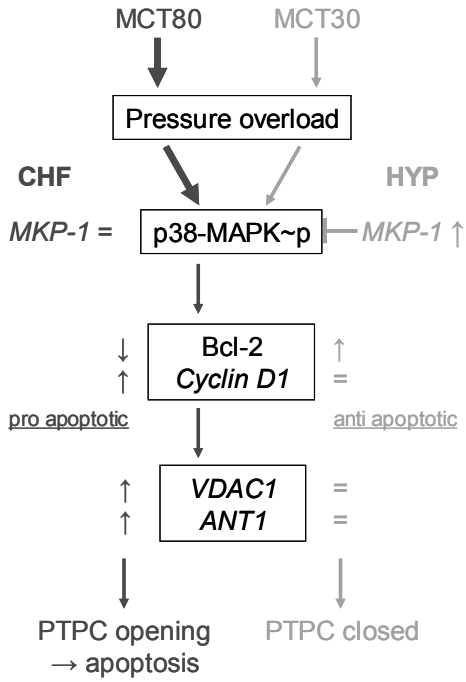

◄Figure 5: Schematic representation of pivotal signalling pathways early in the development of compensated or decompensated hypertrophy. As discussed in the accompanying text, increased MKP-1 expression in the HYP group dephosphorylates p38-MAPK, blocking this pro-death effector. This is associated with increased anti-apoptotic bcl-2 expression and unchanged levels of both VDAC1 and ANT1, resulting in blocked apoptotic signalling. In contrast, due to unchanged MKP-1 levels in the CHF group, p38-MAPK signalling is maintained, which is associated with a decrease in anti-apoptotic bcl-2, an increase in cyclin D1 expression, and ultimately increased levels of VDAC1 and ANT1 leading to PTPC opening and subsequent apoptosis.
↑: upregulation
↓: downregulation
=: unregulated
p38-MAPK~p: phosphorylated p38-MAPK

myocardial remodelling, hearts that will eventually develop heart failure appear to be sensitized to apoptosis, in contrast to compensated hearts which seem to have become more resistant. Similar changes have recently been described by Kang *et al.*[50], both in vivo and in vitro.

The concept that there are signalling pathways specifically linked to either compensated or decompensated hypertrophy, has been gaining more acceptance over the last couple of years, for a recent review see[5]. However, the time point at which these discriminating signals are activated, i.e., the suggested transition of hypertrophy to heart failure, is unknown. Our observation that discriminating pathways have already been invoked very early in myocardial remodelling, and not after compensation has failed, challenges the paradigm that there is in fact such a transition.

Clinical Relevance

Primary pulmonary hypertension is a disease which usually has a rapid course. Patients become symptomatic with non-specific complaints in about two years. Upon presentation, patients may show rapid development of right failure (NYHA Class III - IV), some with only moderately increased pressures, whereas a sub-group of patients show pressures up to systemic levels who remain NYHA Class I, indicating successful

compensatory RV hypertrophy. The ability to make a reliable early prognosis concerning the progression of the disease state will be invaluable to clinicians. The use of diagnostic expression micro-arrays may therefore be ideal to distinguish patients at risk early after clinical presentation. However much work remains to be done before such diagnostic arrays are proven to be reliable and highly reproducible[51]. Our data indicate that such early differences can be detected, in an animal model for right ventricular hypertrophy secondary to pulmonary hypertension. These data may provide target genes for phenotypical screening early in the development of heart failure, and suggest potential targets for early clinical intervention.

Acknowledgement
We sincerely thank the people at the Micro-Array Department (MAD) of the Institute for life Sciences (SILS) at the Faculty of Science (FNWI) from the University of Amsterdam (UvA), The Netherlands, for their help and printing of the arrays used in this study.

Parts of these data were presented in a poster-session at the annual Keystone symposium "Molecular Biology of Cardiac Disease", March 7 - 12, 2004, Keystone, USA.

Reference List

(1) Levy D, Garrison RJ, Savage DD, Kannel WB, Castelli WP. Prognostic implications of echocardiographically determined left ventricular mass in the Framingham Heart Study. *N Engl J Med* 1990 May 31;322(22):1561-6.

(2) Condorelli G, Morisco C, Stassi G, Notte A, Farina F, Sgaramella G, de Rienzo A, Roncarati R, Trimarco B, Lembo G. Increased Cardiomyocyte Apoptosis and Changes in Proapoptotic and Antiapoptotic Genes bax and bcl-2 During Left Ventricular Adaptations to Chronic Pressure Overload in the Rat. *Circulation* 1999 June 15;99(23):3071-8.

(3) Frey N, Olson EN. Cardiac Hypertrophy: The Good, the Bad, and the Ugly. *Annu Rev Physiol* 2003 January 1;65(1):45.

(4) Chien K. Molecular biology of cardiac hypertrophy and heart failure. Grace A, Hunter J, editors. In *Molecular Basis of Cardiovascular Disease*, Chapter 9 , 211-250. 1999.

(5) Morisco C, Sadoshima J, Trimarco B, Arora R, Vatner DE, Vatner SF. Is treating cardiac hypertrophy salutary or detrimental: the two faces of Janus. *Am J Physiol Heart Circ Physiol* 2003 April 1;284(4):H1043.

(6) Doggrell SA, Brown L. Rat models of hypertension, cardiac hypertrophy and failure. *Cardiovascular Research* 1998 July 1;39(1):89-105.

(7) Wilson DW, Segall HJ, Pan LC, Lame MW, Estep JE, Morin D. Mechanisms and pathology of monocrotaline pulmonary toxicity. *Crit Rev Toxicol* 1992;22(5-6):307-25.

(8) Bernocchi P, Ceconi C, Pedersini P, Pasini E, Curello S, Ferrari R. Skeletal muscle metabolism in experimental heart failure. *J Mol Cell Cardiol* 1996 November;28(11):2263-73.

(9) Ceconi C, Condorelli E, Quinzanini M, Rodella A, Ferrari R, Harris P. Noradrenaline, atrial natriuretic peptide, bombesin and neurotensin in myocardium and blood of rats in congestive cardiac failure. *Cardiovasc Res* 1989 August;23(8):674-82.

(10) Wolkart G, Stromer H, Brunner F. Calcium Handling and Role of Endothelin-1 in Monocrotaline Right Ventricular Hypertrophy of the Rat. *Journal of Molecular and Cellular Cardiology* 2000 November;32(11):1995-2005.

(11) Seyfarth T, Gerbershagen HP, Giessler C, Leineweber K, Heinroth-Hoffmann I, Ponicke K, Brodde OE. The Cardiac [beta] -Adrenoceptor-G-protein(s)-adenylyl Cyclase System in Monocrotaline-treated Rats. *Journal of Molecular and Cellular Cardiology* 2000 December;32(12):2315-26.

(12) Brunner F, Wolkart G, Haleen S. Defective Intracellular Calcium Handling in Monocrotaline-Induced Right Ventricular Hypertrophy: Protective Effect of Long-Term Endothelin-A Receptor Blockade with 2-Benzo[1,3]dioxol-5-yl-3-benzyl-4-(4-methoxy-phenyl-)- 4-oxobut-2-enoate-sodium (PD 155080). *J Pharmacol Exp Ther* 2002 February 1;300(2):442-9.

(13) Wassen FW, Schiel AE, Kuiper GG, Kaptein E, Bakker O, Visser TJ, Simonides WS. Induction of thyroid hormone-degrading deiodinase in cardiac hypertrophy and failure. *Endocrinology* 2002 July;143(7):2812-5.

(14) Leineweber K, Brandt K, Wludyka B, Beilfuss A, Ponicke K, Heinroth-Hoffmann I, Brodde OE. Ventricular Hypertrophy Plus Neurohumoral Activation Is Necessary to Alter the Cardiac {beta}-Adrenoceptor System in Experimental Heart Failure. *Circ Res* 2002 November 29;91(11):1056-62.

(15) Kogler H, Hartmann O, Leineweber K, van Nguyen P, Schott P, Brodde OE, Hasenfuss G. Mechanical Load-Dependent Regulation of Gene Expression in Monocrotaline-Induced Right Ventricular Hypertrophy in the Rat. *Circ Res* 2003 July 3;01.

(16) Ecarnot-Laubriet A, Assem M, Poirson-Bichat F, Moisant M, Bernard C, Lecour S, Solary E, Rochette L, Teyssier J-R. Stage-dependent activation of cell cycle and apoptosis mechanisms in the right ventricle by pressure overload. *Biochimica et Biophysica Acta (BBA) - Molecular Basis of Disease* 2002 April 24;1586(3):233-42.

(17) Korstjens IJ, Rouws CH, van der Laarse WJ, Van der ZL, Stienen GJ. Myocardial force development and structural changes associated with monocrotaline induced cardiac hypertrophy and heart failure. *J Muscle Res Cell Motil* 2002;23(1):93-102.

(18) Versluis JP, Heslinga JW, Sipkema P, Westerhof N. Contractile reserve but not tension is reduced in monocrotaline-induced right ventricular hypertrophy. *Am J Physiol Heart Circ Physiol* 2004 March 1;286(3):H979-H984.

(19) Hudig F, Bakker O, Wiersinga WM. Amiodarone decreases gene expression of low-density lipoprotein receptor at both the mRNA and the protein level. *Metabolism* 1998 September;47(9):1052-7.

(20) Snijders AM, Nowak N, Segraves R, Blackwood S, Brown N, Conroy J, Hamilton G, Hindle AK, Huey B, Kimura K, Law S, Myambo K, Palmer J, Ylstra B, Yue JP, Gray JW, Jain AN, Pinkel D, Albertson DG. Assembly of microarrays for genome-wide measurement of DNA copy number. *Nat Genet* 2001 November;29(3):263-4.

(21) Edgar R, Domrachev M, Lash AE. Gene Expression Omnibus: NCBI gene expression and hybridization array data repository. *Nucl Acids Res* 2002 January 1;30(1):207-10.

(22) Tusher VG, Tibshirani R, Chu G. Significance analysis of microarrays applied to the ionizing radiation response. *PNAS* 2001 April 24;98(9):5116-21.

(23) Stouffer SA, Guttman L, Suchman EA, Suchman EA. Measurement and Prediction. Princeton University Press . 1950.

(24) Lame MW, Jones AD, Wilson DW, Dunston SK, Segall HJ. Protein Targets of Monocrotaline Pyrrole in Pulmonary Artery Endothelial Cells. *J Biol Chem* 2000 September 8;275(37):29091-9.

(25) Yoshihara F, Nishikimi T, Horio T, Yutani C, Nagaya N, Matsuo H, Ohe T, Kangawa K. Ventricular adrenomedullin concentration is a sensitive biochemical marker for volume and pressure overload in rats. *Am J Physiol Heart Circ Physiol* 2000 February 1;278(2):H633-H642.

(26) Flashman E, Redwood C, Moolman-Smook J, Watkins H. Cardiac Myosin Binding Protein C: Its Role in Physiology and Disease. *Circ Res* 2004 May 28;94(10):1279-89.

(27) Miyauchi T, Yorikane R, Sakai S, Sakurai T, Okada M, Nishikibe M, Yano M, Yamaguchi I, Sugishita Y, Goto K. Contribution of endogenous endothelin-1 to the progression of cardiopulmonary alterations in rats with monocrotaline-induced pulmonary hypertension. *Circ Res* 1993 November;73(5):887-97.

(28) Jones JE, Mendes L, Rudd MA, Russo G, Loscalzo J, Zhang YY. Serial noninvasive assessment of progressive pulmonary hypertension in a rat model. *Am J Physiol Heart Circ Physiol* 2002 July 1;283(1):H364-H371.

(29) Klein I, Ojamaa K. Thyroid Hormone and the Cardiovascular System. *N Engl J Med* 2001 February 15;344(7):501-9.

(30) Kim SZ, Cho KW, Kim SH. Modulation of endocardial natriuretic peptide receptors in right ventricular hypertrophy. *Am J Physiol Heart Circ Physiol* 1999 December 1;277(6):H2280-H2289.

(31) Vikstrom KL, Bohlmeyer T, Factor SM, Leinwand LA. Hypertrophy, Pathology, and Molecular Markers of Cardiac Pathogenesis. *Circ Res* 1998 April 20;82(7):773-8.

(32) Eaton S. Control of mitochondrial [beta]-oxidation flux. *Progress in Lipid Research* 2002 May;41(3):197-239.

(33) Galland S, Georges B, Le Borgne F, Conductier G, Dias JV, Demarquoy J. Thyroid hormone controls carnitine status through modifications of gamma-butyrobetaine hydroxylase activity and gene expression. *Cell Mol Life Sci* 2002 March;59(3):540-5.

(34) Heidebreder M, Frolich F, Johren O, Dendorfer A, Qadri F, Dominiak P. Hypoxia rapidly activates HIF-3{alpha} mRNA expression. *FASEB J* 2003 August 1;17(11):1541-3.

(35) Rong R, Ahn JY, Huang H, Nagata E, Kalman D, Kapp JA, Tu J, Worley PF, Snyder SH, Ye K. PI3 kinase enhancer-Homer complex couples mGluRI to PI3 kinase, preventing neuronal apoptosis. *Nat Neurosci* 2003 November;6(11):1153-61.

(36) Gill SS, Pulido OM, Mueller RW, McGuire PF. Immunochemical localization of the metabotropic glutamate receptors in the rat heart. *Brain Research Bulletin* 1999 January 15;48(2):143-6.

(37) Gonzalez-Juanatey JR, Pineiro R, Iglesias MJ, Gualillo O, Kelly PA, Dieguez C, Lago F. GH prevents apoptosis in cardiomyocytes cultured in vitro through a calcineurin-dependent mechanism. *J Endocrinol* 2004 February;180(2):325-35.

(38) Ravingerova T, Barancik M, Strniskova M. Mitogen-activated protein kinases: a new therapeutic target in cardiac pathology. *Mol Cell Biochem* 2003 May;247(1-2):127-38.

(39) Kaiser RA, Bueno OF, Lips DJ, Doevendans PA, Jones F, Kimball TF, Molkentin JD. Targeted Inhibition of p38 Mitogen-activated Protein Kinase Antagonizes Cardiac Injury and Cell Death Following Ischemia-Reperfusion in Vivo. *J Biol Chem* 2004 April 9;279(15):15524-30.

(40) Fuller SJ, Davies EL, Gillespie-Brown J, Sun H, Tonks NK. Mitogen-activated protein kinase phosphatase 1 inhibits the stimulation of gene expression by hypertrophic agonists in cardiac myocytes. *Biochem J* 1997 April 15;323 (Pt 2):313-9.

(41) Bueno OF, De Windt LJ, Lim HW, Tymitz KM, Witt SA, Kimball TR, Molkentin JD. The Dual-Specificity Phosphatase MKP-1 Limits the Cardiac Hypertrophic Response In Vitro and In Vivo. *Circ Res* 2001 January 19;88(1):88-96.

(42) Park MT, Choi JA, Kim MJ, Um HD, Bae S, Kang CM, Cho CK, Kang S, Chung HY, Lee YS, Lee SJ. Suppression of Extracellular Signal-related Kinase and Activation of p38 MAPK Are Two Critical Events Leading to Caspase-8- and Mitochondria-mediated Cell Death in Phytosphingosine-treated Human Cancer Cells. *J Biol Chem* 2003 December 12;278(50):50624-34.

(43) Remondino A, Kwon SH, Communal C, Pimentel DR, Sawyer DB, Singh K, Colucci WS. {beta}-Adrenergic Receptor-Stimulated Apoptosis in Cardiac Myocytes Is Mediated by Reactive Oxygen Species/c-Jun NH2-Terminal Kinase-Dependent Activation of the Mitochondrial Pathway. *Circ Res* 2003 February 7;92(2):136-8.

(44) Montoya J, Perez-Martos A, Garstka HL, Wiesner RJ. Regulation of mitochondrial transcription by mitochondrial transcription factor A. *Mol Cell Biochem* 1997 September;174(1-2):227-30.

(45) Ekstrand MI, Falkenberg M, Rantanen A, Park CB, Gaspari M, Hultenby K, Rustin P, Gustafsson CM, Larsson NG. Mitochondrial transcription factor A regulates mtDNA copy number in mammals. *Hum Mol Genet* 2004 May 1;13(9):935-44.

(46) Fosslien E. Review: Mitochondrial medicine--cardiomyopathy caused by defective oxidative phosphorylation. *Ann Clin Lab Sci* 2003;33(4):371-95.

(47) Garnier A, Fortin D, Delomenie C, Momken I, Veksler V, Ventura-Clapier R. Depressed mitochondrial transcription factors and oxidative capacity in rat failing cardiac and skeletal muscles. *J Physiol (Lond)* 2003 September 1;551(2):491-501.

(48) Crompton M, Barksby E, Johnson N, Capano M. Mitochondrial intermembrane junctional complexes and their involvement in cell death. *Biochimie* 2002;84(2-3):143-52.

(49) Weiss JN, Korge P, Honda HM, Ping P. Role of the Mitochondrial Permeability Transition in Myocardial Disease. *Circ Res* 2003 August 22;93(4):292-301.

(50) Kang PM, Yue P, Liu Z, Tarnavski O, Bodyak N, Izumo S. Alterations in Apoptosis Regulatory Factors During Hypertrophy and Heart Failure. *Am J Physiol Heart Circ Physiol* 2004 March 4;00556.

(51) van den IJssel P, Eijk P, Hopmans E, Kasanmoentalib S, Ylstra B. Quality Of In-House Made High-Density Microarrays. Encyclopedia of Diagnostic Genomics & Proteomics (EDGP) , 1108-1112. 12-9-2004.

Chapter 3

Maladaptive Myocardial Hypertrophy In Pressure Overload Does Not Evolve From An Adaptive Precursor State

Henk P.J. Buermans[1], René J. P. Musters[1], Mark van de Wiel[2]
Marian J. Zuidwijk[1], Cornelis van Hardeveld[1], Bauke Ylstra[2]
Frans C. Visser[3], Walter J. Paulus[1], Warner S. Simonides[1]

1. Laboratory for Physiology, Institute for Cardiovascular Research (ICaR-VU), VU University Medical Center, Van der Boechorststraat 7, 1081 BT Amsterdam, The Netherlands.

2. Micro-array core facility
VU University Medical Center, Van der Boechorststraat 7, 1081 BT Amsterdam, The Netherlands.

3. Department of Cardiology, Institute for Cardiovascular Research (ICaR-VU), VU University Medical Center, De Boelelaan 1117, 1081 HV Amsterdam, The Netherlands.

Submitted for publication

Table of contents

Abstract

Background-In pressure overload, maladaptive myocardial hypertrophy is presumed to evolve from an adaptive precursor state. This presumption was tested in a rat model of monocrotaline (MCT)-induced pulmonary hypertension(PH) using two doses of MCT. Methods and Results-After administration of 30 mg/kg (HYP-group), adaptive right ventricular(RV) hypertrophy was observed over a 25 day period whereas after 80 mg/kg (CHF-group), adaptive RV hypertrophy evolved from day 19 into maladaptive RV hypertrophy. RV myocardium of HYP and CHF was compared by micro-array analysis at day 10, when RV phenotypes were identical, at day 19, when RV phenotypes started to diverge and at day 25, when RV phenotypes differed. Differential gene expression between HYP and CHF was already present at day 10. The number of genes with differential expression between HYP and CHF remained almost constant (day 10: 13; day 19: 13; day 25: 16). Self-organizing-maps(SOM)-clustering revealed for several gene-clusters earlier up- or downregulation in CHF than in HYP. Gene-Ontology-analyses and real-time PCR showed genes promoting cell-cycling such as cyclin-B1 to be among the early (day 10) upregulated genes in CHF. In HYP, the rise in cyclin-B1 occurred later (day 19) and was accompanied by higher expression of the G2/M-transition inhibitor Gadd45a. Conclusions-The early presence of differentially expressed genes and the constancy of their number over time indicates RV myocardium of HYP and CHF to differ already shortly after imposition of the overload without a shared adaptive precursor state. Premature upregulation of genes promoting cell-cycling without suppressed G2/M-transition characterized future development of a maladaptive phenotype.

Introduction

Cardiac hypertrophy is often perceived as an initial and beneficial adaptive response to pressure overload[1]. Many patients with arterial hypertension, aortic stenosis or primary PH indeed remain asymptomatic for a prolonged period of time before heart failure develops. Prior to heart-failure development, a transition from adaptive to maladaptive ventricular hypertrophy is presumed to have occurred. Numerous processes in the cardiac myocyte, such as signal transduction[2, 3], use of energy substrates[4] and calcium handling[5] have been implicated in this transition but there is no agreement on the process or combination of processes that is ultimately responsible for the transition from adaptive to maladaptive left ventricular (LV) hypertrophy. Furthermore, the paradigm of such a transition is challenged both by epidemiological studies, which showed LV hypertrophy to be associated with higher morbidity and mortality[6, 7] and by clinical studies, which observed a higher prevalence of LV hypertrophy in aortic stenosis patients presenting with heart failure[8, 9]. These studies suggest that pressure overload-induced ventricular hypertrophy becomes maladaptive immediately following imposition of the overload stimulus. Usually the adaptive and maladaptive outcomes are presumed to emerge from an identical adaptive precursor state that occurs subsequent to imposition of the overload stimulus and prior to the emergence of the final hypertrophic phenotype. The transition to maladaptive hypertrophy is hereby presumed to result from the inability of the compensatory mechanisms to cope with the magnitude of the overload[2, 10], while adaptive hypertrophy remains a mere continuation of the precursor state.

We recently introduced a modification of the established rat monocrotaline (MCT) model for PH and right ventricular (RV) hypertrophy, which by using two different doses of MCT (30 or 80 mg/kg bw) allows for the controlled induction within 25 days of either an adaptive (30 mg/kg bw) or maladaptive (80 mg/kg bw) RV hypertrophic phenotype[11]. For both doses of MCT, the RV response proceeds through an initial phase of RV hypertrophy (day 14-19). From day 19 on, the animals that received 80 mg/kg progress towards decompensation and premature death around day 25-28. In these rats, decompensation is evident from progressive weight loss and signs of right-sided failure such as ascites and pleural effusion. In contrast, compensated RV hypertrophy develops in the animals that received 30 mg/kg since these animals show no signs of failure up to 84 days after MCT injections[11]. This model of controlled phenotypical outcome provides the unique opportunity to characterize the myocardial response to pressure overload during the initial stages after imposition of the overload stimulus before phenotypical differences become apparent. Using micro-

array analyses in this model, we observed significant differences in gene-expression levels between the two MCT doses at day 14 after the MCT injections when the hypertrophic response in both groups was identical[11]. Similar results were reported by Sharma *et al*. during development of LV hypertrophy in homozygous transgenic TGRmRen2-27 rats that progressed either towards adaptive hypertrophy or maladaptive hypertrophy with failure[12]. This early detection of differential gene expression in both studies challenges the presence of a common adaptive precursor state for the two phenotypical outcomes. In the present study, gene-expression profiles were obtained in the MCT-induced PH model at an earlier stage, namely 10 days following administration of either 30 or 80 mg/kg MCT and subsequently compared to gene-expression profiles 19 and 25 days following administration of MCT. The following questions were addressed: 1) Do RV myocardial gene-expression profiles differ 10 days after MCT administration between rats receiving 30 or 80 mg/kg MCT? 2) How does a difference in gene-expression profile evolve over time, i.e., does the number of differentially expressed genes rise over time as one would expect if both phenotypical outcomes progressively diverge from a common precursor, or does the number of differentially expressed genes fall over time as a result of the HYP group catching up in gene expression after a smaller initial stimulus? 3) What is the identity of the genes that are differentially expressed, are these genes associated with specific pathways and can these pathways be related to phenotypical outcome?

Methods

Animals

Animals were treated according to the national guidelines and with the permission of the Institutional Animal Care and Use Committee (IACUC) of the VU University Medical Center Amsterdam, the Netherlands. Male Wistar Rats, weighing 180-200 g (Harlan, Zeist, The Netherlands) were housed individually (250 cm^2/animal) and received food and water ad libitum.

A total of 36 animals were randomly assigned to three groups. All animals received a single subcutaneous injection with either saline (control group: CON, n=12), 30 mg MCT/kg body weight (stable adaptive hypertrophy group: HYP, n=12) or 80 mg MCT/kg body weight (maladaptive hypertrophy, congestive heart failure group: CHF, n=12). At day 10, 19 and 25 after treatment, four animals from each group were randomly picked and sacrificed with a halothane overdose. Lungs were excised, hearts were rinsed by perfusion and the left ventricle (LV) and right ventricle (RV) and interventricular septum (IVS) were separated. All tissues were weighed and snap frozen in liquid nitrogen and stored at -80 ºC. Three animals per group per time point were used for the micro-arrays analysis.

Force Measurements

A parallel group of CON (n=4), HYP (n=5) and CHF animals (n=4) was used for assessing RV contractile properties by analysis of isolated trabeculae at 25 days after imposition of pressure overload. The heart was rapidly excised and a trabecula was isolated from the RV as described in detail before[13]. Trabeculae were stretched to 87% of the length (L_{max})at which maximum force (F_{max}) was developed, yielding a passive force of ~8% of Fmax. Trabeculae were equilibrated for 45 min at a stimulation frequency of 0.5 Hz. The force-frequency relationship (FFR) was determined by measuring the developed active force relative to baseline (0.2 Hz) in response to a stepwise increase in the stimulation frequency up to 8 Hz. Length and dry-weight of the trabeculae were determined to calculate the cross-sectional area, assuming a cylindrical preparation.

Micro-Array Experimental Procedures, Data Handling, Statistical Analysis And Real-Time PCR

The Compugen Rat OligoLibrary™ representing 4803 genes was used. Protocols concerning all procedures can be found in the *additional methods section*. This section also contains information regarding data handling and statistical ANOVA

analysis. Figure 1 schematically depicts the micro-array data handling and analysis steps as performed.

Self Organizing Maps Clustering

Significantly-regulated genes were clustered using a self-organizing-map (SOM) with the Tigr Multiple-experiment-viewer (MeV) software package[14]. Control values per time point were set to zero. Prior to clustering, average expression values per group were mean centered and normalized for genes and arrays. The HYP and CHF expression profiles were entered as a single profile per gene. Expression plots were generated by superimposing the HYP and CHF expression profiles for each cluster. This ensured that the HYP and CHF expression profiles for each single gene were present in the same cluster. A 4-by-4 SOM cluster was generated using Pearson correlation as metric with 600K iterations and cluster $p<0.05$.

Gene-Ontology Classifications

Genes in each of the 16 resulting SOM-clusters were analysed for over-represented themes using the Expression Analysis Systematic Explorer (EASE)[15] tool. Clustered genes were tested for over-representation of specific transcription factor bindings

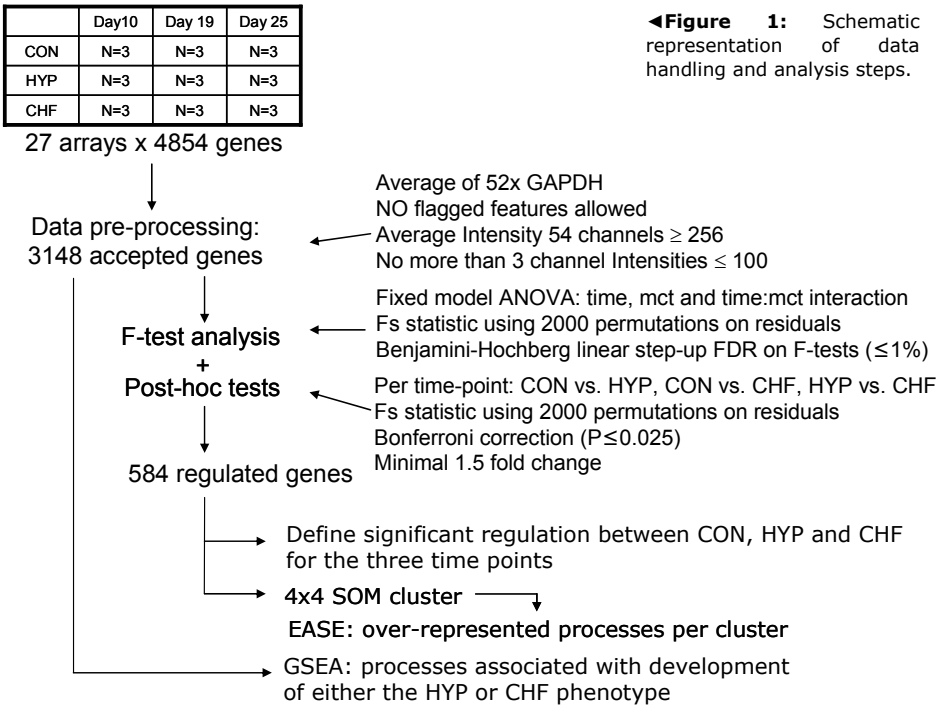

◄**Figure 1:** Schematic representation of data handling and analysis steps.

sites (TFBS), GenMapp and KEGG pathways and the gene ontology classifications for molecular function, cellular component and biological processes, with the enhanced annotation option enabled (same official gene symbol, Homologene COGs, Homologenes and same gene symbol for human, mouse and rat). The background population used were the 3148 genes that were analyzed in the ANOVA analysis. Gene classifications needed to represented at least three genes and have a EASE-test p-value below 0.05 to be considered over-represented.
The HYP vs. CHF group comparisons for each time point were explored using the Gene set enrichment analysis (GSEA)[16] java-package. Only GenMapp pathways were included in this analysis. Due to the low number of replicates, 1000 permutations on genes were used. In consideration with the known issues of possible overestimation of significance levels when using this type of permutation, the FDR q-val cutoff was set at 0.05 instead of the 0.25 value used in the methodological manuscript[16].

Statistical Analysis For Real-Time-PCR And Hypertrophic Parameters
MCT parameters, real-time PCR and FFR measurements were evaluated for significant differences with a two-factor ANOVA with Bonferroni corrected post-hoc tests. Significant and positive correlation between the array and real-time PCR was determined with a Pearson correlation test ($p<0.05$). Data in Tables and Figures are presented as means ± standard error unless stated otherwise. * : $p<0.05$ rel to CON same time point, † : $p<0.05$ rel to HYP same time point.

Additional Methods Section

Total RNA Isolation

Total RNA isolation and real-time PCR were performed as previously described[11]. A common reference RNA pool for the micro-array procedures was constructed by pooling the RNA from IVS samples of animals sacrificed at 19 and 25 days.

Micro-Array Procedures

Array printing: The Compugen Rat OligoLibrary™ was purchased from Sigma-Aldrich. Oligonucleotides were printed on Motorola CodeLink™ activated slides (Amersham Biosciences) using an Perkin Elmer Piezorray non-contact micro dispensing printer. Features were spotted in duplicates divided into two separate regions on the array surface.

Preparation of labelled cDNA probe: Three animals per time point per group were selected for micro-array analysis. cDNA strands were generated from 30 µg total RNA taken from the RV as previously described[11, 17]. In short, cDNA was synthesis was performed using an oligo-dT [(dT)20-VN] primer (Invitrogen) and SuperScript™ II Reverse Transcriptase (Invitrogen) with incorporation of aminoallyl-dUTP. Probes were indirectly labelled with Fluorolink Cy3 and Cy5 mono-functional dyes for the Reference pool and RV samples, respectively.

Micro-array hybridization: Prior to use, the slides were processed following guidelines provided in the manufacturers protocol. Pairs of labelled reference pool (Cy3) and RV sample (Cy5) were combined in a hybridization mix containing 50% formamide and 2x SSC. Hybridization time was set to 14 hours at 37 ºC with agitation, using a Perkin Elmer HybArray 12™ hybridization station. Detailed information on the probe generation and hybridization procedures can be found at http://www.vumc.nl/microarrays/onderzoek/index.html?protocols.html~hoofd.

Data Acquisition And Processing

Slides were scanned at a 10 µm resolution for Cy3 and Cy5 intensities using a Perkin-Elmer Multi Laser Micro-Array Scanner operated by the ScanArray Express v1.0 software. Array images were processed with Imagene v5.1. Spot signal intensities had to be at least three times higher than the local background to allow further processing. Mean Cy3 and Cy5 intensities were background corrected and duplicate signals for each feature on the array were averaged. The number of GAPDH replicates (52x) were averaged. To ensure a balanced design for a robust analysis of variance framework, only genes without flags in any of the 27 arrays were selected for analysis. In addition, genes with a average spot intensity over all 54 channels of

the 27 arrays below 256, were excluded from further processing, as were genes with more than three of the 54 channel intensities below 100. For the remaining genes, Cy3 and Cy5 mean channel intensities were log2 transformed, mean centered and standardized.

Micro-Array Data Analysis

We performed a modified analysis of variance (ANOVA) method to test for differential expression in our dataset[18]. This F-statistic estimates the error variance by borrowing cross-gene information using the James-Stein shrinkage concept as described by Cui *et al*.[19]. This approach is appropriate for datasets with a small number of biological replicates, as in our case, n=3 per group and is supposed to result in a more stable estimate of the error variance.

To evaluate the 3148 genes for differential expression, a fixed model ANOVA was used. Factors included in the ANOVA analysis were array, MCT treatment, time point and the interaction between MCT treatment and time point. Significance of the interaction factor would indicate that the effect of MCT treatment is not constant over time. P-values were calculated using 2000 permutations on residuals, using the Fs statistic. Benjamini-Hochberg linear step-up false discovery rate (FDR) corrections[20] were performed separately on the F-tests for MCT treatment, Time point and interaction factor (FDR<1%). Bonferroni corrected post-hoc tests ($p<0.025$) were performed for all three time points separately for the CON vs. HYP, CON vs. CHF and HYP vs. CHF comparisons. Per gene this lead to three post-hoc t-tests per time point. Additionally, a minimal 1.5 fold change for post-hoc comparisons was included. All calculations were performed in R-statistics v2.0.1 using the Maanova package v0.98.3.

Results

MCT-Induced RV Hypertrophy

Subcutaneous injection of MCT resulted in a progressive increase in lung weight for both the HYP and CHF groups. This increase was already significant at day ten, while a significant difference between the HYP and CHF group was observed at day 25. The increase in lung weight is indicative of increased pulmonary vascular resistance[21, 22] resulting in RV hypertrophy as evidenced by the increase in RV to LV + IVS weight ratio at day 19 and 25 for both the HYP and CHF groups. These parameters are shown in Table 1 with the body weights of these animals at the time of sacrifice. Growth curves are depicted in Figure 2, indicating the drastic fall in body weight in the CHF group after day 19. In agreement with our earlier data, these animals showed secondary signs of heart failure, including pleural effusion and ascites. Contractile properties of RV trabeculae at day 25 were subsequently analyzed to assess myocyte function in both hypertrophy groups relative to controls.

Contractile Characteristics Of RV Trabeculae And FFR

Maximal active force of trabeculae expressed per unit cross-sectional area did not differ between the experimental groups (CON: 22 ± 3, HYP: 40 ± 9 and CHF: 25 ± 6 mN/mm2). Control trabeculae exhibited a positive FFR between 0.2 and 8 Hz, in agreement with earlier reports[23], while those from the CHF group showed no potentiation (Figure 2). In contrast, trabeculae of the HYP group displayed a potentiation of force similar to control trabeculae. The difference in FFR between the HYP and the CHF group is indicative of the presence of maladaptive hypertrophy in the CHF group and adaptive hypertrophy in the HYP group.

Inter-Group Differences In Gene Expression

RV gene-expression profiles were determined for the three groups at day 10, 19 and 25. The total number of genes analyzed after pre-processing equalled 3148. When comparing CON to HYP, 8, 123 and 386 genes were differentially expressed at day 10, 19 and 25, respectively. When comparing CON to CHF, 42, 125 and 454 genes

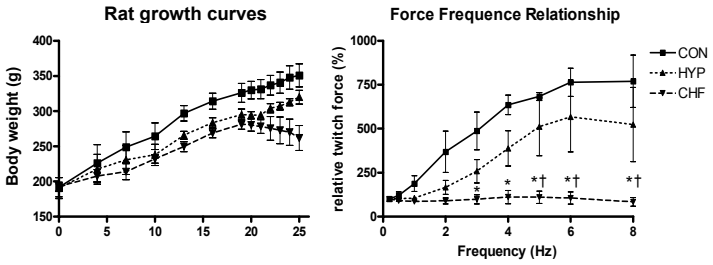

◄**Figure 2:** Left panel: Growth curves of the CON, HYP and CHF animals up to day 25. Data represent Mean ± SD. Right panel: Force frequency relationship. Active twitch force is expressed relative to that at 0.2 Hz (100%). Data represent Mean ± SE.

		Lung (g)	RV (mg)	RV / LV+IVS (mg/mg)	Body weight (g)
Day 10	CON	1.07 ± 0.04	151 ± 8	0.22 ± 0.02	248 ± 4
	HYP	1.39 ± 0.02 *	149 ± 7	0.24 ± 0.01	226 ± 4 *
	CHF	1.39 ± 0.05 *	130 ± 11	0.24 ± 0.01	229 ± 4
Day 19	CON	1.29 ± 0.03	159 ± 5	0.20 ± 0.01	333 ± 8
	HYP	1.57 ± 0.10 *	185 ± 17	0.25 ± 0.01 *	302 ± 4 *
	CHF	1.80 ± 0.03 *	188 ± 13	0.28 ± 0.02 *	285 ± 4 *
Day 25	CON	1.31 ± 0.02	147 ± 11	0.18 ± 0.01	351 ± 8
	HYP	1.72 ± 0.06 *	329 ± 24 *	0.40 ± 0.02 *	320 ± 5 *
	CHF	2.22 ± 0.14 *†	295 ± 13 *	0.42 ± 0.01 *	262 ± 9 *†

▲**Table 1:** Measured parameters for the CON, HYP and CHF groups at 10, 19 and 25 days after MCT injections.

were differentially expressed at day 10, 19 and 25, respectively. The increase over time in the number of differentially expressed genes observed in both the HYP and CHF groups is consistent with the progression of RV hypertrophy. In contrast, when comparing HYP to CHF the number of differentially expressed genes is almost constant with 13 genes differentially expressed on day 10, 13 genes on day 19 and 16 genes on day 25. Even more remarkable, when expressed relative to the total number of differentially expressed genes, the number of genes that are differentially expressed between the HYP and CHF groups fell progressively (day 10: 23.6%; day 19: 7.5%; day 25: 3.1%). Furthermore, as evident from Figure 3A, the genes with differential expression between the HYP and CHF groups varied at each time point, whereas genes with differential expression between the CON and HYP or CON and CHF groups showed considerable overlap at successive time points (Figures 3B and 3C).

The total number of differentially expressed genes equalled 584. A complete listing of these 584 genes is given in Online Results supplement A. The array data set has been deposited in the Gene-expression Omnibus[24] as series GSE3675.

Time-Dependent Changes In Gene Expression

To evaluate the time-dependent expression alterations of individual genes in the HYP and CHF groups, a 4-by-4 Self Organizing Map (SOM) clustering was performed on all 584 differentially expressed genes (Figure 4 A through P). At each time point, the expression of an individual gene in HYP (green lines) or CHF (red-lines) was

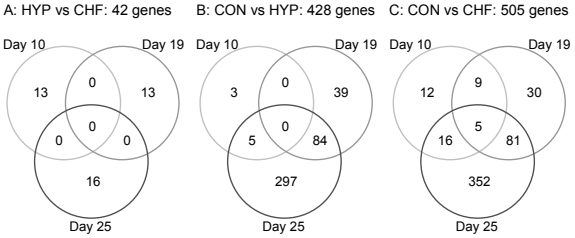

◄**Figure 3:** Overlap of significantly regulated genes at the three time points for each of the three pair-wise group comparisons, i.e., HYP vs. CHF (A), CON vs. HYP (B) and CON vs. CHF (C), respectively.

expressed relative to control levels, which was set to zero. Opposite expression profiles ended up at opposing sides of the cluster grid, with continuously downregulated genes predominantly located in the top row, and continuously upregulated genes in the bottom row. The middle two rows contain genes whose expression shifts over time.

In clusters J and K and to a lesser extent in clusters A, C and O, upregulated or downregulated individual genes occurred earlier in CHF (red lines) than in HYP (green lines) as evident from the red lines rising or falling on day 10 and the green lines displaying a similar pattern only at day 19. At day 25, up- or downregulation of gene expression had become similar in CHF and HYP as evident from the overlap of red and green lines. This finding implies that development of CHF phenotype is related more to the timing of gene expression than to changes in expression of specific genes. Earlier upregulation of expression of genes in the CHF group could be explained by faster elevation of RV wall stress because of more rapid development of PH after administration of 80 mg/kg MCT.

An ontology analysis for each of these 16 clusters, indicated significant over-representation of several biological themes. Genes with protein products located in the mitochondria showed a significant call in clusters A through D and G. All these clusters had progressively downregulated expression levels. The same clusters also contained genes encoding protein products associated with cell metabolism, e.g., lipid metabolism, mitochondrial fatty-acid beta-oxidation and amino acid metabolism. Another over-represented theme was cell-cycling in cluster J. Genes encoding for protein products of the extracellular space were over-represented in cluster D, which corresponded with continuous downregulation over time, as well as in cluster P which corresponded with continuous upregulation over time. A complete overview of over-represented classes is given for each cluster in Online Results supplement B.

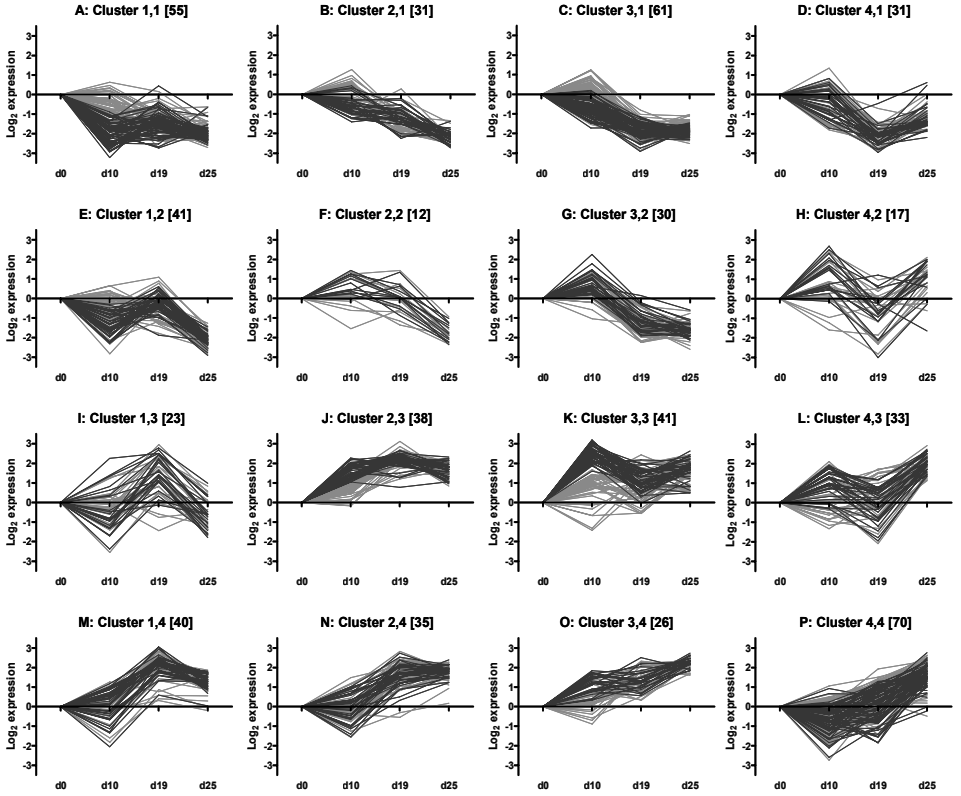

▲**Figure 4:** Expression profiles for all genes in the 16 clusters were corrected for control values per time point. HYP (green lines) and CHF (red lines) expression patterns were superimposed. The total number of genes per cluster is indicated in brackets next to the cluster designation. Note the expression differences at day 10 for clusters J and K while profiles overlap at day 19 and 25.

Inter-Group Differences In Gene Expression Using Gene Set Enrichment Analysis

Gene-expression differences on day 10, 19 and 25 between HYP and CHF were further analysed using the GSEA program to assess differential activation of specific GenMapp pathways (Table 2). GenMapp pathways showing significant enrichment scores for the HYP vs. CHF comparisons again included cell cycle and electron transport chain (ETC). For the cell-cycle pathway 7 genes were upregulated at day 10. The position of the upregulated genes in the cell-cycle pathway is indicated in Figure 1 of online Results supplement C. For the ETC, 15 genes were upregulated at day 10 and 12 genes downregulated at day 25, predominantly affecting complexes I, IV and V. These observations suggest that relative to the HYP group, oxidative phosphorylation activity in the CHF group is upregulated early and downregulated

	Pathway	Gene number - Regulated	Normalized Enrichment score (| NES|)	FDR q-val
day 10	G protein signalling	10 - Down in CHF	1.81	0.034
	Electron transport chain	15 - Up in CHF	1.71	0.038
	Cell cycle	7 - Up in CHF	2.01	0.005
	Ribosomal proteins	20 - Up in CHF	1.67	0.035
day 19	Ribosomal proteins	19 - Up in CHF	2.26	0.001
day 25	Electron transport chain	12 - Down in CHF	1.92	0.010
	Proteasome degradation	11 - Down in CHF	1.80	0.019

▲**Table 2:** Summary of pathways implicated by a GSEA of CHF relative to the HYP group, at all three time points. Indicated for each GenMapp pathway are the number of genes supporting the pathway, expression level in the CHF group relative to the time-matched HYP group, the absolute value of the normalized enrichment score and the FDR q-value.

late during development of maladaptive hypertrophy. The position of the up- or downregulated genes in the ETC is indicated in Figure 2 of online Results supplement C. Other GenMapp pathways showing significant enrichment scores were related to G-protein signalling, ribosomal proteins and proteasome degradation.

Real-Time PCR Confirmation

As a reliability check, the micro-array data were tested for a significant correlation with SYBR-green based real-time PCR. Figure 5 shows bar graphs with the micro-array and real-time PCR data with a correlation plot between both methods for a selection of genes. Figure 3 in Online Results Supplement 3 shows the correlation plots for several other confirmed genes. Overall, over 80% of checked genes showed significant positive Pearson correlation p-values.

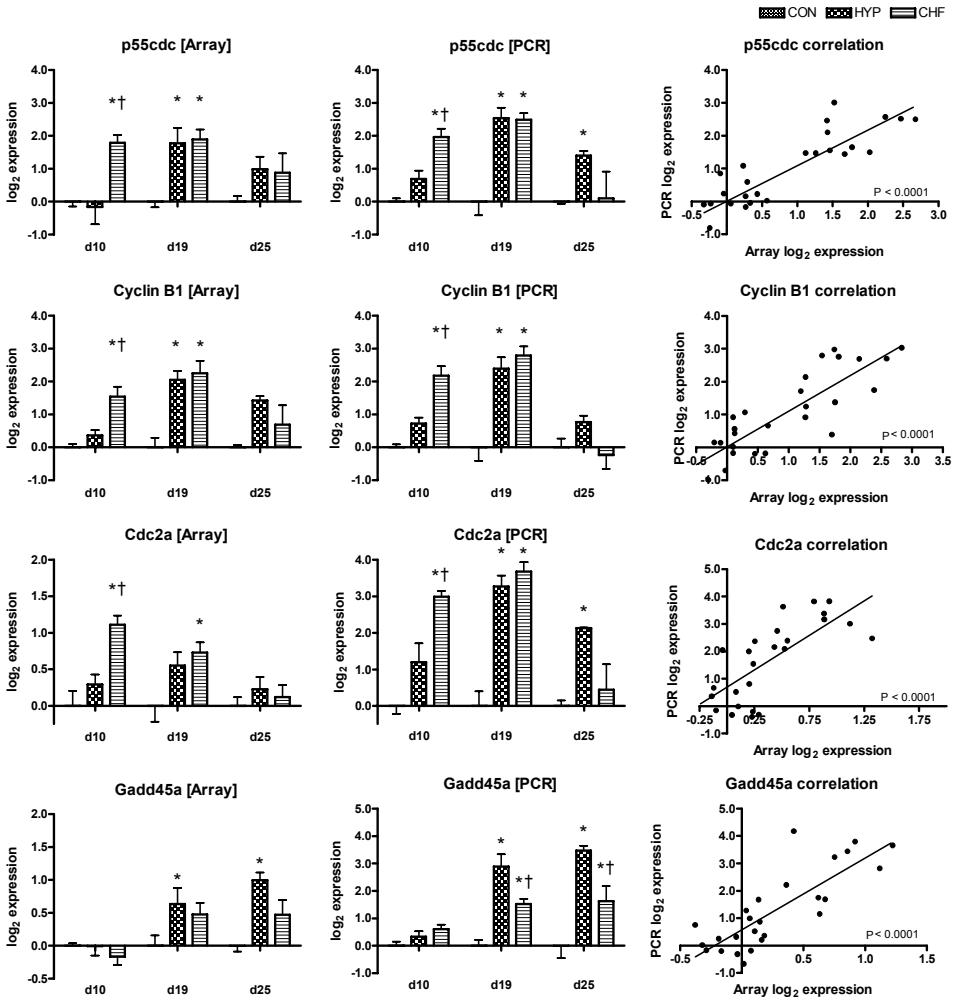

▲**Figure 5:** Log_2 expression values for array and real-time PCR data and an array-PCR correlation-plot for heme-oxygenase1 (HO1) and the cell cycle related genes cell division cycle control protein 2 (Cdc2a / Cdk1), growth arrest and DNA-damage-inducible-alpha (Gadd45a), cyclin B1 and cell division cycle 20 homolog (p55cdc / cdc20). For each time point the CON values were set to zero.

Discussion

The present study observed the following findings: 1) A comparison of gene-expression profiles between HYP and CHF groups revealed the number of differentially expressed genes to be small and to remain almost constant at the different time points (day 10: 13; day 19: 13 and day 25: 16). 2) SOM-clustering of all differentially expressed genes detected important differences in the time-course of up- or downregulation of gene expression. For several clusters of genes, up- or downregulation of gene expression occurred earlier in CHF (day 10) than in HYP (day 19) but later (day 25) gene-expression profiles of these two groups were largely overlapping. This implies development of the CHF phenotype to result from differences in timing of up- or downregulation of gene expression and not from up- or downregulation of specific genes. The varying identity of the differentially expressed genes between the HYP and CHF groups over time (Figure 3A) also fits the observation of a phase shift of gene expression between the HYP and CHF groups whereby the HYP group progressively catches-up in terms of its gene-expression profile with the CHF group (Figure 4). 3) In the CHF group, both ontology analysis of the SOM clusters and GSEA showed initial (day 10) upregulation of genes involved in cell-cycling and electron transport chain. Premature upregulation of these genes seems to predispose RV myocardium to a maladaptive hypertrophic phenotype in experimental MCT-induced PH.

Controlled Induction Of RV Hypertrophy Or Failure

The present study used a previously described[11] modification of the rat MCT model of PH-induced RV hypertrophy which allows for controlled induction of either adaptive or maladaptive RV hypertrophy. The impaired FFR of isolated trabeculae in the CHF group, but not in the HYP group, illustrate the critical difference in contractile function between the adaptive and maladaptive forms of RV hypertrophy (Figure 2). The observed difference in FFR may be related to the previously reported lower RV expression level of SERCA2a in CHF relative to HYP at 25 days after MCT injections[11], since SERCA2a activity is a determinant of the frequency-dependent increase in Ca^{2+}-transient amplitude which underlies the positive FFR in rat trabeculae[23].

Since the outcome for both groups was known in advance, RV myocardial gene-expression profiles could be characterized at early stages of development of either adaptive or maladaptive RV hypertrophy well before functional or morphological differences between groups became apparent. Moreover, the stimulus for hypertrophy was similar in both groups, namely pressure overload, and differed only in severity. This avoided comparison of gene-expression profiles of adaptive and

maladaptive hypertrophy induced by different stimuli such as pressure overload and exercise training.

Differences In Gene-Expression Profiles Between HYP And CHF Groups

The number of differentially expressed genes between HYP and CHF groups was small and remained almost constant throughout the entire observation period. Small differences in myocardial gene expression were also observed in a mouse model of graded LV pressure overload when animals developing adaptive LV hypertrophy were compared to maladaptive LV hypertrophy[25]. Relative to the number of differentially expressed genes observed in the comparison between CON and HYP groups or CON and CHF groups, differential gene expression between HYP and CHF groups actually fell over time despite progressive phenotypic divergence. Absence of an initial identical gene-expression profile in HYP and CHF groups and absence of a progressive rise in the number of differentially expressed genes between HYP and CHF groups argue against a common adaptive hypertrophic phenotype from which both HYP and CHF phenotypes evolved.

Variation In Gene-Expression Profiles Over Time

The 16 clusters that were generated with the SOM analysis can be separated into two main categories, i.e., those clusters that do not show a difference in expression levels between the HYP and CHF groups at any of the three time points (B, D-I, L-N, and P) and those that show a difference in expression between the two hypertrophic phenotypes at day 10, with later disappearance of the observed difference (clusters J and K and to a smaller degree clusters A, C and O). Genes assigned to the first set of clusters can be regarded as genes involved in general hypertrophic remodelling. Many genes that were previously thought to be involved in the progression from adaptive to maladaptive hypertrophy can be found in these clusters. These genes showed altered expression levels relative to the control group, but no difference between the HYP and CHF groups. These genes included genes encoding for proteins involved in fatty-acid beta-oxidation (FAbOx)[4], genes encoding for mitochondrial proteins[26] and genes encoding for components of the extracellular matrix[27]. For the second set of SOM clusters, genes in the CHF group appear to be regulated prior to those in the HYP group. This catch-up of gene expression observed in the HYP group can be explained by the lower intensity of the hypertrophic stimulus to which the HYP group was subjected. These findings suggest the magnitude of the hemodynamic stimulus to be of critical importance for eventual development of a maladaptive hypertrophy phenotype. These findings are also in line with previous experiments in

dogs which developed maladaptive hypertrophy during LV pressure overload when baseline wall-stress prior to imposition of the aortic band was already elevated[28, 29].

Identity Of Differentially Expressed Genes

Identification of the genes significantly different between the HYP and CHF groups reveals information on the processes associated with development of either adaptive or maladaptive hypertrophy. Caution needs to be exerted when drawing conclusions based on over-representation of biological themes from a relatively small number of differentially regulated genes. In this study the number of differentially expressed genes between the HYP and CHF groups was relatively small and using the EASE-program this could render interpretation of over-representation of biological themes unreliable. Therefore, a GSEA approach was used to evaluate the differences in expression levels between the HYP and CHF groups in terms of over-representation of biological themes. The GSEA analysis indicated several GenMapp pathways such as cell-cycling and electron transport with differential expression between the HYP and CHF groups (Table 2).

In the cell-cycle pathway at day 10, three of seven genes showed a significant increase in expression levels in the CHF group relative to both the CON and HYP group, i.e., cell division cycle control protein 2 (Cdc2a / cdk1), cyclin B1 (Ccnb1) as well as cell division cycle 20 homolog (Cdc20), all three of which were confirmed by real-time PCR (Figure 5). The other four genes, i.e., pituitary tumor-transforming gene 1 (PTTG1), proliferating cell nuclear antigen (PCNA), Cyclin D1 (Ccnd1) and cell division cycle 25 homolog A (Cdc25a), had increased expression in CHF relative to HYP.

As a result of downregulation of cell-cycle related genes during postnatal development[30] cardiac myocytes are considered to remain in the G1 phase of the cell-cycle during their entire life-span. Increased levels of cell-cycle related genes have however been reported during hypertrophic ventricular remodelling[11, 12, 31, 32]. In the present study, increased mRNA levels of both cyclinB1 and cdk1 were observed 10 days after MCT administration in the CHF group and 19 days after MCT administration in both HYP and CHF groups. Upregulation of cyclinB1 and cdk1 indicates a progression from the G1 phase of the cell-cycle to the S and G2 phases. Subsequent nuclear translocation of the cyclinB1-Cdk1 complex (M-phase promoting factor; MPF), is a requisite for the G2/M transition. The activity of the MPF complex is inhibited by GADD45a which binds to the MPF complex and dissociates it. The present study observed significantly higher expression levels of GADD45a in the HYP groups relative to both the CON and CHF groups at days 19 and 25 following MCT administration. Hence, 10 days after MCT administration the upregulation of cyclinB1

and cdk1 in the CHF group occurs in the absence of GADD45a upregulation. This situation favours G2/M transition which can be deleterious in terminally differentially cells as it leads to mitotic catastrophe or apoptosis[33, 34]. The latter could relate to the maladaptive hypertrophic phenotype observed in the CHF group. In contrast, in the HYP group upregulation of cyclinB1 and cdk1 occurs later, at a time when expression of GADD45a is already increased. This prevents the deleterious effects of G2/M transition and could thereby preclude the development of maladaptive hypertrophy in this group.

Conclusion

In the present model of controlled induction of HYP and CHF phenotypes, genes that are differentially expressed between HYP and CHF groups are already observed early after imposition of the hypertrophy stimulus, which argues against the existence of an adaptive precursor state during development of adaptive or maladaptive hypertrophy. Furthermore, the number of differentially expressed genes remains constant over time. For several clusters of genes, up- or downregulation of gene expression occurred earlier in CHF (day 10) than in HYP (day 19) but later (day 25) gene-expression profiles of these two groups were largely overlapping. Gene-ontology analyses of these early regulated genes in the CHF group revealed involvement of cell-cycling genes. Premature upregulation of cell-cycling genes therefore predisposes RV myocardium to a maladaptive hypertrophic phenotype.

Reference List

(1) Grossman W, Jones D, McLaurin LP. Wall stress and patterns of hypertrophy in the human left ventricle. *J Clin Invest* 1975 July;56(1):56-64.

(2) Frey N, Olson EN. Cardiac Hypertrophy: The Good, the Bad, and the Ugly. *Annu Rev Physiol* 2003 January 1;65(1):45.

(3) Chien K. Molecular biology of cardiac hypertrophy and heart failure. Grace A, Hunter J, editors. In *Molecular Basis of Cardiovascular Disease*, Chapter 9 , 211-250. 1999.

(4) Lehman JJ, Kelly DP. Gene regulatory mechanisms governing energy metabolism during cardiac hypertrophic growth. *Heart Fail Rev* 2002 April;7(2):175-85.

(5) Wolkart G, Stromer H, Brunner F. Calcium Handling and Role of Endothelin-1 in Monocrotaline Right Ventricular Hypertrophy of the Rat. *Journal of Molecular and Cellular Cardiology* 2000 November;32(11):1995-2005.

(6) Levy D, Garrison RJ, Savage DD, Kannel WB, Castelli WP. Prognostic implications of echocardiographically determined left ventricular mass in the Framingham Heart Study. *N Engl J Med* 1990 May 31;322(22):1561-6.

(7) Manyari DE. Prognostic implications of echocardiographically determined left ventricular mass in the Framingham Heart Study. *N Engl J Med* 1990 December 13;323(24):1706-7.

(8) Buermans HPJ, Paulus WJ. Iconoclasts topple adaptive myocardial hypertrophy in aortic stenosis. *Eur Heart J* 2005 September 1;26(17):1697-9.

(9) Kupari M, Turto H, Lommi J. Left ventricular hypertrophy in aortic valve stenosis: preventive or promotive of systolic dysfunction and heart failure? *Eur Heart J* 2005 April 28;ehi290.

(10) Morisco C, Sadoshima J, Trimarco B, Arora R, Vatner DE, Vatner SF. Is treating cardiac hypertrophy salutary or detrimental: the two faces of Janus. *Am J Physiol Heart Circ Physiol* 2003 April 1;284(4): H1043.

(11) Buermans HPJ, Redout EM, Schiel AE, Musters RJP, Zuidwijk M, Eijk PP, van Hardeveld C, Kasanmoentalib S, Visser FC, Ylstra B, Simonides WS. Microarray analysis reveals pivotal divergent mRNA expression profiles early in the development of either compensated ventricular hypertrophy or heart failure. *Physiol Genomics* 2005 May 11;21(3):314-23.

(12) Sharma UC, Pokharel S, van Brakel TJ, van Berlo JH, Cleutjens JPM, Schroen B, Andre S, Crijns HJGM, Gabius H, Maessen J, Pinto YM. Galectin-3 Marks Activated Macrophages in Failure-Prone Hypertrophied Hearts and Contributes to Cardiac Dysfunction. *Circulation* 2004 November 9;110(19):3121-8.

(13) Musters RJP, van der Meulen ET, van der Laarse WJ, van Hardeveld C. Differential Effects of Norepinephrine on Contractile Recovery of Rat Trabeculae Following Metabolic Inhibition. *Journal of Molecular and Cellular Cardiology* 1998 February;30(2):435-40.

(14) Saeed AI, Sharov V, White J, Li J, Liang W, Bhagabati N, Braisted J, Klapa M, Currier T, Thiagarajan M, Sturn A, Snuffin M, Rezantsev A, Popov D, Ryltsov A, Kostukovich E, Borisovsky I, Liu Z, Vinsavich A, Trush V, Quackenbush J. TM4: a free, open-source system for microarray data management and analysis. *Biotechniques* 2003 February;34(2):374-8.

(15) Hosack D, Dennis G, Sherman B, Lane H, Lempicki R. Identifying biological themes within lists of genes with EASE. *Genome Biology* 2003;4(10):R70.

(16) Subramanian A, Tamayo P, Mootha VK, Mukherjee S, Ebert BL, Gillette MA , Paulovich A, Pomeroy SL, Golub TR, Lander ES, Mesirov JP. Gene set enrichment analysis: A knowledge-based approach for interpreting genome-wide expression profiles. *PNAS* 2005 September 30;0506580102.

(17) Bergman AM, Eijk PP, Ruiz van Haperen VWT, Smid K, Veerman G, Hubeek I, van den IJssel P, Ylstra B, Peters GJ. In vivo Induction of Resistance to Gemcitabine Results in Increased Expression of Ribonucleotide Reductase Subunit M1 as the Major Determinant. *Cancer Res* 2005 October 15;65(20):9510-6.

(18) Kerr MK, Martin M, Churchill GA. Analysis of variance for gene expression microarray data. *J Comput Biol* 2000;7(6):819-37.

(19) Cui X, Hwang JTG, Qiu J, Blades NJ, Churchill GA. Improved statistical tests for differential gene expression by shrinking variance components estimates. *Biostat* 2005 January 1;6(1):59-75.

(20) Reiner A, Yekutieli D, Benjamini Y. Identifying differentially expressed genes using false discovery rate controlling procedures. *Bioinformatics* 2003 February 12;19(3):368-75.

(21) Wilson DW, Segall HJ, Pan LC, Lame MW, Estep JE, Morin D. Mechanisms and pathology of monocrotaline pulmonary toxicity. *Crit Rev Toxicol* 1992;22(5-6):307-25.

(22) Jones JE, Mendes L, Rudd MA, Russo G, Loscalzo J, Zhang YY. Serial noninvasive assessment of progressive pulmonary hypertension in a rat model. *Am J Physiol Heart Circ Physiol* 2002 July 1;283(1):H364-H371.

(23) Janssen PML, Stull LB, Marban E. Myofilament properties comprise the rate-limiting step for cardiac relaxation at body temperature in the rat. *Am J Physiol Heart Circ Physiol* 2002 February 1;282(2):H499-H507.

(24) Edgar R, Domrachev M, Lash AE. Gene Expression Omnibus: NCBI gene expression and hybridization array data repository. *Nucl Acids Res* 2002 January 1;30(1):207-10.

(25) Rothermel BA, Berenji K, Tannous P, Kutschke W, Dey A, Nolan B, Yoo KD, Demetroulis E, Gimbel M, Cabuay B, Karimi M, Hill JA. Differential Activation of Stress-Response Signaling in Load-Induced Cardiac Hypertrophy and Failure. *Physiol Genomics* 2005 July 20;00061.

(26) Rosenberg P. Mitochondrial dysfunction and heart disease. *Mitochondrion* 2004 September;4(5-6):621-8.

(27) Wong K, Boheler KR, Petrou M, Yacoub MH . Pharmacological Modulation of Pressure-Overload Cardiac Hypertrophy : Changes in Ventricular Function, Extracellular Matrix, and Gene Expression. *Circulation* 1997 October 7;96(7):2239-46.

(28) Koide M, Nagatsu M, Zile MR, Hamawaki M , Swindle MM, Keech G, DeFreyte G, Tagawa H, Cooper G, IV, Carabello BA. Premorbid Determinants of Left Ventricular Dysfunction in a Novel Model of Gradually Induced Pressure Overload in the Adult Canine. *Circulation* 1997 March 18;95(6):1601-10.

(29) Ross J, Jr. On Variations in the Cardiac Hypertrophic Response to Pressure Overload. *Circulation* 1997 March 18;95(6):1349-51.

(30) Chen HW, Yu SL, Chen WJ, Yang PC, Chien CT, Chou HY, Li HN, Peck K, Huang CH, Lin FY, Chen JJW, Lee YT. Dynamic changes of gene expression profiles during postnatal development of the heart in mice. *Heart* 2004 August 1;90(8):927-34.

(31) Setoguchi M, Leri A, Wang S, Liu Y, De Luca A, Giordano A, Hintze TH, Kajstura J, Anversa P. Activation of cyclins and cyclin-dependent kinases, DNA synthesis, and myocyte mitotic division in pacing-induced heart failure in dogs. *Lab Invest* 1999 December;79(12):1545-58.

(32) Ecarnot-Laubriet A, Assem M, Poirson-Bichat F, Moisant M, Bernard C, Lecour S, Solary E, Rochette L , Teyssier J-R. Stage-dependent activation of cell cycle and apoptosis mechanisms in the right ventricle by pressure overload. *Biochimica et Biophysica Acta (BBA) - Molecular Basis of Disease* 2002 April 24;1586(3):233-42.

(33) Castedo M, Perfettini JL, Roumier T, Kroemer G. Cyclin-dependent kinase-1: linking apoptosis to cell cycle and mitotic catastrophe. *Cell Death Differ* 2002 December;9(12):1287-93.

(34) Datwyler DA, Magyar JP, Weikert C, Wightman L, Wagner E, Eppenberger HM. Reactivation of the mitosis-promoting factor in postmitotic cardiomyocytes. *Cells Tissues Organs* 2003;175(2):61-71.

Chapter 4

Early Adaptive And Maladaptive Hypertrophic Myocardial Proteome Responses During Pressure Overload

Henk P.J. Buermans[1], Marian Zuidwijk[1], René J.P. Musters[1]
Cornelis van Hardeveld[1], Connie R. Jiménez[2], Frans C. Visser[3]
Walter J. Paulus[1], Warner S. Simonides[1]

1. Laboratory for Physiology, Institute for Cardiovascular Research (ICaR-VU), VU University Medical Center, Van der Boechorststraat 7, 1081 BT Amsterdam, The Netherlands.

2. Department of Molecular and Cellular Neurobiology, Research Institute Neurosciences, Faculty of Earth and Life Sciences Vrije Universiteit, De Boelelaan 1085, 1081 HV Amsterdam, The Netherlands.

3. Department of Cardiology, Institute for Cardiovascular Research (ICaR-VU), VU University Medical Center, De Boelelaan 1117, 1081 HV Amsterdam, The Netherlands.

Submitted for publication

Table of contents

Abstract

Ventricular hypertrophy is a general response of the heart to overload and depending on the degree and the duration of the overload, either and an adaptive or maladaptive hypertrophic phenotype may evolve. We recently observed myocardial gene-expression differences between adaptive and maladaptive hypertrophy early after the imposition of pressure overload, challenging the existence of a common hypertrophy precursor state preceding the development of either of these phenotypes. In the present study, myocardial protein-expression levels were evaluated for significant differential expression early after the imposition of pressure overload between control rats and rats developing either adaptive or maladaptive hypertrophy.

Adaptive or maladaptive hypertrophy phenotypes were induced by subcutaneous injections of either 30 (HYP-group) or 80 (CHF-group) mg monocrotaline(MCT)/kg body weight, respectively. At 10 days after MCT injections when RV phenotypes were identical, right ventricular (RV) cytosolic-protein fractions from HYP, CHF and time matched control (CON) animals were separated and compared using 2-dimensional gel electrophoresis. When comparing CON to HYP, CON to CHF and HYP to CHF, 5, 15 and 23 protein-spots showed significant differential expression, respectively. MALDI-TOF mass spectrometry identification of a subset of proteins indicated fatty acid metabolism, reactive oxygen species handling and apoptosis signalling to be already altered at 10 days after the imposition of pressure overload between the HYP and CHF groups.

In conclusion, the observed differences at the myocardial protein-expression level between the HYP and CHF groups at 10 days after the imposition of pressure overload, further argues against the existence of a common hypertrophic precursor state.

Introduction

Ventricular hypertrophy is a general adaptive mechanism of the heart to increased workload and is aimed at normalizing ventricular wall stress. Depending on the duration and the degree of the overload, either an adaptive or maladaptive hypertrophy phenotype will evolve over time. Numerous processes have been associated with hypertrophic ventricular remodelling, e.g., re-expression of the fetal-gene programme[1, 2], alterations in calcium handling[3], altered energy metabolism substrate[4, 5], extracellular matrix composition[6] and signal transduction cascades[7]. Still, it remains uncertain which of these changes or combination of changes are critical for the development of either an adaptive of maladaptive hypertrophy phenotype. Moreover, the time point at which these crucial alterations are initiated during remodelling remains largely unknown.
It is generally presumed that both the adaptive and maladaptive phenotypes evolve from a common hypertrophy precursor state and that maladaptive remodelling becomes evident after compensation mechanisms have failed to maintain normal pump function. However, this concept has recently been challenged by clinical[8, 9] and epidemiological[10, 11] studies, which suggest that ventricular hypertrophy is already maladaptive immediately after the imposition of pressure overload.

The monocrotaline(MCT)-dose controlled model of either an adaptive or maladaptive ventricular hypertrophy phenotype due to graded pulmonary hypertension provides the unique opportunity to study the right-ventricular(RV) responses at early time points after the imposition of pressure overload[12, 13]. At 10 days after MCT injections, micro-array analyses revealed RV myocardial gene-expression profiles that were already specifically associated with either the adaptive or maladaptive phenotypical outcome, though no RV hypertrophy had yet developed. These observations also argue against a hypertrophy precursor state common for both the adaptive and maladaptive phenotypes[13]. However, it is unknown whether in parallel to the differences observed at the transcription level, differences in protein expression occur between adaptive and maladaptive remodelling at day 10. More specifically, changes at the transcription level do not necessarily lead to altered protein-expression levels, and, changes at the protein level may be observed in the absence of differential transcription regulation.

In this study, using the MCT-dose controlled model, we compared the adaptive and maladaptive hypertrophy phenotypes at day 10 after the imposition of pressure

overload to test for significant differential protein-expression levels using 2-dimensional gel electrophoresis (2DGE). The aim of this study was threefold:
1) Is there evidence that supports the presence of differential protein expression at 10 days after the imposition of pressure overload. 2) What is the identity of differentially expressed proteins and do these proteins provide clues to critical alterations that could mediate either adaptive or maladaptive remodelling. 3) How does differential protein expression relate to alterations at the transcription level of their corresponding genes.

Methods

Animals

Animals were treated according to the national guidelines and with the permission of the Institutional Animal Care and Use Committee (IACUC) of the VU University Medical Center Amsterdam, the Netherlands.

Monocrotaline(MCT)-dose controlled induction of adaptive hypertrophy (HYP; 30 mg MCT/kg body weight (bw), n=4) and maladaptive hypertrophy (CHF; 80 mg MCT/kg bw, n=4) was performed as previously described[12, 13]. Animals were sacrificed 10 days after subcutaneous MCT injections. Lungs were excised, hearts were rinsed by perfusion and the left ventricle (LV), right ventricle (RV) and interventricular septum (IVS) were separated. All tissues were snap frozen in liquid nitrogen and stored at -80 ºC.

Protein Sample Preparation For 2DGE

The RV from three animals per group were used in the 2DGE experiments. All chemicals were electrophoresis-grade from Sigma unless stated otherwise. Approximately 15 mg RV tissue was homogenized in 400 µL lysis buffer (8 mol/L urea, 4% w/v CHAPS, 50 mmol/L DTT) using a glass-glass homogenizer, for a total of 10 strokes per sample. The homogenate was left on ice for 45 min. and centrifuged for 15 min. at 14.000 g at 4 ºC. A total of 150 µg protein (Bradford method) from the supernatant fraction was prepared in 450 µL lysis buffer with 0.5% v/v IPG buffer pH3-10-non-linear (NL) (Amersham biosciences). A pool of equal amounts of protein of each of the nine samples was run in parallel to the nine individual samples and served as the preparative gel for MALDI-TOF protein identification.

Isoelectric Focusing, SDS-Page, And MALDI-TOF Mass Spectrometry

The protein pool for the preparative gel and the three individual samples per experimental condition were processed in parallel. Protein samples were applied to IPG gels (Immobiline DryStrip 24 cm, pH 3-10 non-linear (NL), Amersham biosciences). Gel rehydration and isoelectric focusing were performed over night (o/n) on an Ettan™ IPGphor™ II IEF System (Amersham biosciences) at 50 µA per strip (65 kVh: 30 V, 12 h; 500 V, 1 h; 100 V, 1 h and 8000 V, 8h [step-n-hold gradient type]) at 20 ºC, in strip holders covered with Immobiline DryStrip Cover Fluid. After focusing, the IPG strips were wrapped in plastic foil and stored at -80 °C.

Second dimension SDS-PAGE separations was performed as described[14] with minor modifications. Individual IPG strips were applied to simultaneously cast [1-1.5 mm] 12% dyracryl gels (12% dyracryl, 0.365 mol/L Tris pH8.8, 0.1% SDS, 0.1% APS and

0.5 µl TEMED). The gels were run in 1x Tris-glycin-SDS buffer at 15 ºC for 24h at 12 W followed by 4h at 15 W using the Isodalt System (Amersham Biosciences).
After second dimension separation the nine sample gels were silver stained as described by Shevchenko *et al*.[15], with minor modifications. Three parallel staining batches were performed, each containing one gel from each experimental condition. After staining the gels were stored in 0,2 % HAc/10% MeOH at 4°C. The preparative gel was fixed in 10% Methanol/7% acetic acid o/n and subsequently washed 3 times for 10 min. with distilled water. This gel was stained with Sypro-Ruby fluorescent staining solution for 3 h, directly followed by a Coomassie staining (34% Methanol, 3% phosphoric acid, 15% w/v ammoniumsulphate, 0.1% Coomassie brilliant blue G250).
Protein spots of interest were manually excised from the Sypro-Ruby/Coomassie stained gel. In-gel trypsin digestion, MALDI-TOF procedures and database searches were performed as described[15, 16] with minor modifications.

Quantification And Statistical Analysis Of 2DGE Gels
The silver-stained 2D gels were scanned using a densitometer (Bio-Rad). Computer assisted matching and quantifications of corresponding protein spots across multiple gels was done using PDQuest image analysis software (v7.0; Bio-Rad). Only spots matched to all nine gels were selected for processing and statistical analysis. Spot intensities per gel were normalized to the total quantity of valid spots. Spots with average intensities outside the 5-95th percentile interval were excluded from further analysis. To test for significant differential expression, a modified analysis of variance (ANOVA) method was performed which uses an F-statistic to estimate the error variance by borrowing cross-gene information using the James-Stein shrinkage concept[17, 18]. Bonferroni corrected post-hoc tests ($p<0.05$) were performed for the three pair-wise comparisons. A minimal 1.5-fold change between groups was included. P-values were calculated using 1000 permutations on residuals.

Quantitative Real-Time PCR
Realtime-PCR experiments were performed as previously described[12]. Gene expression was normalized to HPRT levels. The gene-specific primer sequences used were (5' to 3'): Echs1 (NM_078623, F: GCC-ACT-GAT-GAC-CGG-AGA-GA, R: GGT-GGA-GAA-AGG-TAT-GGC-TGC); Fabp3 (NM_024162, F: TCG-TGA-CAC-TGG-ACG-GAG-G, R: GCC-ATG-GGT-GAG-AGT-CAG-GAT); Hspb1 (NM_031970, F: AAT-ACA-CGC-TCC-CTC-CAG-GTG, R: GAT-TGT-GTG-ACT-GCT-TTG-GGC); Prdx2 (NM_017169, F: CCC-TCT-GCT-TGC-TGA-TGT-GAC, R: GAG-GCC-CCT-GTA-AGC-GAT-G); Hprt

(M63983, F: ATG-GGA-GGC-CAT-CAC-ATT-GT, R: ATG-TAA-TCC-AGC-AGG-TCA-GCA-A).

Statistical Analysis Of PCR And Hypertrophy Parameters

Significant differences were evaluated using a one-way ANOVA with the Bonferroni multiple testing correction. Differences with a p-value smaller than 0.05 were considered significant.

Results

MCT-Induced RV Hypertrophy

At 10 days after subcutaneous injection of either 30 or 80 mg MCT/kg bw, a significant increase in lung weight for both the HYP and CHF groups relative to CON was observed. This is indicative of increased pulmonary vascular resistance[19, 20]. In agreement with previous observations, this increase in pulmonary pressure did not yet result in RV hypertrophy at day 10, i.e., both RV weight and the RV to LV + IVS weight ratio did not show a significant increase[13]. Body weight of both MCT injected groups showed a small, yet significant difference relative to the CON group. These parameters are shown in Table 1.

Between-Group Differences In Protein Expression

The SDS-PAGE gels showed a high level of reproducibility. Representative images of corresponding sections from all nine individual gels are shown in Figure 1. A total of 396 protein spots were matched across all gels. Spots with average intensities

	CON (n=4)	HYP (n=4)	CHF (n=4)
BW (g)	251 ± 5	230 ± 7 *	222 ± 3 *
RV (mg)	162 ± 9	147 ± 7	144 ± 10
RV to LV+S (mg / mg)	0.243 ± 0.006	0.234 ± 0.002	0.229 ± 0.007
Lung (g)	1.13 ± 0.01	1.42 ± 0.02 *	1.49 ± 0.07 *

▲**Table 1:** Measured parameters for the CON, HYP and CHF groups at 10 days after MCT injections. Data represent Mean ± SE and significant differences are indicated with * : $p<0.05$ relative to CON.

Name + symbol	Protein accession	Pred *p*I	Pred mass	Protein score CI(%)	Nr of Fragments
Fatty acid-binding protein-3, heart (Fabp3)	P07483	5.92	16.4	99.70	1
Peroxiredoxin 2 (Prdx2)	P35704	5.34	21.7	99.43	3
Enoyl-CoA hydratase, mitochondrial (Echs1)	P14604	8.40	31.5	99.99	8
Heat-shock protein beta-1 (Hspb1)	P42930	6.12	22.9	99.43	4

▲**Table 2:** Name and protein accession number of the four identified proteins. Indicated are the predicted *p*I and mass, protein identity confidence interval (CI) and the number of protein fragments on which the identification was based.

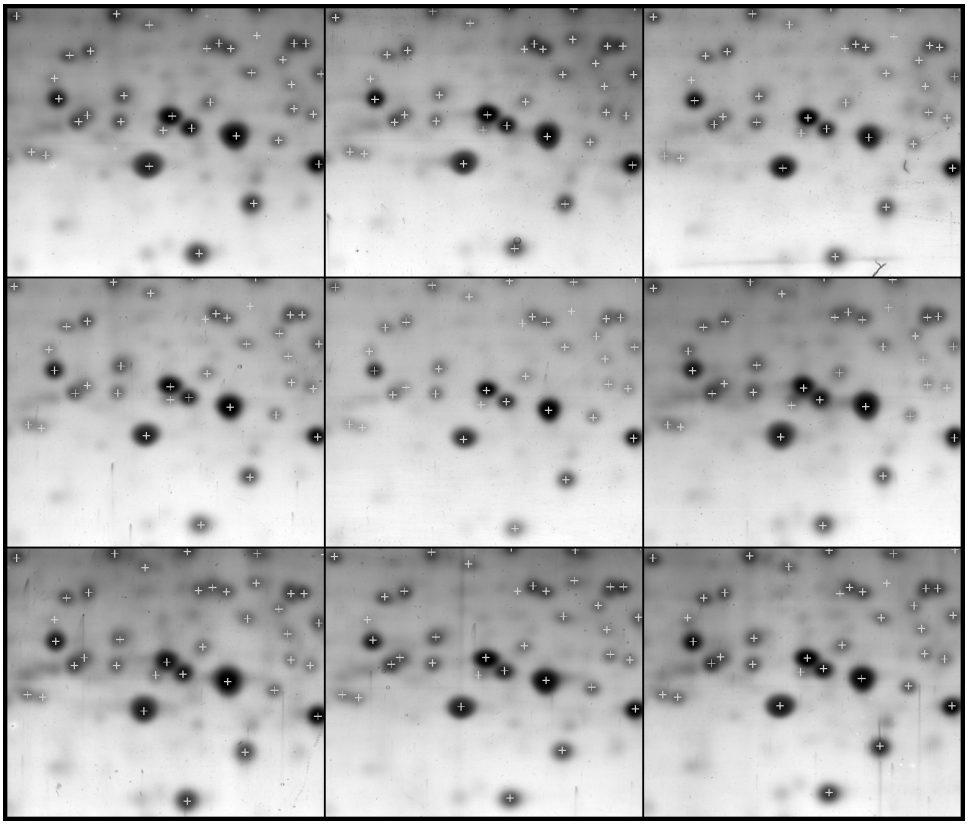

▲**Figure 1:** SDS-PAGE images from corresponding segments from the gels. Crosses mark matched spots in all nine gels. Sections represent a mass range of ~20 to 25 kDa and isoelectric-point range of ~5 to 7.

outside the 5-95th percentile range were excluded from further analysis. The remaining 353 spots were tested for significant differential expression between the three replicate groups. When comparing CON to HYP, CON to CHF and HYP to CHF, 5, 15 and 23 spots were differentially expressed, respectively. Some proteins were significantly regulated in more than one of the pair-wise comparisons. The total number of unique protein spots with significant differential expression was 35 (Figure 2).

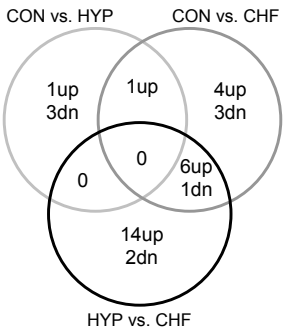

►**Figure 2:** The number of significantly differentially-expressed proteins for each pair-wise comparison as indicated by the ANOVA analysis. Also indicated are the number of upregulated (up) and downregulated (dn) proteins.

Identity Of Differentially Expressed Proteins

Of the 35 differentially expressed protein spots, 20 were excised from the preparative gel to be identified using MALDI-TOF mass spectrometry. Four proteins were positively identified. Table 2 list the names, protein accession number, predicted mass and pI as well as the protein score for positive identification for these spots. The position of these four protein spots with corresponding mass and pI on the SDS-PAGE gel is indicated in Figure 3. An example of the protein fragments from the trypsin digest that identified the Echs1 protein is shown in Figure 4.

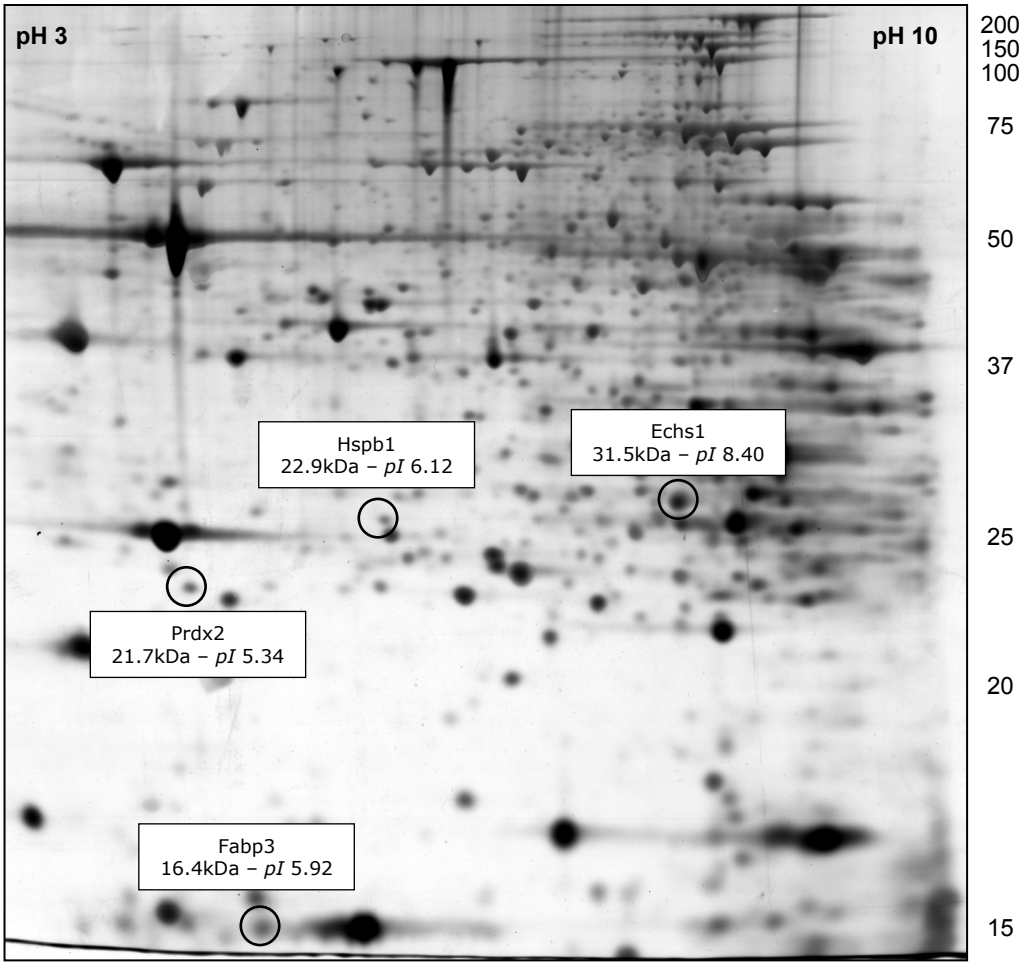

▲**Figure 3:** Representative image of a silver-stained SDS-PAGE gel. Mass and *pI* markers are indicated at the right and top of the image, respectively. Significantly differentially regulated and identified protein spots are marked in the image.

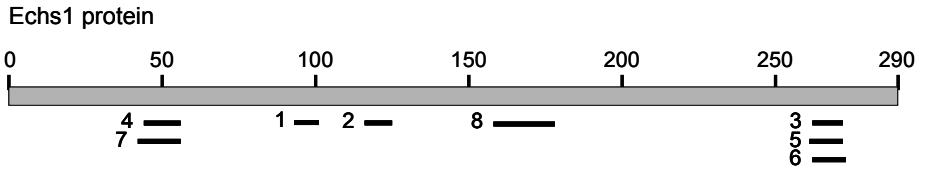

Fragment	Observed Mass	begin	end	length	sequence
1	863.46	93	101	8	AFAAGADIK
2	1311.6656	116	125	9	FLSHWDHITR
3	1335.6271	262	272	10	LFYSTFATDDR
4	1425.8171	44	56	12	NSSVGLIQLNRPK
5	1463.7162	261	272	11	KLFYSTFATDDR
6	1491.724	262	273	11	LFYSTFATDDRR
7	1610.1927	42	56	14	GKNSSVGLIQLNRPK
8	2111.1201	158	178	20	AQFGQPEILLGTIPGAGGTQR

▲**Figure 4:** Protein fragments from the Echs1-trypsin digest identified by MALDI-TOF mass spectrometry. Top: schematic representation of the Echs1 protein spanning 290 amino-acid residues from N- to C-terminus. Protein fragments 1 through 8 (horizontal bars) are aligned relative to their position on the Echs1 protein. Bottom: Protein fragments in ascending order of observed mass. Indicated are start and end amino-acid position on the Echs1 protein strand, fragment length and amino-acid sequence per fragment.

Quantitative Real-Time PCR

Realtime PCR was used to assess whether the altered protein expression observed for the four identified proteins were a result of changes at the transcription level of their corresponding genes. Only Echs1 mRNA-expression levels showed a similar downregulation in the CHF group relative to both HYP and CON as was found for the protein-expression levels. Expression levels for both the protein and their matching mRNA transcripts are shown in Figure 5.

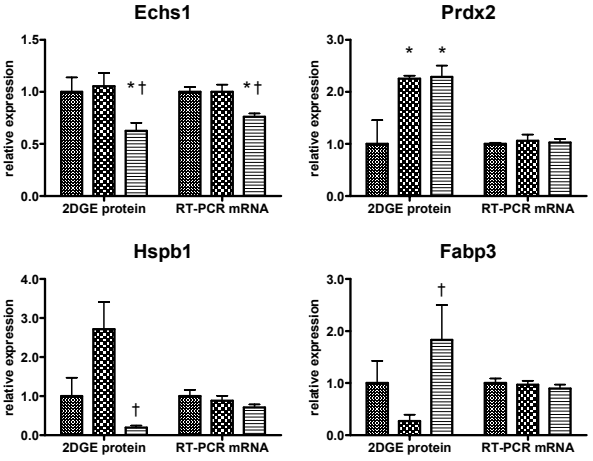

◄**Figure 5:** Expression profiles of the identified significantly differentially expressed proteins from both 2DGE and real-time PCR experiments. Control expression levels were set to 1. Data represent Mean ± SE and significant differences are indicated with * : $p<0.05$ rel to CON; †: $p<0.05$ rel to HYP.

Discussion

In the present study, global proteome profiling using 2-dimensional gel electrophoresis at the early stages during the development of either adaptive or maladaptive RV hypertrophy in a MCT-dose controlled rat model for pulmonary hypertension, yielded the following results:
1) When comparing RV myocardial protein-expression levels at 10 days after the imposition of pressure overload, 5 proteins displayed significant differential expression between the CON and HYP groups, 15 proteins between the CON and CHF groups and 23 proteins between the HYP and CHF groups. 2) Evaluation of function of identified proteins with significant differential expression levels indicated alterations at the level of fatty acid metabolism, reactive oxygen species handling and apoptosis-related signalling to be present already early during myocardial remodelling. 3) Only for specific proteins could altered protein-expression levels be related to changes at the transcription level of their corresponding genes.

Induction Of Adaptive Or Maladaptive Hypertrophy
The model used in this study allows for the controlled induction of either an adaptive or maladaptive hypertrophic RV phenotype by a subcutaneous injection of either 30 or 80 mg MCT/kg body weight, respectively[12, 13]. Early stages during the development of either an adaptive or maladaptive phenotype can therefore be reliably characterized during the period just after the imposition of pressure overload and before functional or morphological differences between groups become apparent.
In previous studies using this model, significant differences in mRNA-expression levels between RV myocardial tissue from HYP and CHF animals were determined by micro-array expression profiling at 10, 14, 19 and 25 days after MCT injections[12, 13]. When considering day 10 after the imposition of pressure overload, of the total of 55 genes with significant differential expression levels, 13 displayed a significance call in the HYP vs. CHF comparison (23.6%). The present study suggests that these differences are more distinct at the proteome level, i.e., 23 of 35 protein spots (67%). This indicates that the divergence of adaptive and maladaptive remodelling at the early stages after the imposition of pressure overload results in more pronounced responses at the proteome level than can be observed at the mRNA-transcript level. This is substantiated by the observation that alterations at the protein level could only be related to changes at the transcription level for the Echs1 protein.
However, it cannot be excluded that the differences in observations between both studies may partially be explained by differences in the statistical procedures used to determine significant differential expression. In addition, the micro-arrays assayed a

defined set of 4803 genes, while in the 2DGE experiments an unknown number of cytosolic proteins were assayed.

Alterations In Fatty Acid Transport And Mitochondrial Beta-Oxidation

Of the identified proteins which show significant differential expression, Fabp3 and Echs1 could be related to alterations in energy metabolism substrate. Under physiological conditions, mitochondrial fatty-acid (FA) β-oxidation generates approximately 70% of the total ATP production in the heart. However, severe downregulation of FA oxidation, accompanied by increased glycolysis and glucose oxidation are observed at the advanced stages of ventricular hypertrophy due to pressure overload[4, 5]. Long chain-FA (LCFA) are broken down in four steps during β-oxidation, generating reduced flavin adenine dinucleotide (FADH2), reduced nicotinamide adenine dinucleotide (NADH) and acetyl-CoA. The second step of this cycle is provided by Echs1, which catalyzes the hydration of 2-trans-enoyl-coenzyme-A (CoA) intermediates to L-3-hydroxyacyl-CoAs.

Significantly reduced Echs1 mRNA and protein levels in the maladaptive hypertrophy group at day 10 after the imposition of pressure overload indicate that the switch towards glucose as the predominant metabolic substrate may already have been initiated. The adaptive hypertrophy group did not show these changes at day 10, indicating that the shift towards glucose metabolism is indeed associated with maladaptive hypertrophic remodelling. Micro-array Echs1-expression profiles from previous experiments are in agreement with these findings[13]. Mitochondrial beta-oxidation shutdown may lead to intracellular lipid accumulation[21]. Lipid accumulation has been shown to occur in human non-ischemic heart failure[22] and has been associated with lipotoxicity leading to apoptosis in multiple cell types, including cardiac myocytes[23, 24] and with cardiac contractile dysfunction in Zucker diabetic fatty rats[22] and obese (ob/ob) mice[25].

In response to increased intracellular lipids, levels of fatty-acid binding proteins (Fabps) are increased[23]. In line with this, our data show significantly higher expression levels of the heart-specific Fabp (Fabp3) form in the maladaptive relative to the adaptive-hypertrophy group. Fabps are a group of ~15kDa cytoplasmic proteins which are highly expressed in tissues dependent on FA metabolism. Fabps are involved in gene-expression regulation via peroxisome proliferator activated receptor alpha (PPARα), protection against detergent-like properties of local high long-chain FA (LCFA) concentrations and intracellular transport of hydrophobic compounds, such as LCFA[26].

The increase in Fabp3 may affect cardiac-myocyte function on multiple levels. It could serve as a protective mechanism in response to the toxic effects of increased

cellular lipid accumulation. Also, LCFA-Fabp3 complexes may participate with PPARα in upregulation of FA metabolism-related genes in order to increase FA metabolism and counteract intracellular lipid accumulation[4, 21]. Indeed, the upstream promotor sequence of the Echs1 gene contains functional PPARα response elements[27, 28] and Echs1 expression in the CHF group at day 19 appeared to be normalized, i.e., no longer significantly different from CON and HYP levels[13].

Alterations In Peroxide Handling

Peroxiredoxins (Prdxs) are involved in cellular proliferation, protection against oxidative stress through degradation of H_2O_2, organic hydroperoxides and peroxynitrite, as well as modulation of intracellular signalling routes that use H_2O_2 as the 2nd messenger. Prdxs contain conserved redox-active cysteine residues in their catalytic center which are involved in the enzymatic peroxidase activity. Peroxide substrates oxidize these cysteine-residues to sulfenic acids, leading to a reversible inactivation of the peroxidase activity[29]. Although Prdxs have relatively low catalytic efficiencies ($\sim 10^5$ M^{-1} s^{-1})[30] compared to glutathione peroxidases ($\sim 10^8$ M^{-1} s^{-1})[30] and catalases ($\sim 10^6$ M^{-1} s^{-1})[31], Prdxs contribute significantly to intracellular-peroxide clearance due to their abundant expression levels. The detected increase in Prdx2-protein levels in both the adaptive and maladaptive phenotypes indicates Prdx2 to be involved in general hypertrophic remodelling. These increased Prdx2 levels could provide additional tolerance to peroxide stress.

We recently observed early activation of the cdc2-cyclinB complex during maladaptive- but not adaptive-hypertrophic remodelling[13]. Activation of the cdc2-cyclinB complex causes untimely progression through the G2/M transition of the cell cycle. Chang *et al*. showed that the active cdc2-cyclinB complex is able to phosphorylate Prdx2 and subsequently deactivate this Prdx2 in vitro[32]. Loss of Prdx2-peroxidase activity would lead to intracellular H_2O_2 accumulation which is needed for progression through the cell cycle[32]. It is tempting to speculate that via this mechanism, H_2O_2 levels will be higher in CHF relative to HYP. Mitogen-activated protein kinases have been shown to be activated by H_2O_2 in a dose dependent manner, in which Erk1/2 appeared to be activated at lower doses than Jnk and p38[33,34]. Early stages of adaptive remodelling would then be associated with pro-hypertrophic Erk1/2 activation while during maladaptive remodelling, pro-apoptotic Jnk and p38 signalling would be present in addition to Erk. Previous observations at 14 days after MCT injections, indeed found increased p38-phosphorylation levels to be associated with maladaptive remodelling[12].

Heat Shock Protein Survival Signalling

In this study we observed a significantly higher expression of the Hspb1/Hsp27 protein in the HYP group relative to the CHF group, with no significant differences relative to CON levels. Hsp27 expression has been associated with increased survival after cytotoxic stimuli. Different mechanisms have been proposed to mediate the survival properties of Hsp27 overexpression, many of which interfere with pro-apoptotic signalling[35].

The lower Hsp27-expression levels observed in the maladaptive hypertrophy group, relative to the adaptive hypertrophy group, could indicate a more apoptosis-prone myocardium at the early stages during maladaptive remodelling. This is in line with previous observation using this model[12, 36].

Conclusion

In this study using the MCT-dose controlled induction of either an adaptive or maladaptive hypertrophic phenotype, significant differences in protein expression were observed between the HYP and CHF groups at 10 days after the induction of pressure overload. This, in conjunction with our previous observations of mRNA-expression differences between HYP and CHF at 10 days after the imposition of pressure overload, further argues against the existence of a common adaptive precursor state during the development of either an adaptive or maladaptive hypertrophy phenotype. Moreover, our data indicate that early during the development of either an adaptive or maladaptive hypertrophic response, differences in pro-survival signalling as well as in fatty acid metabolism may already be present. Differences in the rise of pressure overload over time between the HYP and CHF groups are likely to be responsible for the observed differences between these two groups through differential activation of signal transduction pathways that mediate the protein and mRNA expression levels.

Reference List

(1) Chien KR, Knowlton KU, Zhu H, Chien S. Regulation of cardiac gene expression during myocardial growth and hypertrophy: molecular studies of an adaptive physiologic response. *FASEB J* 1991 December 1;5(15):3037-46.

(2) Bar MH, Kreuzer J, Cojoc A, Jahn L. Upregulation of embryonic transcription factors in right ventricular hypertrophy. *Basic Res Cardiol* 2003 September;98(5):285-94.

(3) Brunner F, Wolkart G, Haleen S. Defective Intracellular Calcium Handling in Monocrotaline-Induced Right Ventricular Hypertrophy: Protective Effect of Long-Term Endothelin-A Receptor Blockade with 2-Benzo[1,3]dioxol-5-yl-3-benzyl-4-(4-methoxy-phenyl-)- 4-oxobut-2-enoate-sodium (PD 155080). *J Pharmacol Exp Ther* 2002 February 1;300(2):442-9.

(4) Lehman JJ, Kelly DP. Gene regulatory mechanisms governing energy metabolism during cardiac hypertrophic growth. *Heart Fail Rev* 2002 April;7(2):175-85.

(5) Stanley WC, Recchia FA, Lopaschuk GD. Myocardial Substrate Metabolism in the Normal and Failing Heart. *Physiol Rev* 2005 July 1;85(3):1093-129.

(6) Wang D, Oparil S, Feng JA, Li P, Perry G, Chen LB, Dai M, John SWM, Chen YF. Effects of Pressure Overload on Extracellular Matrix Expression in the Heart of the Atrial Natriuretic Peptide-Null Mouse. *Hypertension* 2003 May 19;01.

(7) Frey N, Olson EN. Cardiac Hypertrophy: The Good, the Bad, and the Ugly. *Annu Rev Physiol* 2003 January 1;65(1):45.

(8) Buermans HPJ, Paulus WJ. Iconoclasts topple adaptive myocardial hypertrophy in aortic stenosis. *Eur Heart J* 2005 September 1;26(17):1697-9.

(9) Kupari M, Turto H, Lommi J. Left ventricular hypertrophy in aortic valve stenosis: preventive or promotive of systolic dysfunction and heart failure? *Eur Heart J* 2005 April 28;ehi290.

(10) Levy D, Garrison RJ, Savage DD, Kannel WB, Castelli WP. Prognostic implications of echocardiographically determined left ventricular mass in the Framingham Heart Study. *N Engl J Med* 1990 May 31;322(22):1561-6.

(11) Manyari DE. Prognostic implications of echocardiographically determined left ventricular mass in the Framingham Heart Study. *N Engl J Med* 1990 December 13;323(24):1706-7.

(12) Buermans HPJ, Redout EM, Schiel AE, Musters RJP, Zuidwijk M, Eijk PP, van Hardeveld C, Kasanmoentalib S, Visser FC, Ylstra B, Simonides WS. Microarray analysis reveals pivotal divergent mRNA expression profiles early in the development of either compensated ventricular hypertrophy or heart failure. *Physiol Genomics* 2005 May 11;21(3):314-23.

(13) Buermans HPJ, Musters RJP, van de Wiel M, Zuidwijk M, van Hardeveld C, Ylstra B, Visser FC, Paulus WJ, Simonides WS. Maladaptive myocardial hypertrophy in pressure overload does not evolve from an adaptive precursor state. *Submitted manuscript*.

(14) Jimenez CR, Eyman M, Lavina ZS, Gioio A, Li KW, van der Schors RC, Geraerts WP, Giuditta A, Kaplan BB, van Minnen J. Protein synthesis in synaptosomes: a proteomics analysis. *J Neurochem* 2002 May;81(4):735-44.

(15) Shevchenko A, Wilm M, Vorm O, Mann M. Mass spectrometric sequencing of proteins silver-stained polyacrylamide gels. *Anal Chem* 1996 March 1;68(5):850-8.

(16) Jimenez CR, Stam FJ, Li KW, Gouwenberg Y, Hornshaw MP, De Winter F, Verhaagen J, Smit AB. Proteomics of the Injured Rat Sciatic Nerve Reveals Protein Expression Dynamics During Regeneration. *Mol Cell Proteomics* 2005 February 1;4(2):120-32.

(17) Kerr MK, Martin M, Churchill GA. Analysis of variance for gene expression microarray data. *J Comput Biol* 2000;7(6):819-37.

(18) Cui X, Hwang JTG, Qiu J, Blades NJ, Churchill GA. Improved statistical tests for differential gene expression by shrinking variance components estimates. *Biostat* 2005 January 1;6(1):59-75.

(19) Wilson DW, Segall HJ, Pan LC, Lame MW, Estep JE, Morin D. Mechanisms and pathology of monocrotaline pulmonary toxicity. *Crit Rev Toxicol* 1992;22(5-6):307-25.

(20) Jones JE, Mendes L, Rudd MA, Russo G, Loscalzo J, Zhang YY. Serial noninvasive assessment of progressive pulmonary hypertension in a rat model. *Am J Physiol Heart Circ Physiol* 2002 July 1;283(1):H364-H371.

(21) Djouadi F, Brandt JM, Weinheimer CJ, Leone TC, Gonzalez FJ, Kelly DP. The role of the peroxisome proliferator-activated receptor [alpha] (PPAR[alpha]) in the control of cardiac lipid metabolism. *Prostaglandins, Leukotrienes and Essential Fatty Acids* 1999;60(5-6):339-43.

(22) Sharma Saum, Adrogue JV, Golfman Leon, Uray Ivan, Lemm John, Youker Keit, Noon Gp, Frazier Oh, Taegtmeyer Hein. Intramyocardial lipid accumulation in the failing human heart resembles the lipotoxic rat heart. *FASEB J* 2004 November 1;18(14):1692-700.

(23) Van Bilsen M, de Vries JE, van der Vusse GJ. Long-term effects of fatty acids on cell viability and gene expression of neonatal cardiac myocytes. *Prostaglandins, Leukotrienes and Essential Fatty Acids* 1997 July;57(1):39-45.

(24) de Vries JE, Vork MM, Roemen TH, de Jong YF, Cleutjens JP, van der Vusse GJ, Van Bilsen M. Saturated but not mono-unsaturated fatty acids induce apoptotic cell death in neonatal rat ventricular myocytes. *J Lipid Res* 1997 July 1;38(7):1384-94.

(25) Christoffersen C, Bollano E, Lindegaard MLS, Bartels ED, Goetze JP, Andersen CB, Nielsen LB. Cardiac Lipid Accumulation Associated with Diastolic Dysfunction in Obese Mice. *Endocrinology* 2003 August 1;144(8):3483-90.

(26) Glatz JFC, van der Vusse GJ. Cellular fatty acid-binding proteins: Their function and physiological significance. *Progress in Lipid Research* 1996 September;35(3):243-82.

(27) Marcus SL, Miyata KS, Zhang B, Subramani S, Rachubinski RA, Capone JP. Diverse Peroxisome Proliferator-Activated Receptors Bind to the Peroxisome Proliferator-Responsive Elements of the Rat Hydratase/Dehydrogenase and Fatty Acyl-CoA Oxidase Genes but Differentially Induce Expression. *PNAS* 1993 June 15;90(12):5723-7.

(28) Zhang B, Marcus SL, Sajjadi FG, Alvares K, Reddy JK, Subramani S, Rachubinski RA, Capone JP. Identification of a Peroxisome Proliferator-Responsive Element Upstream of the Gene Encoding Rat Peroxisomal Enoyl-CoA Hydratase/3-Hydroxyacyl-CoA Dehydrogenase. *PNAS* 1992 August 15;89(16):7541-5.

(29) Woo HA, Chae HZ, Hwang SC, Yang KS, Kang SW, Kim K, Rhee SG. Reversing the Inactivation of Peroxiredoxins Caused by Cysteine Sulfinic Acid Formation. *Science* 2003 April 25;300(5619):653-6.

(30) Hofmann B, Hecht HJ, Flohe L. Peroxiredoxins. *Biological Chemistry*383(3-4):347-64.

(31) Slinker BK, Stephens RL, Fisher SA, Yang Q. Immediate-early Gene Responses to Different Cardiac Loads in the Ejecting Rabbit Left Ventricle. *Journal of Molecular and Cellular Cardiology* 1996 July;28(7):1565-74.

(32) Chang TS, Jeong W, Choi SY, Yu S, Kang SW, Rhee SG. Regulation of Peroxiredoxin I Activity by Cdc2-mediated Phosphorylation. *J Biol Chem* 2002 July 5;277(28):25370-6.

(33) Kwon SH, Pimentel DR, Remondino A, Sawyer DB, Colucci WS. H2O2 regulates cardiac myocyte phenotype via concentration-dependent activation of distinct kinase pathways. *Journal of Molecular and Cellular Cardiology* 2003 June 1;35(6):615-21.

(34) Wei S, Rothstein EC, Fliegel L, Dell'Italia LJ, Lucchesi PA. Differential MAP kinase activation and Na+/H+ exchanger phosphorylation by H2O2 in rat cardiac myocytes. *Am J Physiol Cell Physiol* 2001 November 1;281(5):C1542-C1550.

(35) Concannon CG, Gorman AM, Samali A. On the role of Hsp27 in regulating apoptosis. *Apoptosis* 2003 January;8(1):61-70.

(36) Ecarnot-Laubriet A, Assem M, Poirson-Bichat F, Moisant M, Bernard C, Lecour S, Solary E, Rochette L, Teyssier J-R. Stage-dependent activation of cell cycle and apoptosis mechanisms in the right ventricle by pressure overload. *Biochimica et Biophysica Acta (BBA) - Molecular Basis of Disease* 2002 April 24;1586(3):233-42.

Chapter 5

General Discussion

Table of contents

Adaptive vs. Maladaptive Myocardial Hypertrophy

This thesis is focused on gene-expression alteration during the development of right-ventricular hypertrophy in a rat model for pulmonary hypertension. The aim of this research was to determine putative hypertrophic signalling events that drive general hypertrophy and to distinguish between processes at the transcriptome level that are specifically associated with the development of either an adaptive or maladaptive hypertrophic phenotype, due to pressure overload. The adaptations of the heart, e.g., alterations in signal transduction cascades, energy metabolism and calcium handling, are a result of changes in the expression level of specific genes. A better understanding of the gene-expression alterations during the development of ventricular hypertrophy may therefore allow for the identification of key processes involved in myocardial remodelling.

Cardiac hypertrophy has long been thought to represent an adaptive or beneficial response mechanism of the heart to increased workload, in which elevated wall stress is normalized by thickening of the ventricular wall[1] and adequate blood flow is maintained. However, depending on the degree and level of the overload, the adaptive response may progress to a state of impaired contractile capability, leading to heart failure. In the MCT-dose-controlled model of graded pulmonary hypertension and defined phenotypical outcome described in this thesis, the term maladaptive hypertrophy does not exclude the existence of a compensatory phase during ventricular remodelling. In fact, for both MCT doses, the RV response is first thought to proceed through an initial phase of RV hypertrophy, i.e., days 14-19. At the end of this phase, the balance between beneficial and detrimental signals shifts towards maladaptive remodelling, causing the adaptive or maladaptive characters of the response to become discernable. This implies that prior to the shift in balance from beneficial towards detrimental signalling, the hypertrophy observed in both these phenotypes is likely to be identical. However, this paradigm of ventricular hypertrophy does not take into account the possibility that adaptive and maladaptive myocardial remodelling may already have diverged at an early stage during the overload.

1: Myocardial Hypertrophy

The observed decreases in plasma T3 and body weight between days 19 and 25, are indicative of the development of the maladaptive phenotype. However, these two parameters do not provide any direct information regarding the contractile function of the RV of the heart. Therefore, it is essential for the unambiguous interpretation of the data presented in this thesis to have a clear set of definitions of what characterizes the adaptive and maladaptive hypertrophic phenotypes.

Defining Hypertrophy Phenotypes

Dorn II *et al.* devised a simple scheme with criteria to differentiate between these two phenotypes (Figure 1)[2]. First of all, hypertrophy at the individual cardiac myocyte level has to be evident, i.e., increased cell size, and not just an increase of the heart or ventricle itself. In the MCT model, RV myocyte cross-sectional area (CSA) for the HYP and CHF groups at day 19 after MCT injections showed a similar increase in size for both MCT-injected groups relative to control levels (CON vs. HYP vs. CHF; 258 ± 54 vs. 462 ± 5* vs. 473 ± 26* μm^2). Interestingly, myocyte CSA at day 25 for the three groups showed comparable levels to those observed at day 19 (232 ± 19 vs. 467 ± 50* vs. 476 ± 51* μm^2) (unpublished observations; Figure 2). This indicates that the parallel addition of sarcomeres, i.e., concentric remodelling, had already reached a maximum level at day 19. The additional increase in RV weight observed between day 19 and 25 may be explained both by excessive extracellular matrix deposition and/or increased myocyte length through the addition of sarcomeres in series to existing ones, i.e., eccentric remodelling.

As a second differentiating criterion between either an adaptive or maladaptive hypertrophy phenotype, a measure of cardiac myocyte contractility should be provided. SERCA2a is an important contributor to cardiac myocyte contractility since SERCA2a activity is a determinant of the frequency-dependent increase in Ca^{2+}-transient amplitude which governs the positive FFR in rat trabeculae[3]. SERCA2a-mRNA expression was shown to be significantly downregulated at day 25 in the CHF group relative to both CON and HYP animals. In line with these observations, positive force-frequency relationships were observed for both the CON and HYP animals at day 25, whereas CHF animals did not show this potentiation.

The increases in cardiac myocyte CSA in both hypertrophy groups and the differences in FFR responses between the two groups, indicate the adaptive and maladaptive nature of the HYP and CHF hypertrophy phenotypes, respectively. However, more data may be added to further characterize the adaptive and maladaptive hypertrophy phenotypes in the MCT-dose-controlled hypertrophy model. In addition to cardiac

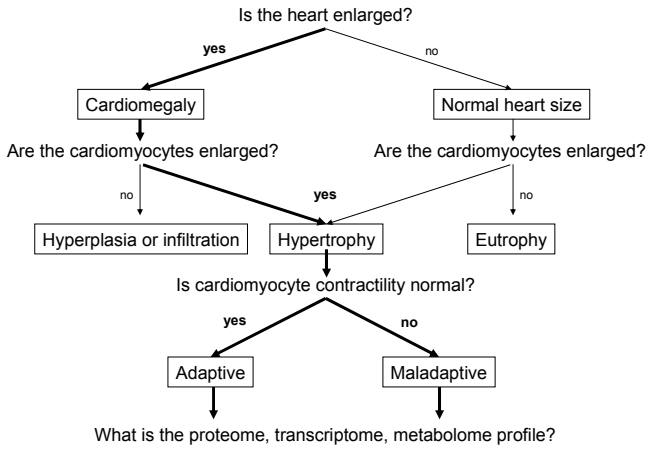

◄Figure 1 - Simple criteria for classifying cardiac hypertrophy phenotypes. See accompanying text. Adapted from Dorn II[2] *et al*.

myocyte CSA, myocyte volume determinations could better characterize the eccentric remodelling response between day 19 and 25. Also, the increases in RV mass for both the HYP and CHF groups could partially be related to immune-related cell types, i.e., macrophage[4] and mast cells[5], which have been shown to infiltrate hypertrophic myocardium during conditions of pressure overload. Additional parameters that could be used to determine the functional characteristics underlying the adaptive or maladaptive phenotypes include calcium sensitivity, end-diastolic and systolic pressures, fractional shortening, ejection fraction and wall stress, as a classical parameter. In fact, a recent publication by Hessel *et al.* characterized the RV hemodynamics in the MCT-dose controlled RV hypertrophy model[6]. At four weeks after MCT injections, RV end-systolic pressure (PES) and relaxation time constant (tau) were maintained in the adaptive hypertrophy group. However, in the maladaptive group, these parameters were significantly altered relative to both controls and MCT30 animals, i.e., increased PES and decreased tau. The RV ejection fraction was significantly reduced in the MCT30 group (rel. to CON), as well as in the MCT80 group (rel. to CON and HYP). Moreover, this paper also suggests that the eccentric remodelling observed in the MCT model may, in part, be due to myocyte slippage[6].

Natriuretic Peptive Levels

Plasma brain natriuretic peptide levels have recently been proposed as a diagnostic and prognostic marker in heart failure[7, 8]. Surprisingly, plasma BNP-32 levels did not allow differentiation between the adaptive and maladaptive hypertrophy phenotypes. BNP mRNA expression on the arrays showed a similar profile. Nevertheless, plasma BNP levels at day 25 showed a significant correlation with RV to LV+IVS ratio

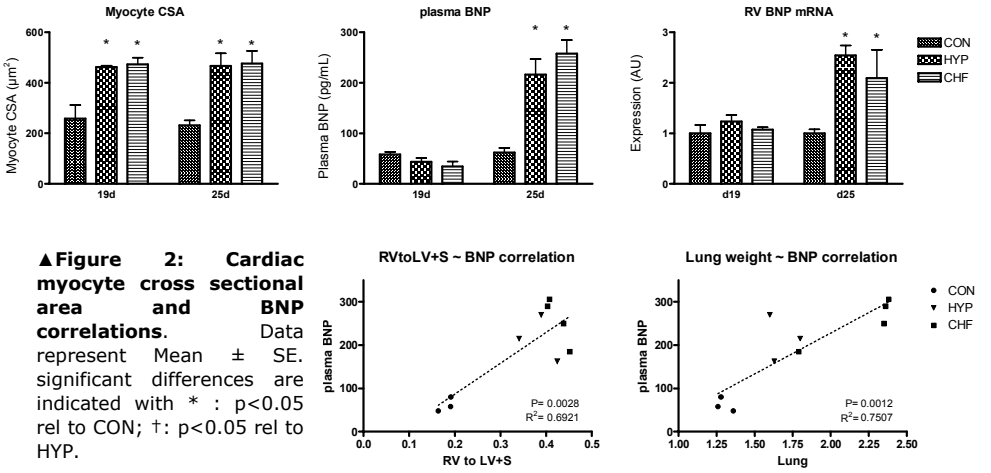

▲Figure 2: Cardiac myocyte cross sectional area and BNP correlations. Data represent Mean ± SE. significant differences are indicated with * : p<0.05 rel to CON; †: p<0.05 rel to HYP.

(p=0.0028, R^2=0.69) and lung weight (p=0.0012, R^2=0.75) (Figure 2). These data suggest that elevations of plasma BNP levels are a late event during RV hypertrophy development and not to be a reliable predictor of outcome in this model. Similar findings have been reported when BNP mRNA transcript levels of hearts from hypertensive homozygous renin-overexpressing (Ren-2) rats that progressed to early HF were compared with those of Ren-2 rats that remained compensated[9].

Left Ventricular Alterations Due To RV Hypertrophy

Evidence is emerging that RV hypertrophy in the MCT model also affects the LV of these hearts. A likely mechanism for these alterations is through increased plasma noradrenalin levels, leading to reduced total β-adrenergic receptor density in both the LV and RV through downregulation of the β1 receptor isoform[10]. As a result of diminished β1-adrenergic receptor densities, ventricular protein and mRNA expression may be altered. Proteome analysis comparing both RV and LV to their corresponding time-matched control ventricles at 20-24 days after injection of 50 mg MCT/kg bw, indicated protein expression changes unique to either ventricle, i.e., no overlap was observed between proteins that were significantly regulated in the RV and LV[11].

However, the time point at which these additional alterations emerge, as well as to how these factors contribute to the overall phenotype are poorly understood. Therefore, physiological as well as molecular parameters should be determined not only in RV, but also in LV and IVS. Nonetheless, it is without question that the primary trigger for these additional events is the hypertrophic response of the RV to pressure overload.

Alternative Models For Adaptive vs. Maladaptive Remodelling

In the literature, several studies have been described that used animal models to study adaptive and maladaptive myocardial hypertrophy. Most of these studies focussed on end-stage phenotypes to investigate molecular processes associated with the development of either adaptive or maladaptive hypertrophy, making it difficult to discern between primary and secondary hypertrophic responses to pressure overload. The primary molecular hypertrophic responses that drive either adaptive or maladaptive remodelling can only be visualized at time points prior to the divergence of these two phenotypes. However, the time point at which this divergence of the two phenotypes actually occurs, is not known, and is likely to differ between models and different species. Visualizing the primary events leading to either of the hypertrophic phenotypes can only be achieved in animal models for which phenotypical outcome is known in advance, e.g., exercise induced hypertrophy[12-14] and the MCT-dose controlled model[15], or, when a reliable assessment of phenotypical outcome can be obtained at early time points during ventricular remodelling, without affecting the normal remodelling processes, e.g., through plasma profiling or procuring biopsies.

The hypertensive homozygous renin transgenic TGR (mRen-2) (Ren-2) rats[16] have recently been used to study early events during myocardial remodelling[9, 17]. All Ren-2 rats develop cardiac hypertrophy, although only a subset of these animals rapidly progress towards a maladaptive phenotype (12-14 weeks of age), while the remaining rats develop an adaptive hypertrophy state (sacrificed at 17 weeks of age). Micro-array analyses performed on LV tissue from both the adaptive and maladaptive rats indicated 48 genes with higher expression and 14 genes with lower expression in the Ren-2 rats that developed heart failure compared to those that developed compensated hypertrophy. In a parallel series of experiments, LV myocardial biopsy material was obtained from these Ren2 rats at a time point prior to phenotypical divergence, i.e., 10 weeks of age. End-point phenotype of the individual rats was determined by longitudinal follow-up observations up to 17 weeks of age. Analysis performed on the 10 week biopsy samples using qPCR indicated that from the set of regulated genes both thrombospondin-2[9] and Galectin-3[17] were already upregulated in the rats that would later progress to heart failure, while for those that remained in a compensated hypertrophy state, the expression of these two genes was comparable to that in time-matched Sprague-Dawley control rats.

Similar to the emergence of two groups for the Ren-2 rats in 17 weeks, a single dose of 40 mg MCT / kg body weight leads to subsets of animal phenotypes, either with or without characteristic signs of heart failure within 4 weeks after MCT injections[18]. However, an analogous approach to the one described above is not feasible for this

model due to the thin RV wall which does not allow for the procurement of tissue biopsy samples.

Another frequently used approach to investigate differences in gene-expression between adaptive and maladaptive ventricular remodelling is to compare exercise-induced left-ventricular hypertrophy with maladaptive remodelling. Strøm *et al.* first evaluated gene-expression differences between LV myocardium of male Wistar rats after 7.5 weeks of intermittent treadmill exercise with age matched sedentary rats[13]. Next, they focussed, using qPCR, on metabolism related genes, and confirmed the differential expression of both upregulated genes, i.e., fatty acid translocase (FAT/CD36), fatty acid binding protein 4 (FABP4), fatty acid transport protein (Slc27a1) and glucokinase regulatory protein (GCKR), as well as downregulated genes, i.e., uncoupling protein 2 (UCP2) in the exercise group. An additional set of qPCR experiments focussed on UCP2 and CD36 expression in the non-infarcted ventricular regions of the LV three weeks after myocardial infarction (MI). This revealed that CD36 was only upregulated in the exercise hypertrophy group, i.e., the MI animals did not show a significant difference in expression relative to control animals. UCP2 expression was downregulated in adaptive exercise-induced hypertrophy, while expression of this gene was upregulated after MI relative to control animals. In general, downregulation of fatty acid metabolism-related genes is observed during hypertrophic remodelling[19, 20]. Interestingly, upregulation of such genes was observed in the exercise-induced hypertrophy group. From these studies the authors concluded that the exercise-induced adaptive hypertrophy group showed signs of a successful switch in metabolism[13]. However, this study did not provide a large scale comprehensive gene-expression comparison between adaptive and maladaptive hypertrophy responses, as was presented in a study by Kong et al[12]. Exercise-induced cardiac hypertrophy was compared to hypertrophy and heart failure in Dahl salt-sensitive rats[12]. A similar degree of hypertrophy was achieved in both groups when compared to time-matched control animals. However, several distinct clusters of genes could be discerned, i.e., genes with expression alterations that were specific for either the adaptive or maladaptive group and genes that showed similar gene-expression changes in both hypertrophy groups relative to controls. These results are comparable to those described in Chapter 2 of this thesis, i.e., clusters V, IV and III, respectively. However, the identity of the genes within these clusters varied substantially between these studies. The authors concluded from these model-specific gene-expression responses that activation of different signalling cascades is associated with either model, e.g., inflammation, oxidative stress, apoptosis and acute stress responses.

A more drastic view of model-specific responses was presented by Aronow *et al.*. They initially hypothesized that the hypertrophic response of the myocardium which is observed in human cardiomyopathies and in a wide variety of animal models, is the result of a conserved hypertrophic gene-expression program[21]. When they compared LV myocardium obtained from three transgenic mouse models for cardiac hypertrophy to their non-transgenic control animals, the number of differentially expressed genes did appear to be correlated with the observed phenotypic severity. However, when the gene-expression alterations of the three transgenic mouse models were compared, no common conserved transcription program could be observed for these models. Rather, unique transcriptional responses to each individual genetic cause of hypertrophy were found[21].

The studies described above provide valuable information on processes that discern between adaptive and maladaptive ventricular hypertrophy. However, the remodelling response observed for the MI model is a complex mixture of pressure and volume overload, making extrapolation to isolated pressure overloaded concentric hypertrophy difficult.
Also, one must keep in mind that during exercise-induced cardiac hypertrophy, neither an increase in resting left ventricular systolic pressure[14] nor in mean arterial pressure[13] is observed. Moreover, exercise training has an on/off nature. In contrast to a chronic pathological stimulus, the profile of intermittent stimuli in time may allow the ventricle to adapt successfully.

2: Time Dependent Remodelling Processes

The myocardial gene-expression alterations in the RV during the development of pressure overload, were determined in two separate micro-array experiment series, i.e., day 14 (Chapter 2; set 1) and days 10, 19 and 25 (Chapter 3; set 2). To obtain a complete picture of the time-dependency of gene-expression alterations, these two datasets may be combined. This may appear to be straightforward, however there are some fundamental differences between these two data sets that need to be taken into account.

Differences Between Expression Array Data sets
When comparing the experimental setup of both array series, several common as well as different features become apparent. An identical oligonucleotide-library set representing 4803 features was spotted in duplicate on different areas of the arrays, albeit with an overall different spatial distribution due to the different array printing techniques used. Also, both experiment series used the common reference design setup, but different RNA pools were used for each of these series to hybridize the CON, HYP and CHF samples. In addition, the amount of total RNA used per channel was reduced from 100 to 30 µg in the second set, yet the generation of labelled cDNA strands was identical. Also, the hybridization techniques differed from the custom setup, including a pre-hybridization for set 1, whereas for experiment set 2, automated hybridization, without pre-hybridization, was used. These methodological differences between micro-array experiment series, as well as different data pre-selection criteria, lead to different sets of genes to be analysed after pre-processing the raw data, i.e., 3060 and 3148 genes analysed in Chapters 2 and 3, respectively. In total, 3335 unique features were analysed, of which 2823 were overlapping between datasets (Table 1).

Statistical (re)Considerations
A more important difference between the array series is that the statistics used to test for significant differential gene expression between experimental groups was different between the two array experiment series. The relatively simple Z-test used for statistical inference for array set 1 could not be used for the second, more complex data set. The structure of the second set, i.e., containing the experimental factors time and MCT, as well as the interaction between these two factors, called for a more suitable statistical framework which would be able to cover the structure of this dataset.

Linear models[22], e.g., Maanova[23, 24] and Limma[25], can be used for the analysis of two-colour micro-array expression data and allow for the incorporation and analysis of multiple experimental factors at once in one dataset. Re-analyzing the day 14 dataset using a similar approach to the one described in Chapter 3 is possible, as is integration of the day 14 dataset into the day 10-19-25 dataset and analysing all four time points in a multifactorial design. In retrospect however, a mixed-model Anova using the fixed factors MCT (CON, HYP, CHF), Time (d10, d14, d19, d25), the interaction between the Time and MCT factor, and the random factors Array (45 in total), Spot (two duplicates per array) and the hybridization sessions (d14 vs d10+d19+d25), would be able to efficiently cover all expression data. However, a thorough re-analysis of the entire dataset containing all four time points, including GSEA and/or EASE over-representation analyses on individual Self-organizing-Map clusters, falls outside the scope of this discussion. However, at some points in the discussion, a few relatively simple data manipulations will be presented, although the remainder will focus on processes as discussed in Chapters 2, 3 and 4.

Increase In Pulmonary Arterial Pressure In Time

MCT leads to dose-dependent damage and remodelling of the pulmonary arterioles. A higher MCT dose does not only lead to more extensive vascular damage and remodelling, but is also likely to give rise to an accelerated increase in pulmonary arterial pressure (PAP) compared to lower doses, as is depicted in the left panel of

	Chapter 2 (set1)	Chapter 3 (set2)
Days after MCT injection	14	10, 19, 25
Arrays	6 per group	3 per group per time point
Reference pool	Equal amounts of RNA from all three groups from RV and LV	IVS from all three groups at days 19 and 25
totalRNA per sample	100µg	30µg
Hybridization	Custom setup With pre-hybridization	Perkin Elmer HybArray 12™ No pre-hybridization
Gene selection	Max three flagged datapoints of six arrays per group per gene	No flagged datapoints allowed in entire dataset
Genes analysed	3060	3148
Statistical test	Z-score	R/Maanova

▲Table 1 - Methodological differences between micro-array experiments.
See accompanying text.

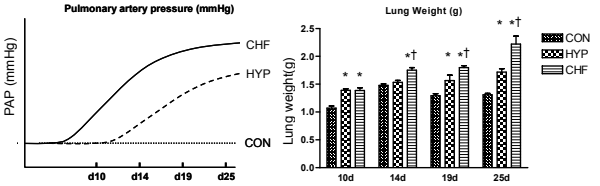

►**Figure 3** – PAP and Lung weight in time. Data represent Mean ± SE and significant differences are indicated with * : $p<0.05$ rel to CON; †: $p<0.05$ rel to HYP.

Figure 3. The rise in PAP is related to the increase in lung weight[26, 27] (Figure 3 – right panel). Possibly, this delayed and dampened, increase in pressure-overload in the MCT30 group allows the ventricle to adapt gradually, in contrast to the MCT80 group, where pressure increases shortly and sharply after MCT administration, which may tip the delicate balance between detrimental and beneficial processes already early during remodelling.

The expression patterns of the cell-cycle related genes cyclin B1, cell division cycle control protein 2 (Cdc2a), cell division cycle control protein 20 (cdc20/p55cdc), as well as aurora kinase-B (AurkB), fit the above described profile, i.e., an earlier upregulation in the CHF than in HYP. This response may represent a futile response of the myocardium to increase the number of cardiac myocytes, i.e., adult cardiac myocytes are unable to proceed through the cell cycle, and in fact, may be detrimental, ultimately leading to decompensation. However, it may just as well be that these changes represent cell division responses originating from other ventricular cell types, e.g., endothelial cells, vascular smooth muscle cells or cardiac fibroblasts. The heterogeneous cell population of the heart makes unambiguous interpretation of the mRNA-expression data difficult. To cope with this problem, Wang *et al.* recently proposed a method that allows for computational deconvolution of the mixed cell-type tissue expression profiles, by incorporating expression profiles of the individual cell types present in that mixed tissue[28]. Alternatively, immunofluorescence may be used to detect changes in protein levels, or, in situ hybridizations may be used to measure mRNA levels to determine the cellular origin of the observed changes.

Correlation to lung weight may identify unknown pressure-overload-responsive genes although actual pressure measurements would be preferable. In parallel, significant correlation with the RV to LV+IVS weight ratio, or RV weights alone, would implicate hypertrophy-associated gene-expression processes. Table 2, summarizes the number of significant positively and negatively correlated genes for several parameters. Interestingly, though only a few genes were correlated to body-weight alterations in the experiment series and none to liver weight, in total 138 genes displayed significant correlations to lung weight. This indicates an obvious link between lung weight changes and RV hypertrophy. The largest number of genes was found to be

	Liver	Body weight	Lung	RV	RV / LV+S
POS	0	10	63	134	130
NEG	0	4	75	205	187
total	0	14	138	339	317

▲**Table 2 - Significant correlation with physical parameters**. Significant positive or negative correlation between the expression data derived from the array and physical parameters was determined with a Pearson correlation test. Genes having a Benjamini-Hochberg false discovery rate(FDR)[29] corrected p-value below 0.01, i.e., a maximum of 1% FDR genes in the list or significantly regulated genes, and with a Pearson correlation coefficient greater than 0.7 or below -0.7, were considered to be significantly correlated.

significantly correlated to the RV weight. An EASE[30] gene-ontology over-representation analysis indicated cell adhesion and extracellular space to be represented in the top ranking processes for the positively correlated genes, while fatty acid metabolism and mitochondrion were top ranking in the negatively correlated genes (data not shown). In Chapter 3 - Figure 4, these same gene categories were shown to be present in clusters displaying either predominantly up- or downregulated genes. Also, in a model of transverse aortic constriction, these same classifications emerged when correlating gene-expression alterations to LV parameters[31], indicating that LV and RV myocardial remodelling show a substantial number of parallel cellular responses to pressure overload.

Dynamic Processes Associated With Maladaptive Remodelling

Highly dynamic gene-expression alterations were observed during the development of both adaptive and maladaptive ventricular hypertrophy, with simultaneous alterations of many related and unrelated processes over time. These highly variable expression profiles illustrate the importance of proper timing when comparing mRNA and protein-expression levels between different experimental models, or even within one model.

At different time points during ventricular remodelling, changes at the metabolism substrate level could be inferred. The switch from fatty acids towards glucose as the predominant substrate for energy metabolism in the established hypertrophied heart is a well known fact[19, 20]. Chapter 2 provided the first evidence of altered mitochondrial biogenesis between the HYP and CHF groups at day 14 during myocardial remodelling in the form of CHF-specific downregulation of the mitochondrial transcription factor A (mtTFA). Chapter 3 showed a more extensive picture of altered substrate metabolism, predominantly at days 19 and 25 after MCT

injections, though with little differences between the two hypertrophy groups. The late events in the shift in metabolism were paralleled by a decrease in the expression of the transcription cofactor peroxisome proliferative activated receptor-α (PPARα) coactivator-1a (PGC-1a) (Chapter 3, online results supplement), with an overall decrease in expression of genes with corresponding mitochondrial proteins, as described in the previous paragraph and Chapter 3.

Unexpected was the observed CHF-specific downregulation of mitochondrial enoyl-CoA hydratase (Echs1) at both the mRNA and protein levels already at day 10 after MCT injections in Chapter 4, as determined by qPCR and 2-dimensional gel electrophoresis, respectively. However, the micro-array data indicated that this downregulation was abolished at day 19, while it was again downregulated at day 25, both in the HYP and CHF groups relative to control levels. Moreover, a gene set enrichment analysis (GSEA) that specifically focussed on the differences between the HYP and CHF groups, indicated elevated gene-expression levels in CHF compared to HYP at day 10 for genes implicated in the mitochondrial electron transport chain (mETC). However, at day 25 these elevated expression levels in CHF had decreased to a level below that of the HYP group, suggesting reduced mETC activity in the CHF group at day 25. This argues for a possible biphasic regulation for at least a part of the metabolism-related genes during ventricular remodelling.

The GSEA analysis mentioned in the previous paragraph also indicated cell-cycle regulation to be associated with phenotypical outcome. The delayed increase in cyclinB1 and Cdk1 levels in HYP relative CHF, as well as increased Gadd45a expression levels in the HYP group at later time points, could prevent potentially detrimental G2/M checkpoint transition in adaptive remodelling. The gene-expression data obtained at day 14 after MCT injections, pointed to detrimental p38-MAPK related processes triggering apoptosis, and subsequent maladaptive remodelling. However, at the other time points examined, p38-related processes and apoptosis related gene-expression alterations could not be detected.

Overall, these observations attest to phases, or, successive waves of detrimental processes over time that ultimately culminate into maladaptive remodelling.

3: Clinical Implications

Patients with PAH display right atrial (RA) and RV enlargement, reduced RV function, displacement of the interventricular septum and tricuspid regurgitation. A subpopulation of patients who have been diagnosed with having pulmonary arterial hypertension (PAH), may die within months after diagnosis, while others survive for decades, reflecting the CHF and HYP groups as characterized using the MCT model in this thesis. A hemodynamic predictor of survival for patients with idiopathic PAH (IPAH), is mean PAP. The detection of pericardial effusion by echocardiography has negative prognostic implications, as does indexed RA area. Also a reduced performance in the 6 minute walking test (6MWT) for PAH patients has been observed. A detailed overview of clinical parameters for prognosis determination was recently described by McLaughlin *et al.*[32]. However, the sum of clinical parameters is insufficiently able to reliably determine prognosis, pressing the need for additional parameters.

Halting, or even reversing progression of detrimental myocardial remodelling, is essential for proper patient care. The data presented within this thesis may provide information for the further research and development of new biomarkers that allow for accurate patient prognosis. Though many of the genes that were assayed display similar regulation for both the HYP and CHF groups relative to the control animals and display highly variable expression patterns in time, a small set of genes did show commitment differential expression between the adaptive and maladaptive hypertrophy groups.

From this subset of genes it may be possible to device a method that allows for prediction of phenotypical outcome, at least for MCT rats. A combination of gene-expression profiles for growth arrest and DNA-damage-inducible alpha (Gadd45a), which has significantly higher expression levels in the HYP groups at days 19 and 25 rel. to CHF and CON, and heme-oxygenase 1 (HO1), which has higher expression levels in the CHF group rel. to both HYP and CON at days 10, 19 and 25 (Figure 4), may be able to predict the emergence of either an adaptive or maladaptive hypertrophic phenotype.

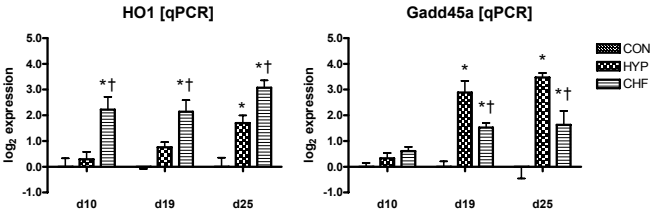

►**Figure 4 - GADD45a and HO1 expression profiles.** Data represent Mean ± SE and significant differences are indicated with * : p<0.05 rel to CON; †: p<0.05 rel to HYP.

The micro-array data from all four time points may also provide a more solid basis, or at least a starting point, for the development of a set of prognostic arrays for phenotypical outcome. Figure 5 shows the results of a simple approach taken to determine if there indeed is a subset of genes at each of the time points that may differentiate between the CON, HYP and CHF groups. For each of the four time points, the three experimental groups show complete or near complete separation. Still, one must keep in mind that only three to six arrays per group were used, which is a too small sample population for such predictor analyses. Thus, more research has to be done to confirm these claims, not only in MCT rats but also in other models for either adaptive or maladaptive ventricular remodelling, and a human patient population. The development of a diagnostic array which could classify patients on the basis of many differentiating genes may appear to be ideal, however, the major disadvantage is that one needs to obtain cardiac muscle tissue to perform the tests, which may not be easily accessible.

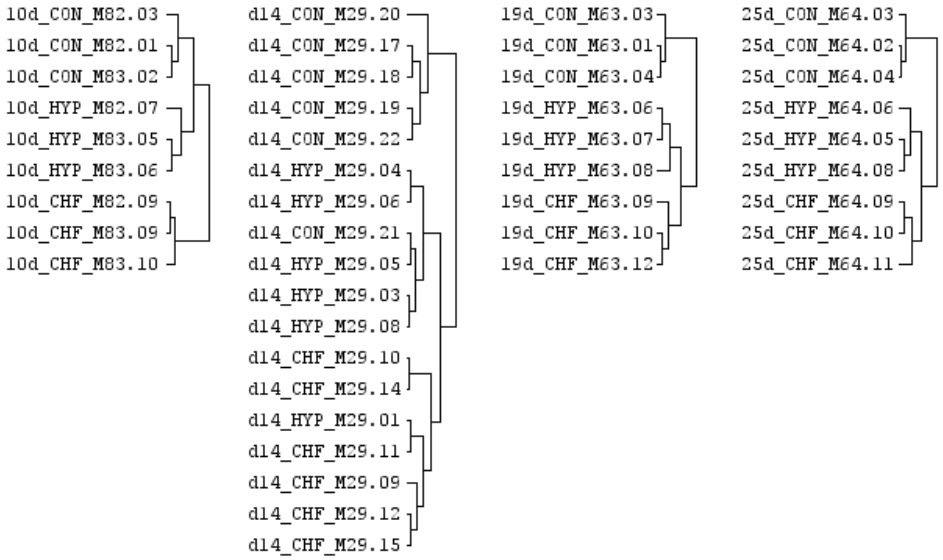

▲Figure 5 - Hierarchical clustering separates the three experimental groups per time point. Classical One way ANOVA ($p \leq 0.01$) between groups for each separate time point. Significantly regulated genes were mean centered and normalized for genes followed by mean center and normalize per sample. Data were hierarchically clustered using average linkage and euclidean distance. Clustering was based on 37, 47, 122 and 381 significantly regulated genes for time points 10, 14, 19 and 25 days post MCT injections, respectively. Anova analyses and clustering were performed in the Tigr multiple experiment viewer which is part of the TM4 software package[33]. From left to right, sample tree dendrograms are shown for days 10, 14, 19 and 25, respectively. Note that the CON, HYP and CHF samples form separate clusters at each time point, except at day 14, where almost complete separation is seen.

4: Perspectives For Further Studies

At several points in the previous paragraphs, proposals for further research have already been mentioned, and some additional options will be presented here.

Extension Of The Expression Arrays Analyses

The total genome of the taxus Rattus norvegicus, comprising 20 autosomes, one sex chromosome and a mitochondrial chromosome, contains an estimated 33.991 gene transcripts, ~20.000 of which may represent protein-coding genes (www.ensembl.org). The arrays used in the studies described in this thesis represented only ~24% of the whole protein-coding genome. New series of experiments covering a larger extent of the rat genome is likely to identify more genes with expression alterations that are associated with myocardial remodelling. Particularly, more genes may be identified that drive the differentiation between the adaptive and maladaptive hypertrophy groups. The new generation of arrays that are now available contain enough unique probe sequences to effectively cover the entire rat genome, e.g., Affymetrix and Agilent-technologies.

The expression profiles obtained in this thesis were mainly focussed on the RV myocardium, with only a small representation of LV profiles (n=2 per group, Chapter 2). Still, a small number of genes was indicated to be regulated in the LV. Extending the array analyses to other (extra)myocardial tissue components at different time points could further characterize this response and potentially reveal the origin of these additional effects.

Proteome Analyses

The 2-dimensional gel electrophoresis experiments displayed a high reproducibility, which is essential if one would like to extend the current day 10 analyses to span multiple time points, several tissue components and/or subcellular organelle fractions. Over 10% of the total number of regulated genes coded for genes with corresponding proteins that localized to the mitochondria, identifying it as an important affected subcellular compartment in heart failure.

One shortcoming of the proteome analysis described in Chapter 4 is the relatively low number of positively identified significantly regulated proteins. A higher success-rate percentage will profoundly increase the value of the data presented. Moreover, in general, proteins may be subject to multiple forms of post-translational modifications like phosphorylation, acetylation, glycosilation. The study as it was performed was unable to detect such modification.

Unexplored here, but related to proteome analyses, is serum or plasma protein profiling. Blood is more conveniently collected than a small piece of ventricular tissue. Also urinary biomarkers may be explored as a potential means to classify patients to either a good or bad prognosis.

General Extrapolation

To assess whether the findings assembled in Chapters 2, 3 and 4, represent more generally applicable mechanisms, it will be essential to specifically explore these alterations in other animal models representing human cardiomyopathies as well as in the human patient population at risk.

5: Conclusions

Does maladaptive right-ventricular hypertrophy evolve from an adaptive precursor state? The evidence presented in this thesis, accumulated by different techniques ranging from fundamental protein and mRNA measurements to physiological cardiac function determinations, states that it does not.

Already early after the imposition of pressure overload in the MCT model for controlled phenotypical outcome, the adaptive and maladaptive hypertrophy groups differ at both the proteome and transcriptome levels. Maladaptive remodelling was associated with signs of aberrant cell-cycle progression, decreased mitochondrial beta-oxidation of fatty acids and increased mitochondrial electron transport chain activity at 10 days after MCT injections. At 14 days, decreased mitochondrial biogenesis paired with pro-death effector signalling via p38 MAPK were observed for maladaptive remodelling, while at day 25, decreased mitochondrial electron transport chain activity could be inferred from the micro-array expression data. These successive waves of detrimental processes over time ultimately culminate into maladaptive remodelling.

Reference List

(1) Grossman W, Jones D, McLaurin LP. Wall stress and patterns of hypertrophy in the human left ventricle. *J Clin Invest* 1975 July;56(1):56-64.

(2) Dorn GW, II, Robbins J, Sugden PH. Phenotyping Hypertrophy: Eschew Obfuscation. *Circ Res* 2003 June 13;92(11):1171-5.

(3) Janssen PML, Stull LB, Marban E. Myofilament properties comprise the rate-limiting step for cardiac relaxation at body temperature in the rat. *Am J Physiol Heart Circ Physiol* 2002 February 1;282(2):H499-H507.

(4) Shioi T, Matsumori A, Kihara Y, Inoko M, Ono K, Iwanaga Y, Yamada T, Iwasaki A, Matsushima K, Sasayama S. Increased Expression of Interleukin-1¯ and Monocyte Chemotactic and Activating Factor/Monocyte Chemoattractant Protein-1 in the Hypertrophied and Failing Heart With Pressure Overload. *Circ Res* 1997 November 19;81(5):664-71.

(5) Hara M, Ono K, Hwang MW, Iwasaki A, Okada M, Nakatani K, Sasayama S, Matsumori A. Evidence for a Role of Mast Cells in the Evolution to Congestive Heart Failure. *J Exp Med* 2002 February 4;195(3):375-81.

(6) Hessel MHM, Steendijk P, den Adel B, Schutte CI, van der Laarse A. Characterization of right ventricular function after monocrotaline-induced pulmonary hypertension in the intact rat. *Am J Physiol Heart Circ Physiol* 2006 May 26;00369.

(7) Morisco C, Sadoshima J, Trimarco B, Arora R, Vatner DE, Vatner SF. Is treating cardiac hypertrophy salutary or detrimental: the two faces of Janus. *Am J Physiol Heart Circ Physiol* 2003 April 1;284(4): H1043.

(8) Nagaya MD N, Nishikimi MD P, Okano MD Y, Uematsu MD P, Satoh MD P, Kyotani MD P. Plasma Brain Natriuretic Peptide Levels Increase in Proportion to the Extent of Right Ventricular Dysfunction in Pulmonary Hypertension. *Journal of the American College of Cardiology* 1998 January;31(1):202-8.

(9) Schroen B, Heymans S, Sharma U, Blankesteijn WM, Pokharel S, Cleutjens JPM, Porter JG, Evelo CTA, Duisters R, van Leeuwen REW, Janssen BJA, Debets JJM, Smits JFM, Daemen MJAP, Crijns HJGM, Bornstein P, Pinto YM. Thrombospondin-2 Is Essential for Myocardial Matrix Integrity: Increased Expression Identifies Failure-Prone Cardiac Hypertrophy. *Circ Res* 2004 September 3;95(5):515-22.

(10) Leineweber K, Brandt K, Wludyka B, Beilfuss A, Ponicke K, Heinroth-Hoffmann I, Brodde OE. Ventricular Hypertrophy Plus Neurohumoral Activation Is Necessary to Alter the Cardiac {beta}-Adrenoceptor System in Experimental Heart Failure. *Circ Res* 2002 November 29;91(11):1056-62.

(11) Schott P, Singer SS, Kogler H, Neddermeier D, Leineweber K, Brodde OE, Regitz-Zagrosek V, Schmidt B, Dihazi H, Hasenfuss G. Pressure overload and neurohumoral activation differentially affect the myocardial proteome. *Proteomics* 2005 April;5(5):1372-81.

(12) Kong SW, Bodyak N, Yue P, Liu Z, Brown J, Izumo S, Kang PM. Genetic expression profiles during physiological and pathological cardiac hypertrophy and heart failure in rats. *Physiol Genomics* 2005 March 21;21(1):34-42.

(13) Strom CC, Aplin M, Ploug T, Christoffersen TEH, Langfort J, Viese M, Galbo H, Haunso S, Sheikh SP. Expression profiling reveals differences in metabolic gene expression between exercise-induced cardiac effects and maladaptive cardiac hypertrophy. *FEBS Journal* 2005;272(11):2684-95.

(14) Iemitsu M, Maeda S, Miyauchi T, Matsuda M, Tanaka H. Gene expression profiling of exercise-induced cardiac hypertrophy in rats. *Acta Physiologica Scandinavica* 2005;185(4):259-70.

(15) Buermans HPJ, Redout EM, Schiel AE, Musters RJP, Zuidwijk M, Eijk PP, van Hardeveld C, Kasanmoentalib S, Visser FC, Ylstra B, Simonides WS. Microarray analysis reveals pivotal divergent mRNA expression profiles early in the development of either compensated ventricular hypertrophy or heart failure. *Physiol Genomics* 2005 May 11;21(3):314-23.

(16) Pinto YM, Pinto-Sietsma SJ, Philipp T, Engler S, mehl P, Hocher B, Marquardt H, Sethmann S, Lauster R, Merker HJ, Paul M. Reduction in Left Ventricular Messenger RNA for Transforming Growth Factor {beta}1 Attenuates Left Ventricular Fibrosis and Improves Survival Without Lowering Blood Pressure in the Hypertensive TGR(mRen2)27 Rat. *Hypertension* 2000 November 1; 36(5):747-54.

(17) Sharma UC, Pokharel S, van Brakel TJ, van Berlo JH, Cleutjens JPM, Schroen B, Andre S, Crijns HJGM, Gabius H, Maessen J, Pinto YM. Galectin-3 Marks Activated Macrophages in Failure-Prone Hypertrophied Hearts and Contributes to Cardiac Dysfunction. *Circulation* 2004 November 9;110(19):3121-8.

(18) Wassen FW, Schiel AE, Kuiper GG, Kaptein E, Bakker O, Visser TJ, Simonides WS. Induction of thyroid hormone-degrading deiodinase in cardiac hypertrophy and failure. *Endocrinology* 2002 July;143(7):2812-5.

(19) Lehman JJ, Kelly DP. Gene regulatory mechanisms governing energy metabolism during cardiac hypertrophic growth. *Heart Fail Rev* 2002 April;7(2):175-85.

(20) Stanley WC, Recchia FA, Lopaschuk GD. Myocardial Substrate Metabolism in the Normal and Failing Heart. *Physiol Rev* 2005 July 1;85(3):1093-129.

(21) Aronow BJ, Toyokawa T, Canning A, Haghighi K, Delling U, Kranias E, Molkentin JD, Dorn GW. Divergent transcriptional responses to independent genetic causes of cardiac hypertrophy. *Physiol Genomics* 2001 June 6;6(1):19-28.

(22) Kerr MK. Linear models for microarray data analysis: hidden similarities and differences. *J Comput Biol* 2003;10(6):891-901.

(23) Kerr MK, Martin M, Churchill GA. Analysis of variance for gene expression microarray data. *J Comput Biol* 2000;7(6):819-37.

(24) Cui X, Hwang JTG, Qiu J, Blades NJ, Churchill GA. Improved statistical tests for differential gene expression by shrinking variance components estimates. *Biostat* 2005 January 1;6(1):59-75.

(25) Smyth GK, Michaud J, Scott HS. Use of within-array replicate spots for assessing differential expression in microarray experiments. *Bioinformatics* 2005 May 1;21(9):2067-75.

(26) Wilson DW, Segall HJ, Pan LC, Lame MW, Estep JE, Morin D. Mechanisms and pathology of monocrotaline pulmonary toxicity. *Crit Rev Toxicol* 1992;22(5-6):307-25.

(27) Jones JE, Mendes L, Rudd MA, Russo G, Loscalzo J, Zhang YY. Serial noninvasive assessment of progressive pulmonary hypertension in a rat model. *Am J Physiol Heart Circ Physiol* 2002 July 1;283(1):H364-H371.

(28) Wang M, Master SR, Chodosh LA. Computational expression deconvolution in a complex mammalian organ. *BMC Bioinformatics* 2006 July 3;7(1):328.

(29) Reiner A, Yekutieli D, Benjamini Y. Identifying differentially expressed genes using false discovery rate controlling procedures. *Bioinformatics* 2003 February 12;19(3):368-75.

(30) Hosack D, Dennis G, Sherman B, Lane H, Lempicki R. Identifying biological themes within lists of genes with EASE. *Genome Biology* 2003;4(10):R70.

(31) Mirotsou M, Dzau VJ, Pratt RE, Weinberg EO. Physiological genomics of cardiac disease: quantitative relationships between gene expression and left ventricular hypertrophy. *Physiol Genomics* 2006 July 11;00028.

(32) McLaughlin VV, Presberg KW, Doyle RL, Abman SH, McCrory DC, Fortin T, Ahearn G. Prognosis of Pulmonary Arterial Hypertension*: ACCP Evidence-Based Clinical Practice Guidelines. *Chest* 2004 July 1;126(1_suppl):78S-92.

(33) Saeed AI, Sharov V, White J, Li J, Liang W, Bhagabati N, Braisted J, Klapa M, Currier T, Thiagarajan M, Sturn A, Snuffin M, Rezantsev A, Popov D, Ryltsov A, Kostukovich E, Borisovsky I, Liu Z, Vinsavich A, Trush V, Quackenbush J. TM4: a free, open-source system for microarray data management and analysis. *Biotechniques* 2003 February;34(2):374-8.

Chapter 6

Iconoclasts Topple Adaptive Myocardial Hypertrophy In Aortic Stenosis

Henk P.J. Buermans and Walter J. Paulus, M.D., Ph.D., FESC

Laboratory for Physiology, Institute for Cardiovascular Research (ICaR-VU)
VU University Medical Center, Van der Boechorststraat 7, 1081 BT Amsterdam, The Netherlands.

Published in:
European Heart Journal, 2005 Sep;26(17):1697-9

Table of contents

Introduction

For more than thirty years, the development of concentric left ventricular (LV) hypertrophy in pressure overload was considered adaptive because the parallel deposition of new sarcomeres and the corresponding LV wall thickening succeeded to normalize LV systolic wall stress despite the high intracavitary systolic pressure[1]. In aortic stenosis, the validity of this paradigm was demonstrated by hemodynamic studies, which established an inverse relationship between LV systolic wall stress and LV ejection fraction (EF) and by clinical outcome studies, which demonstrated worse postoperative prognosis if LV performance fell below this inverse LV wall stress-LVEF relationship[2, 3]. This clinical paradigm of adaptive myocardial hypertrophy developing during progression of aortic stenosis clearly withstood the test of time despite the mounting epidemiological evidence of LV hypertrophy being associated with excess cardiac mortality and despite the ominous significance of LV hypertrophy in congenital aortic stenosis.

In this issue of the European Heart Journal, Kupari *et al*. are the first to challenge the time-honored concept of adaptive LV hypertrophy in aortic stenosis[4]. In a carefully designed prospective study of patients with isolated aortic stenosis, they observed an inverse relation between LV mass index and LVEF and a higher prevalence of LV hypertrophy in patients suffering of heart failure. They therefore concluded that development of LV hypertrophy was actually promoting heart failure instead of preventing it.

Basic Inspiration

When Kupari *et al*. started their prospective study 5 years ago, they were well ahead of the crowd in appreciating emerging basic evidence on pressure overload-induced myocardial hypertrophy and in translating it to clinical cardiology[5]. During LV pressure overload, the raised biomechanical stress on the cardiac myocytes stimulates various signal transduction pathways to the nucleus[6] and induces autocrine production and secretion of angiotensin II and endothelin, whose receptors are coupled to Gq proteins. It was precisely in a mouse model with cardiorestricted deficiency in Gq signalling that the paradigm of adaptive LV hypertrophy during pressure overload received a first serious blow[7]. After one week of aortic constriction, control mice showed complete normalization of LV systolic wall stress in contrast to the cardiac gene-targeted mice, who had a blunted hypertrophic response and were unable to reduce LV systolic wall stress. After 8 weeks of aortic constriction, despite

initial normalization of wall stress, control mice developed an increase in chamber dimensions and progressive deterioration of LV function with echocardiographic fractional shortening falling from 59 to 35%. In contrast, cardiac gene targeted mice with blunted LV hypertrophy and persistent elevation of LV systolic wall stress showed after 8 weeks only limited LV dilatation and preserved LV function with an echocardiographic fractional shortening of 52%. From these experiments it was concluded that in pressure overload the left ventricle is better off being "stressed out" than being hypertrophied.
In other models of experimental pressure-overload, investigators however clearly succeeded in creating adaptive or physiological hypertrophy. One of these models was a rat model of right ventricular (RV) hypertrophy caused by monocrotaline(MCT)-induced pulmonary hypertension[8]. When rats were given 30 mg/kg of MCT subcutaneously, they developed slow onset pulmonary hypertension and adaptive RV hypertrophy but when rats were given 80 mg/kg of MCT, there was rapid development of pulmonary hypertension, which was accompanied by RV failure and by premature death. Fourteen days after MCT injection, RV hypertrophy was still identical in rats having received 30 or 80 mg/kg of MCT. However, when RV myocardium was subjected to a micro-array analysis 14 days after MCT injection, 63 genes out of the 3010 cardiac genes screened were already differentially expressed between rats that had received 30 mg/kg of MCT and were going to develop adaptive RV hypertrophy and rats that had received 80 mg/kg of MCT and were going to develop RV failure. This study implies that adaptive hypertrophy does not precede maladaptive hypertrophy in pressure-overload and that the magnitude of the initial pressure-overload stimulus predestines the myocardium to development of an adaptive or maladaptive phenotype. In accordance to these results, development of heart failure in the mice-aortic constriction model and in clinical aortic stenosis is related respectively to the tightness of the aortic band and to the progression of valvular stenosis. Clinical trials, which try to slow the progression of valvular stenosis with statins or angiotensin converting enzyme inhibitors could test the validity of this assumption by demonstrating slower progression of valvular stenosis to be accompanied by reduced incidence of heart failure.

Clinical Translation

Before converting to the iconoclastic view that in aortic stenosis LV hypertrophy is maladaptive, a critical appraisal of the evidence provided by Kupari *et al*. seems justified. The following issues are of concern: 1) failure to identify and to characterize

aortic stenosis patients with LV hypertrophy and no heart failure, i.e. with adaptive LV hypertrophy; 2) no demonstration of a persistent elevation of LV wall stress in the aortic stenosis patients without LV hypertrophy and 3) presence of discordant LVEF-LV hypertrophy relationships when LV hypertrophy is assessed either by LV mass index or by relative wall thickness.

Sixty three aortic stenosis patients were free of heart failure and had evidence of LV hypertrophy defined by a LV mass index > 110 g/m^2 in women and by a LV mass index > 134 g/m^2 in men. This group was larger than the group of aortic stenosis patients presenting with heart failure and similar evidence of LV hypertrophy (n=39). Aortic stenosis patients with adaptive LV hypertrophy therefore outnumbered aortic stenosis patients with maladaptive LV hypertrophy in this prospective study population. The investigators failed to look for clinical features discriminating patients with adaptive LV hypertrophy from patients with maladaptive LV hypertrophy. Such discriminating clinical features could have identified an hormonal or environmental background, which predisposes pressure-overload hypertrophy to evolve into a maladaptive phenotype. In this respect, body mass index and arterial blood pressure were significantly higher in the patients who developed heart failure. Obesity and hypertension are established risk factors for LV diastolic dysfunction[9] and as aortic stenosis progresses, these co-morbidities can direct LV hypertrophy towards a maladaptive phenotype with diastolic heart failure. Obesity and hypertension are both associated with insulin resistance, which lowers myocardial nitric oxide (NO) content by reducing protein kinase B-mediated endothelial NO synthase (NOS3) phosphorylation. Myocardial NO content is a potent modulator of the hypertrophy process as recently demonstrated in transgenic mice with cardiac-myocyte restricted NOS3 overexpression[10]. Hence, development of maladaptive LV hypertrophy should not necessarily be ascribed to the hypertrophy gene programme but could also result from deleterious modification of its expression by hormonal and environmental factors.

Normalization of LV wall stress is a key feature of the adaptive hypertrophy paradigm in pressure overload. In the original studies that applied this paradigm to aortic stenosis, failure to normalize LV wall stress was kept responsible both for contractile dysfunction[2] and for poor postoperative outcome[3]. The study by Kupari *et al*. comes to the opposite conclusion as they observe better contractile function in the absence of LV hypertrophy. Absence of LV hypertrophy in their study does however not imply persistent elevation of LV wall stress, which they unfortunately failed to measure. As mentioned before, LV hypertrophy was diagnosed when LV mass index exceeded preset values. Since LV mass index also depends on LV end-diastolic volume index, its use to categorize patients for LV hypertrophy can cause patients with small LV

volumes and moderate increase in LV wall thickness to end up in the group "without LV hypertrophy". This indeed happened as evident from Table 3, which shows patients "without LV hypertrophy" to have elevated septal (13±0.3 mm) and posterior (12±0.4 mm) wall thickness and a LV end-diastolic diameter smaller than the patients "with LV hypertrophy". Patients labeled as having no LV hypertrophy could well have developed sufficient LV hypertrophy to normalize LV wall stress for a small LV cavity and their superior contractile performance was therefore no surprise. To clarify this issue, the study needs to be implemented with an invasive assessment of LV wall stress.

Finally, since LV mass index depends on LV end-diastolic volume index and since LV end-diastolic volume index was significantly larger in the heart failure group, the inverse relation between LV mass index and LVEF can also be explained by an inadequacy of LV hypertrophy to normalize LV wall stress for a large LV cavity. In fact, when LV mass index was replaced by relative wall thickness (i.e. septal and posterior wall thickness divided by end-diastolic diameter), this inadequacy of LV hypertrophy got accounted for and the relation between LVEF and LV hypertrophy actually reversed with a higher LVEF now being observed at a higher relative wall thickness.

Conclusion

Avoidance or modification of maladaptive LV hypertrophy remains a major clinical challenge. The study by Kupari *et al*. deserves credit for being the first to translate recent basic evidence on maladaptive myocardial hypertrophy to the clinical setting of valvular heart disease. At present, their iconoclastic idea on LV hypertrophy in aortic stenosis awaits further confirmation by invasive studies. As with all iconoclastic acts, history will tell if it cleared perspectives or spoiled the view.

Reference List

(1) Grossman W, Jones D, McLaurin LP. Wall stress and patterns of hypertrophy in the human left ventricle. *J Clin Invest* 1975 July;56(1):56-64.

(2) Gunther S, Grossman W. Determinants of ventricular function in pressure-overload hypertrophy in man. *Circulation* 1979 April;59(4):679-88.

(3) Carabello BA, Green LH, Grossman W, Cohn LH, Koster JK, Collins JJ, Jr. Hemodynamic determinants of prognosis of aortic valve replacement in critical aortic stenosis and advanced congestive heart failure. *Circulation* 1980 July;62(1):42-8.

(4) Kupari M, Turto H, Lommi J. Left ventricular hypertrophy in aortic valve stenosis: preventive or promotive of systolic dysfunction and heart failure? *Eur Heart J* 2005 April 28;ehi290.

(5) Marban E. Translation, Translation, Translation: Circulation Research in Cardiology's New Golden Age. *Circ Res* 2005 January 7;96(1):4-5.

(6) Frey N, Katus HA, Olson EN, Hill JA. Hypertrophy of the Heart: A New Therapeutic Target? *Circulation* 2004 April 6;109(13):1580-9.

(7) Esposito G, Rapacciuolo A, Naga Prasad SV, Takaoka H, Thomas SA, Koch WJ , Rockman HA. Genetic Alterations That Inhibit In Vivo Pressure-Overload Hypertrophy Prevent Cardiac Dysfunction Despite Increased Wall Stress. *Circulation* 2002 January 1;105(1):85-92.

(8) Buermans HPJ, Redout EM, Schiel AE, Musters RJP, Zuidwijk M, Eijk PP, van Hardeveld C, Kasanmoentalib S, Visser FC, Ylstra B, Simonides WS. Microarray analysis reveals pivotal divergent mRNA expression profiles early in the development of either compensated ventricular hypertrophy or heart failure. *Physiol Genomics* 2005 May 11;21(3):314-23.

(9) Fischer M, Baessler A, Hense HW, Hengstenberg C, Muscholl M, Holmer S, Doring A, Broeckel U, Riegger G, Schunkert H. Prevalence of left ventricular diastolic dysfunction in the community: Results from a Doppler echocardiographic-based survey of a population sample. *Eur Heart J* 2003 February 2;24(4):320-8.

(10) Janssens S, Pokreisz P, Schoonjans L, Pellens M, Vermeersch P, Tjwa M, Jans P, Scherrer-Crosbie M, Picard MH, Szelid Z, Gillijns H, Van de Werf F, Collen D, Bloch KD. Cardiomyocyte-Specific Overexpression of Nitric Oxide Synthase 3 Improves Left Ventricular Performance and Reduces Compensatory Hypertrophy After Myocardial Infarction . *Circ Res* 2004 May 14;94(9):1256-62.

Chapter 7

Summary & Samenvatting

Table of contents

Adaptive and maladaptive myocardial remodelling due to pressure overload do not evolve from a common hypertrophy precursor stage

Characterization of ventricular proteome and transcriptome profiles

Summary

Heart failure contributed to approximately 287.200 deaths in the year 1999 in the United States and on average, 5 million cases of heart failure exist in the U.S alone. Two recent epidemiological studies, based on two separate populations, indicated an overall higher incidence of heart failure in men, with no decreased incidence over time. For women however, one study showed decreased incidence while the other indicated no change during the last two decades. Both studies indicated an overall increase in the survival rate, in particular for men and young persons. However, this increase in survival rate was less prominent in women and the elderly. With an overall 5 year survival rate of 52% and an increasing elderly population, heart failure remains a major health problem.
Heart failure is a clinical end-point of a syndrome characterized by a progressive loss of pump function, manifested by respiratory distress, pedal edema and ascites, and profound exercise intolerance. Myocardial ventricular hypertrophy is a major risk factor that is associated with a higher incidence of clinical events, morbidity and mortality from cardiovascular disease, generally leading to heart failure. Although myocardial hypertrophy due to pressure overload is aimed at normalizing wall stress, depending on the degree and duration of the overload, the hypertrophic response may progress into a state of compromised cardiac function, ultimately leading to congestive heart failure. Ventricular hypertrophy is both associated with, and characterized by, many known alterations at the transcriptome and proteome expression levels. Well known examples of which are changes in extracellular matrix composition, a switch in energy metabolism substrate, altered signal transduction pathway activity and impaired calcium handling. However, which of the alterations are critical to the development of either an adaptive or maladaptive hypertrophy phenotype is under debate. Moreover, the time point at which the divergence between the phenotypes occurs during pressure overload remains unknown.

The work presented in this thesis was focussed on investigating alterations on the transcriptome and proteome level that occur during myocardial hypertrophic remodelling which are associated with the divergence towards either an adaptive or maladaptive phenotype. Micro-array analysis and 2-dimensional gel electrophoresis were the techniques of choice to determine these pivotal molecular events on both

the transcriptome and proteome level, respectively. To this end, protein- and mRNA-expression levels were compared between adaptive and maladaptive hypertrophy responses to pressure overload over time.

Chapter 2 first describes the animal model representing human pulmonary hypertension (PH) that allowed for the controlled induction of either an adaptive or maladaptive phenotype. Right ventricular (RV) hypertrophy secondary to PH was induced by a single injection of monocrotaline (MCT). A subcutaneous MCT injection of 30 mg/kg leads to stable adaptive RV hypertrophy (HYP) while 80 mg/kg leads to a transient phase of adaptive RV hypertrophy (day 14-19) followed by maladaptive hypertrophy and RV failure (CHF) around day 25-28. This MCT-dose-controlled model for RV hypertrophy provided the unique opportunity to characterize the molecular myocardial changes during the initial stages of pressure overload and was therefore used to investigate ventricular mRNA and protein expression levels well before overt phenotypical differences became apparent.
RV gene-expression profiles generated by a rat oligonucleotide micro-array representing 4803 unique features, were compared between animals developing adaptive hypertrophy, maladaptive hypertrophy and control (CON) animals at 14 days after the imposition of pressure overload. At this time point, the level of developed hypertrophy was identical for both the adaptive and maladaptive hypertrophy phenotypes when compared to control animals.
Of the 3060 selected features for analysis on the arrays, 179 were significantly differentially expressed between the three groups. Clustering of these significantly regulated genes revealed distinct clusters with different expression profiles. Some of these clusters represented genes that were equally differentially expressed in both the adaptive and maladaptive hypertrophy groups relative to control expression levels. Two clusters were found that specifically correlated with phenotypical outcome of either MCT treated group, i.e., one of these clusters represented genes with specifically altered expression levels in the adaptive hypertrophy group only (2 up- and 4 downregulated), while the other represented genes with altered expression levels for the maladaptive hypertrophy group only (25 up and 6 downregulated). Moreover, genes in these specific profiles indicated that processes involving p38-MAPK signalling and apoptosis could be related to the adaptive or maladaptive phenotypical outcome.
These findings indicated that distinct expression profiles and potentially decisive pathways had already been initiated at an early time point during ventricular remodelling, which could indicate that the maladaptive and adaptive groups were already different very early after the imposition of pressure overload.

In Chapter 3 we extended the analysis of gene-expression alterations during adaptive or maladaptive hypertrophic remodelling, to include more time points after MCT injections. Micro-array experiments were performed at day 10, when RV hypertrophy had not yet developed and phenotypes were identical, at day 19 when RV phenotypes started to diverge and at day 25 when RV phenotypes were different. Force frequency relationship (FFR) determinations from isolated rat trabeculae clearly indicated ventricular dysfunction in the CHF group showing a positive FFR response for both the CON and HYP animals at day 25, whereas CHF animals did not show this potentiation.

Out of the 3148 selected features for analysis, an analysis of variance statistical framework identified 584 significantly regulated genes between the three experimental groups over time. When comparing CON to HYP, 8, 123 and 386 genes were differentially expressed at day 10, 19 and 25, respectively. When comparing CON to CHF, 42, 125 and 454 genes were differentially expressed at day 10, 19 and 25, respectively. Some of these genes were significantly regulated at more than one time point, primarily at days 19 and 25. Also, a considerable number of genes existed that were equally regulated in both HYP and CHF group relative to CON. This indicated that there is a general increase in the total number of differentially expressed genes as ventricular remodelling progressed with time. However, when comparing HYP to CHF the number of differentially expressed genes is almost constant with 13, 13 and 16 genes differentially expressed on day 10, 19 and 25, respectively.

Self organizing map clustering was used to visualize the changes in expression of the 584 regulated genes over time. Many of the clusters found represented genes with equal significant differential expression in both hypertrophy groups relative to time-matched control animals, especially at days 19 and 25 after MCT injections. Gene-ontology (GO) over-representation analyses on these clusters of genes, indicated substantial alterations affecting lipid metabolism and the mitochondrial compartments, which predominantly represented downregulated genes. In contrast, clusters of upregulated genes represented extracellular matrix composition, cell adhesion and muscle development. However, for a subset of clusters, the expression levels of the genes in the CHF group had a tendency to be altered just prior to those same genes in the HYP group. Interestingly, genes with corresponding proteins involved in cell-cycle progression control were an over-represented GO classification in these latter clusters.

A gene set enrichment analysis (GSEA) using GenMapp pathways was performed to more specifically characterize differences between the HYP and CHF groups at all three time points. Several pathways were implicated to predispose adaptive and

maladaptive remodelling. Genes with corresponding proteins involved in the mitochondrial electron transport chain showed decreased expression in CHF relative to the HYP at day 25, while the inverse was observed for this pathway at day 10 after imposition of pressure overload. In addition, genes representing the cell cycle control pathway showed higher expression in CHF than HYP at day 10. Of these cell cycle genes, cyclin B1, cdc2a and p55cdc were confirmed by realtime PCR to be differentially overexpressed in the CHF group relative to both HYP and CON. Cyclin B1 and cdc2a have important functions in regulating the G2/M cell-cycle transition. Furthermore, Gadd45a, an inhibitor of G2/M transition, was shown to be overexpressed in the HYP group. This suggested an important role for proper regulation of cell-cycle progression to be associated with phenotypical divergence between adaptive and maladaptive hypertrophy.
These findings further challenged the existence of a "transition to heart failure". More specifically, these data indicated that, instead of adaptive and maladaptive hypertrophic phenotypes evolving from an common hypertrophic precursor state, the myocardial responses in animals developing either of these phenotypes are already different from a very early time point after the imposition of pressure overload. Furthermore a critical role for proper cell-cycle control at the G2/M transition was suggested to be associated with the differentiation between the adaptive and maladaptive phenotypes early after the imposition of pressure overload.

Parallel to the gene-expression analyses in Chapter 3, RV myocardial proteome-expression profiles obtained from animals at 10 days after MCT injections were compared using 2-dimensional gel-electrophoresis in Chapter 4. Of the 353 protein spots that were analysed, 5, 15 and 23 were significantly differentially expressed between the CON to HYP, CON to CHF and HYP to CHF comparisons, respectively. Some proteins were significantly regulated in more than one of the pair-wise comparisons. Of these proteins, mitochondrial Enoyl-CoA hydratase (Echs1) was shown to be specifically downregulated in the CHF group rel. to the HYP and CON groups, which was paralleled by a similar significant decrease at the mRNA level. Echs1 catalyses the second reaction step in the mitochondrial beta-oxidation of fatty acids, suggesting that a change in energy metabolism substrate precedes phenotypical divergence.
These data indicated that not merely specific mRNA levels were different between adaptive and maladaptive remodelling early after the imposition of pressure overload, but that this was also true for specific proteins. These data further substantiated the findings presented in Chapter 3.

Adaptive en maladaptive myocardiale remodelling door druk overbelasting onstaan niet vanuit een overeenkomstig hypertroof voorloper stadium

Karakerizatie van ventriculaire proteoom en transcriptoom profielen

Samenvatting

Hart falen was verantwoordelijk voor ongeveer 287.200 sterfgevallen in 1999 in de Verenigde Staten, waar er alleen al naar schatting 5 miljoen patiënten met hart falen voorkomen. Uit twee recente, op onafhankelijke populaties uitgevoerde epidemiologische studies, is gebleken dat hart falen vaker voorkomt bij mannen, zonder verminderde incidentie door de tijd. Echter, voor vrouwen bleek uit een van deze studies een afgenomen incidentie, terwijl de andere geen verandering aangaf voor de laatste twee decennia. In het algemeen gaven beide studies een toegenomen overlevings kans aan, met name voor mannen en jongere personen. Doch, deze toegenomen overlevingskans was minder evident bij vrouwen en oudere mensen. Met een gemiddelde 5-jarige overlevingskans van 52% en de toenemende vergrijzing van de bevolking blijft hart falen een groot medisch probleem.

Hart falen is het klinische eind-punt van een syndroom dat wordt gekarakterizeerd door progresief verlies van pomp funktie, dat zich kenbaar maakt door ademhalings moeilijkheden, vochtophoping in de benen met ascites, en onverdraagzaamheid van lichaamsbeweging. Myocardiale ventrikel hypertrofie is een van de belangrijkste risico factoren, die geassocieerd zijn met een hogere frequentie van klinische manifestatie, morbiditeit en mortaliteit, die in het algemeen leidden tot hart falen. Hoewel myocardiale hypertrofie als gevolg van druk overbelasting gericht is op normalizatie van wand spanning, is het afhankelijk van de duur en mate van de overbelasting of deze hypertrofe reactie zal doorslaan naar een toestand van belemmerde hart funktie, die uiteindelijk zal leidden tot hart falen. Ventrikel hypertrofie is zowel geassocieerd met, als te karakterizeren door, vele erkende veranderingen op het transcriptoom en proteoom expressie niveau. Bekende voorbeelden hiervan zijn veranderde extracellulaire matrix samenstelling, een substraat wisseling mbt. energie metabolisme, gewijzigde activiteit van signaal transductie routes en belemmerd calcium transport. Echter, er is nog geenszins overeenstemming over welke van deze veranderingen kritiek zouden zijn voor de ontwikkeling van enerzijds een adaptief of anderzijds een maladaptief fenotype. Bovendien is het tijdspunt waarop de splitsing tussen deze twee fenotypes optreed nog altijd onbekend.

Het werk dat in dit proefschrift wordt gepresenteerd, is gericht op het ontrafelen van veranderingen die optreden op het transcriptoom en proteoom niveau tijdens myocardiale hypertrofe remodelling, die geassocieerd zijn met het opsplitsen van de adaptive en maladaptive fenotypes. Micro-array analyses en twee-dimensionle gel electroforese zijn de gebruikte technieken om de kritieke molekulaire voorvallen op respectivelijk het transciptoom en proteoom niveau te bestuderen. Hiervoor zijn eiwit en mRNA expressie niveaus vergeleken tussen adaptive en maladaptive hypertrofe responsen op druk overbelasting in de tijd.

In Hoofdstuk 2 wordt eerst het dieren model voor humane pulmonaire hypertensie (PH) beschreven. Dit model levert de mogelijkheid voor gecontroleerde inductie van hetzij een adaptief of maladaptief fenotype. Rechter ventrikulaire (RV) hypertrofie secundair aan PH werd geïnduceerd door een enkele injectie van monocrotaline (MCT). Een subcutane MCT injectie van 30 mg/kg leidt tot een stabiele adaptive RV hypertrofie (HYP), terwijl 80 mg/kg leidt tot een transiente fase van adaptive hypertrofie (dag 14-19) gevolgd door maladaptive hypertrofie en RV falen (CHF) rond dag 25-28. Dit model van dosis gecontroleerde RV hypertrofie levert de unieke mogelijkheid om de mocelulaire veranderingen gedurende de initiele fase van druk overbelasting the karakterizeren en is om die reden gebruikt om ventriculaire mRNA en eiwit expressie verschillen te bestuderen ruim voordat fenotypische verschillen duidelijk zichtbaar worden.

RV gen-expressie profielen gegenereerd mbv. een rat oligonucleotide micro-array representatief voor 4803 unieke gen-sequenties, werden vergeleken tussen adaptive, maladaptive en controle (CON) dieren op 14 dagen na het opleggen van de druk overbelasting. Op dit tijdspunt is de mate van ontwikkelde hypertrofie identiek voor het adaptive en maladaptive hypertrofe fenotype tov. de controle dieren.

Van de 3060 voor analyse geselecteerde gen-sequenties waren er 179 met significante differentiële expressie tussen de drie groepen. Het clusteren van deze significant gereguleerde genen duidde op afzonderlijke clusters met verschillende expressie profielen. Sommige van deze clusters waren representatief voor genen met gelijke mate van differentiële expressie in zowel adaptive als maladaptive hypertrofie tov. de controle expressie niveaus. Twee clusters werden gevonden die specifieke correlaties vertoonde met de fenotypische uitslag van de twee gebruikte MCT doses, dwz, een van deze clusters was representatief voor genen met specifiek veranderde expressie niveaus in de adaptive hypertrofie groep (2 verhoogde- en 4 verlaagde expressie), terwijl de andere representatief was voor genen met specifiek veranderde expressie niveaus in de maladaptive hypertrofie groep (25 verhoogde- en 6 verlaagde expressie). Bovendien duidde de genen met deze specifieke expressie

profielen op de betrokkenheid van p38-MAPK signalering en apoptose op de uiteindelijke gevormde adaptive en maladaptive fenotypes.
Deze bevindingen gaven aan dat afzonderlijke expressie profielen en potentiëel doorslaggevende routes al op een vroeg tijdspunt tijdens ventriculaire remodelling geinitiëerd waren, wat zou kunnen betekenen dat de maladaptive en adaptive groepen al heel kort na het opleggen van druk overbelasting reeds verschillend zijn.

In hoofdstuk 3 verlengen we de analyse van gen-expressie veranderingen gedurende adaptive of maladaptive remodelling met meerdere tijdspunten na MCT injecties. Micro-array experimenten werden uitgevoerd voor dag 10, wanneer RV hypertrofie nog niet evident was en de fenotypes identiek zijn, voor dag 19, wanneer RV fenotypes uiteen beginnen te lopen en voor dag 25, wanneer RV fenotypes verschillend zijn. Kracht-frequentie relatie (KFR) bepalingen op geïsoleerde ratten trabekels gaven duidelijk gestoorde ventriculaire funktie aan voor de CHF groep. Zowel de CON als de HYP groep vertoonde een positieve KFR response voor dieren op dag 25, terwijl de CHF dieren deze potentiatie niet weergaven.
Van de 3148 voor analyse geselecteerde gen-sequenties werden er 584 genen geïdentificeerd met significante regulatie tussen de drie groepen in de tijd. Voor de CON met HYP vergelijking kwamen 8, 123 en 386 genen differentiëel tot expressie op respectivelijk dag 10, 19 en 25. Voor de CON met CHF vergelijking kwamen 42, 125 en 454 genen differentiëel tot expressie op respectivelijk dag 10, 19 en 25. Een aantal van deze genen waren significant gereguleerd op meer dan een tijdspunt, met name op dagen 19 en 25. Ook was er een aanzienlijk aantal genen met gelijke mate van differentiële expressie in de HYP en CHF groepen tov. de controle expressie niveaus. Deze data gaven aan dat er spake is van een globale toename van differentiële gen expressie bij het vorderen van de ventriculaire remodelling in de tijd. Echter, het aantal differentiële genen voor de HYP met CHF vergelijking was vrijwel constant, met 13, 13 en 16 genen differentiële genen op respectivelijk dag 10, 19 en 25.
Om de expressie veranderingen van de 584 gereguleerde genen in de tijd weer te geven, werd *Self organizing map* clustering toegepast. Veel van de gevonden clusters waren representatief voor genen met gelijke significante differentiële expressie in beide hypertrofie groepen tov. de tijds-controle groep. Dit was met name zo voor 19 en 25 dagen na MCT injecties. Gen-ontologie (GO) over-representatie analyses uitgevoerd op deze clusters van genen gaven aan dat er aanzienlijke veranderingen optraden mbt. het lipide metabolisme en het mitochondriale compartiment, voor genen met voonamelijk verlaagde expressie niveaus. In contrast, clusters met vehoogde gen-expressie waren representatief voor veranderingen in extracellulaire

matrix samenstelling, cel adhesie en spier opbouw. Echter, in een klein aantal clusters was een trend zichtbaar waarbij veranderingen in gen-expressie niveau van de CHF groep eerder optraden dan voor deze zelfde genen in de HYP groep. Interessant genoeg vertoonde genen met corresponderende eiwitten die een regulerende rol spelen in de cel-cyclus progressie, significante GO classificatie over-gerepresentatie in deze laatst genoemde clusters.
Een *gene set enrichment analysis* (GSEA) op GenMapp-routes werd vervolgens uitgevoerd om de verschillen tussen HYP en CHF op de drie tijdspunten specifieker te karakterizeren. Meerdere routes bleken betrokken bij het predisponeren van adaptive en maladaptive remodelling. Genen met corresponderende eiwitten die betrokken zijn in de mitochondriale ademhalingsketen vertoonde verlaagde expressie in CHF tov. HYP op dag 25, terwijl het ongekeerde werd waargenomen voor deze route voor dag 10 na opleggen van de druk overbelasting. Ook kwamen genen die representatief zijn voor de cel-cyclus regulatie route hoger tot expressie in de CHF groep dan in de HYP groep op dag 10. De significant toegenomen expressie van de cel-cyclus genen cyclin B1, cdc2a en p55cdc in de CHF groep tov. HYP en CON, was bevestigd met realtime PCR. Cyclin B1 en cdc2a zijn belangrijk bij regulatie van de G2/M cel-cyclus transitie. Bovendien kwam de G2/M transitie remmer, Gadd45a significant hoger tot expressie in de HYP groep. Dit opperde dat een belangrijke rol van correcte regulatie van de cel-cyclus progressie is weggelegd bij de fenotypische opsplitsing tussen adaptive en maladaptive hypertrofie.
Deze bevindingen legde verdere twijfels bij het bestaan van een "transitie naar hart falen". Specifieker gesteld, deze data geven aan dat de myocardiale responsen in dieren die een van deze fenotypes ontwikkellen, al verschillen op een heel vroeg tijdspunt na te oplegging van druk overbelasting, in paats van dat de adaptive en maladaptive hypertrofe fenotypes onstaan uit een overeenkomstige voorloper toestand. Bovendien, een kritieke rol voor correcte cel-cyclus controle tijdens de G2/M transitie werd geassocieerd met de differentiatie tussen de adaptive en maladaptive fenotypes op een vroeg tijdspunt na de oplegging van druk overbelasting.

Parallel aan de gen-expressie analyses uit Hoofdstuk 3 worden in Hoofdstuk 4 myocardiale RV proteoom-expressie profielen van dieren op 10 dagen na MCT injecties vergeleken mbv. 2-dimensionale gel electroforese. Van de 353 eiwit spots die geanalyseerd zijn, waren er respectivelijk 5, 15 en 23 met significante differentiële expressie tussen de CON vs. HYP, CON vs. CHF en HYP vs. CHF vergelijkingen. Sommige van deze eiwitten kwamen voor in meer dan een van de groeps vergelijking. Van deze eiwitten vertoonde het mitochondriale Enoyl-CoA

hydratase (Echs1) specifieke expressie verlaging in de CHF groep tov. de HYP en CON dieren, en een parallele verlaging in expressie werd gevonden op het mRNA-transcript niveau. Het Echs1 katalyseert de tweede stap van de mitochondriale beta-oxidate van vetzuren, wat inpliceert dat veranderingen in energy metabolisme substraat optreden vóór fenotypische opsplitsing.

Deze data geven aan dat vroeg na de oplegging van druk overbelasting niet alleen specifieke mRNA niveaus verschillen tussen adaptive en maladaptive remodelling, maar dat dit ook geldt voor specifieke eiwitten. Deze data onderbouwde onze bevindingen uit Hoofdstuk 3.

Dankwoord

Soms had ik het zelf niet meer verwacht, maar na vijf jaar is het er dan toch van gekomen: *mijn proefschrift*!. Vanzelfsprekend heb ik het niet zonder hulp voor elkaar kunnen krijgen. Daarom wil ik graag van deze gelegenheid gebruik maken om een aantal mensen te bedanken voor hun inzet en steun.

Paul Eijk, Paul van den IJssel, Bauke Ylstra en alle andere mensen van de micro-array faciliteit. Ik heb altijd met plezier met jullie samengewerkt. Soemini, en vooral in de latere fase van mijn array analyses, Mark van de Wiel, zonder jullie statistische ondersteuning had het zeker niet gelukt.
Connie Jimenez. Heel hoofdstuk 4 had zonder jou proteomics expertise nooit van de grond kunnen komen. Het was me een waar genoegen met je samen te werken.

Mijn twee promotoren. Frans, wat me nog goed is bijgebleven, is dat je van mening was dat slechts 6 arrays per groep toch wel aan de magere kant zou zijn. Je opperde dan ook direkt dat we de experiment serie maar eens flink zouden moeten gaan uitbreidden. Geloof me, als de mogelijkheid er op dat moment was, ik had dat graag gedaan. Walter Paulus. Met de overmaat aan data die uit mijn array experimenten voortkwam, was het noodzaak om dit vooral ondubbelzinnig en duidelijk weg te schrijven. Ik heb veel geleerd tijdens de maanden dat we samen aan het schrijven waren.

Dop & Marian. Jullie twee vormde een solide basis voor de laatste 5 jaar onderzoek. Zonder jullie had het nooit gaan rollen. Zonder jullie had het allemaal nooit tot een goed einde kunnen komen.

René, hou goede moed!

Mijn kamer genoten Arthur, Ronald en Everaldo. Te sterke koffie van de ene, te slap van de andere, en de derde drinkt (vreemd genoeg?) liever thee. Het waren een paar leuke jaren om nooit meer te vergeten. Maar als een van jullie ooit nog eens computer hulp nodig heeft: don't call us !!

Pierre, Barry, Philip en Elif, Jeroen en Carina, John-Paul, Ortwin, Roeland: bedankt voor de (on)vergetelijke vrijdag en zaterdag avonden. Deze waren uitermate geschikt om alle lab frustraties van de hele week te relativeren. Need I sλy more!?

Mijn ouders en Opa's en Oma's voor hun onvoorwaardelijke steun.

Maar natuurlijk moet ik een persoon zeker niet vergeten. Hoewel je pas in 2001 in zicht kwam, zou je in de daarop volgende jaren een zeer grote stempel op mijn werk gaan drukken: mijn Linda. Je vond al dat "hele avond achter de computer zitten werken" en die "rode, gele, groene *vlekken*" maar niets. Maar begreep dat het belangrijk voor me was en bleef me steunen en motiveren, vooral als het minder goed leek te gaan. Als ik jou niet had gehad ..... laten we daar maar niet over gaan speculeren. Vanaf nu hoef je me niet meer te delen met " het promoveren". Kusss

Henk

De Auteur

Henk Buermans werd geboren op 3 mei 1975 te Roosendaal, Nederland. Na het behalen van de MAVO, HAVO en VWO diploma's in de periode 1991 tot 1995, studeerde hij bio-farmaceutische wetenschappen aan de universiteit van Leiden. Aan het eind van deze studie periode liep hij stage bij afdeling Biofarmacie van het Leiden/Amsterdam Center for Drug Reseach onder begeleiding van Dr. J. von der Thussen en Dr. E. Biessen. Een 2^{e} stage werd vervolgens doorlopen bij afdeling Moleculaire en Vasculaire Biologie van de K.U. Leuven, België, onder begeleiding van Dr. P. Verhamme en Prof. Dr. P. Holvoet. Het doctoraal examen Bio-farmaceutische wetenschappen van Universiteit Leiden behaalde hij op 13 februari 2001.
Vanaf juni 2001 t/m december 2005 was hij werkzaam als promovendus bij afdeling Fysiologie van het VU medisch centrum te Amsterdam. Zijn onderzoek in deze periode was gericht op het in kaart brengen van verschillen op zowel gen- als eiwit-expressie niveau die onstaan tussen een pathologische en niet-pathologische vorm van hartspier vergroting tijdens druk overbelasting. Dit onderzoek was onder begeleiding van Dr. W. Simonides, met als promotoren Prof. Dr. F. Visser en Prof Dr. W. Paulus. De behaalde resultaten zijn oa. beschreven in dit proefschrift.
Op het moment van dit schrijven is Henk werkzaam als post-doc, onder begeleiding van Dr. PB 't Hoen bij het Centrum voor Humane en Klinische Genetica van het Leids Universitair medisch centrum. Hier maakt hij deel uit van het Europesche *HeartRepair* project (www.heartrepair.org), waar hij in nauwe samenwerking met Dr. M. van den Hoff van de afdeling Anatomie en Embryologie van het Academisch Medisch Centrum Amsterdam, onderzoek verricht naar gen-expressie dynamiek tijdens de embryonale ontwikkeling van de hartspier circulatie en *in vitro* hartspiercel vorming.